Massive Sterile Neutrinos For Dark Matter Halos

by

Aqsa Yasmin

A thesis submitted in partial fulfillment of the requirements
for the degree of Master of Philosophy in Physics

Supervised by

Prof. Dr. Azad A. Siddiqui

Co-supervised by

Prof. Dr. Asghar Qadir

Department of Physics School of Natural Sciences National University of Sciences and Technology H-12, Islamabad, Pakistan (2021)

FORM TH-4

National University of Sciences & Technology

MS THESIS WORK

We hereby recommend that the dissertation prepared under our supervision by: Aqsa Yasmin, Regn No. 00000278385 Titled: Massive Sterile Neutrinos for Dark Matter Halos be Accepted in partial fulfillment of the requirements for the award of **MS** degree.

Examination Committee Members

1. Name: PROF. TOOBA FEROZE Signature: _____

2. Name: DR. M. ALI PARACHA Signature: _____

External Examiner: DR. MANSOOR UR REHMAN Signature: _____

Supervisor's Name PROF. AZAD A. SIDDIQUI Signature: _____

Co-Supervisor's Name PROF. ASGHAR QADIR Signature: _____

_____ 05.01.2022
Head of Department Date

COUNTERSINGED

Date: 05-01-2022 _____
Dean/Principal

Acknowledgement

I thank Allah the Almighty for His countless blessings.
I feel highly privileged to express my profound gratitude to **Prof. Dr. Asghar Qadir** for his continuous guidance and support throughout my MS. I am truly honored that I was able to work on my entire thesis and research under his guidance. He is undoubtedly the best teacher I ever had and my ideal person. I am very grateful to **Prof. Dr. Azad A. Siddiqui** for his support and backing me up even in the most difficult times.
Thanks to my mother for her love, support, and sacrifices and my brother who have always been very supportive.
Lastly, I would like to thank my late grandfather and grandmother for their unconditional love, I would never have been able to be who I am today without them.

Aqsa Yasmin.

Abstract

This study pertains to an investigative analysis of the Ruffini-Argüelles-Rueda (RAR) model of a self-gravitating gas of about 48 to 345 keV degenerate fermions that form a fully degenerate core, with and without considering the cutoff effects. These fermions are taken to provide the non-baryonic dark matter which lie outside the standard model of Particle Physics and are known as "sterile neutrinos" or "neutralinos". It assumes a degenerate Fermi core surrounded by a partially degenerate Fermi halo. We see if we get the cores collapsing into black holes in such a system enhancing the potential well of the degenerate fermions. In order to conduct an analysis, we use fermions of masses 48 keV, 56 keV, 100 keV, 200 keV, and 348 keV for the calculations. The density profiles and rotation curves show three remarkably different regimes: the quantum core, transition region from quantum to classical effects, and classical halo. We also check the results for masses below 48 keV. Latest research shows that at fermion mass 56 keV a compact core with mass and size close enough to that of Sgr A* is obtained, this gives an excellent explanation to the idea of considering a fermionic core as an alternative to Sgr A*.

Contents

List of Figures

List of Tables

Chapter 1

Introduction

The problem of existence of dark matter (DM) in galaxies and searching for the dark matter particles, their masses, and other properties is one of the most discussed issues in Physics today. The distribution of dark matter in terms of collisionless massive particles was assumed considering different distribution functions like Maxwellian, Fermi-Dirac (FD), and, Bose-Einstein (BE) distribution functions. From the '80s till the present, the dark matter distribution in galaxies has been considered, with a system consisting of self-gravitating massive fermions from fully degenerate regime to semi-degenerate regime [11,12]. The Fermi-Dirac statistics for the fermion masses going from a few eV to keV and the Bose-Einstein condensate from 10^{-25} eV to a few eV were taken into account [12].

In this dissertation, firstly, the mass of dark matter particles is constrained. After that the system is solved at selected values of the degeneracy parameter θ_0 and the temperature parameter β_0, considering the Ruffini-Argüelles-Rueda model known as the RAR model [5, 13], which explains the dark matter distribution for fermion masses ranging from 10 to 65 KeV at a finite temperature. The core density and pressure are obtained for each fermion mass and the corresponding degeneracy and temperature parameters, using the fermionic equations of state. Then the variables like density, mass, and velocity varying with distance for core and halo are found by solving the equilibrium equations, considering the system to be spherically symmetric. The density profiles show three physical regimes: the inner dense core which obeys quantum statistics, the intermediate regime with some quantum corrections implied, and the classical Boltzmann regime. Then different density profiles are considered like the Navarro-Frenk-White (NFW) profile which gives a cuspy core behavior [6] and the Einasto density profile which shows a cored behavior [7], compared with the RAR density profile to see the difference.

A gravitational potential is assumed for the core of a dark matter halo, which could possibly be an alternative to the central black hole, if it would explain all the dynamics of the surroundings, and for these observations a fermionic mass range is assumed. Then the rotation curves for different ino masses are obtained with the corresponding degeneracy and

temperature parameters. The first maximum of the rotation curve gives the core size r_c and the second one gives the halo size r_h. Just like the density profiles, the rotation curves also show different regimes.

The fermion masses ranging from 48 to 345 KeV are then considered, where the mass 345 keV is the critical mass limit, beyond which the gravitational collapse is expected. For the finite size of galaxies, a cutoff is introduced in the fermionic phase space distribution, as already explained in [14] along with a cutoff parameter W just like the degeneracy and temperature parameters. This gives new solutions with the central compact core being an alternative to the black hole case of Sgr A*. For the RAR paper [5], the possibility of a fermion core at the galactic center to be an alternative to the central black hole did not reach the accurate compactness because the cutoff energy was not considered [15]. In the recent work presented in the sixteenth Marcel-Grossmann meeting (MG16), it was pointed out that at fermion mass 56 keV, a compact degenerate quantum core as an alternative to a black hole was obtained with a core mass $\sim 3.6 \times 10^6\ M_\odot$ [10]. This narrows the range from 56 keV to 345 keV. This will be discussed in detail in the last chapter.

So we will see how matter in distributed in a galaxy from the core to halo looking at the density profiles and the rotation curves. We will also see the distribution of baryonic matter in the bulge and disk of a galaxy. The model gives a good explanation for the problem of the formation of supermassive black holes shortly after the Big Bang and the missing black holes in the intermediate mass range. Other than the dark matter, baryonic matter is also present in the core of a galaxy, so this baryonic matter will tend to fall into the degenerate cores and may even form black holes inside. So we will see how much of the baryonic matter falls into the cores so that they collapse.

I will organize my thesis as follows:

In the first chapter, I will explain the background of Einstein's General Relativity Theory and then give an introduction to the elementary concepts of General Relativity. Before Einstein came up with his revolutionary ideas, only Newtonian Physics was known, in which gravity was just a force, General Relativity modified the concept of gravity and the Universe itself. For understanding General Relativity, differential geometry is a key, so I will discuss a few concepts of geometry which led to the development of Einstein's General Theory and his famous Einstein field equations. Then the most general solution of Einstein's field equations, known as the Schwarzschild solution is given, that led to the existence of black holes. Einstein's jaw dropping theories opened a whole new world of research for the future.

In the second chapter, I will discuss Cosmology, different models of the Universe, its evolution from the Big Bang till the present, and how it would possibly evolve in future. Then a little bit of Particle Physics will be explained to better understand different particles which might solve today's major research mysteries. Other than the normal matter, that is the baryonic matter, scientists have hypothesized the existence of dark matter as an entity of this Universe in recent times. Its imprints in the Universe and proposed constituents still stand as a mystery.

In the third chapter, I will discuss Astrophysics leading to the current understanding of black holes as astronomical objects, how the laws of Physics would behave near and inside a black hole, types of black holes, the problem of the formation of supermassive black holes, and their presence at the centers of different galaxies. Then galaxies and their types are explained along with different components of galaxies like bulge, disk, and halo to study the distribution of matter in different components of galaxies.

In the fourth chapter, I will explain the work of Ruffini, Argüelles, and Rueda. In the fifth and final chapter, I will explain my work and conclude the thesis with discussions and findings.

1.1 Background of General Relativity

In 1905, Einstein presented the *Special Theory of Relativity* [16] which deals with the study of uniform linear motion in an inertial frame of reference. With this theory, Einstein was able to change the concept of space and time from Newtonian absolute space and time, where the space was assumed to be continuously spread in all the directions and the time ticking at an even pace. Space and time are relative, according to Einstein, depending on the point of view of an observer. Special Relativity has two basic principles, stated as:
1. *In all the inertial frames, the laws of Physics are all the same.*
2. *The speed of light is constant for all the observers.*

Special Relativity deals with uniform motion. Einstein wanted to expand his concept by dealing with non-uniform motion, that is the accelerated motion. It took him a decade before he succeeded in presenting his new theory of General Relativity in 1915 that deals with the accelerated motion.

1.2 General Relativity

General Relativity is a theory not only about gravity but also about geometry [17, 18]. In General Relativity, space and time are a single 4-dimensional manifold called *spacetime*. It explains that the fabric of spacetime is not flat but gets distorted due to the presence of massive and compact objects. It produces a curvature in the spacetime, that is responsible for the gravitational force. It replaced Newton's universal law of gravitation.

The principles of General Relativity are:

1.2.1 The Equivalence Principle

The equivalence principle states that *the gravity is in some sense the same as the acceleration.*

The effects due to a uniformly accelerated frame of reference having an acceleration "a", cannot be distinguished from an unaccelerated reference frame in a gravitational field with gravity $g = -a$. Consider a man inside an elevator who drops an object which he was holding. It falls down the way it would on the Earth. The elevator may not necessarily be in an Earth-like gravitational field. It could be in a space far from the gravitational effects, say in a rocket, accelerating at 9.8 m/s^2. So inside an elevator, the man cannot decide whether he is in a gravitational field or in space with no gravitational field. Einstein thought of it back in 1907 [18]. For the inertial and gravitational masses to be equal, Eötvos performed an experiment. The expected result from the experiment was null. It was the only evidence on which General Relativity bases.

1.2.2 The General Covariance Principle

The general covariance principle states that *all the physical laws can be simply expressed tensorially.*

It means that in a gravitational field, the laws of Physics are given by the equations which are invariant under any set of transformations [17]. General Relativity deals with arbitrary motion. It gives a better explanation for the macroscopic objects in a gravitational field and faces some limitations when it comes to microscopic objects. In 1913, Einstein proposed the idea that the gravitational field can be incorporated by a metric tensor that gives the line element and the surface element as

$$ds^2 = g_{ab}(x^c)dx^a dx^b, \tag{1.1}$$

where g_{ab} is a *symmetric tensor*. The coefficients of the metric are arbitrary functions of the spacetime position. Ignoring all the gravitational effects, the line element reduces to the Minkowski line element. The components of the metric tensor for this case are:

In Cartesian coordinates

$$g_{00} = 1, \quad g_{11} = -1, \quad g_{22} = -1, \quad g_{33} = -1, \quad g_{ab} = 0 \quad if \quad a \neq b. \tag{1.2}$$

In Polar coordinates

$$g_{00} = 1, \quad g_{11} = -1, \quad g_{22} = -r^2, \quad g_{33} = -r^2 \sin^2\theta, \quad g_{ab} = 0 \quad if \quad a \neq b, \tag{1.3}$$

which gives

$$ds^2 = dr^2 - r^2 d\theta^2 - r^2 \sin^2\theta d\phi^2. \tag{1.4}$$

Maxwell's theory of the electromagnetic field is a field theory that is one of the most powerful theories. Maxwell wanted to incorporate gravity in his theory but he said it was not possible. Einstein succeeded in constructing and giving a physical interpretation to the field theory. Later on, symmetries were taken into account which led to the supergravity theory and the superstring theory.

1.3 The Curvature Tensor

An invariant geometry is required to explain General Relativity, for which tensors serve the purpose. Earlier the differential geometry was for a 3-dimensional plane, curve, and surface. In Relativity and Cosmology, we deal with the 4-dimensional tensors in curved space. For the unification of gravity with the other forces, we need to go beyond 4-dimensions.

The Gauss invariant intrinsic curvature of a surface is generalized to a high dimensional space when a basis vector is carried along two opposite directions and in the opposite order. Then the difference of the two results using covariant derivative will give

$$X^a_{;c;d} - X^a_{;d;c} = (X^a_{,\ c} + \Gamma^a_{\ b\ c} X^b)_{;d} - (X^a_{,\ d} + \Gamma^a_{\ d\ b} X^b)_{;c}, \tag{1.5}$$

where $\Gamma^a_{\ b\ c}$ is called the *Christoffel symbol*, given as

$$\Gamma^a_{\ b\ c} = \frac{1}{2} g^{ad}(g_{bd,c} + g_{cd,b} - g_{bc,d}), \tag{1.6}$$

$$X^a_{;c;d} - X^a_{;d;c} = (\Gamma^a_{\ b\ c,d} - \Gamma^a_{\ d\ b,c}) X^b + (\Gamma^a_{\ d\ f}\Gamma^f_{\ c\ b} - \Gamma^a_{\ c\ f}\Gamma^f_{\ d\ b}) X^b, \tag{1.7}$$

$$X^a_{;c;d} - X^a_{;d;c} = (\Gamma^a_{\ b\ c,d} - \Gamma^a_{\ d\ b,c} + \Gamma^a_{\ d\ f}\Gamma^f_{\ c\ b} - \Gamma^a_{\ c\ f}\Gamma^f_{\ d\ b}) X^b, \tag{1.8}$$

$$X^a_{;c;d} - X^a_{;d;c} = R^a_{bcd} X^b, \tag{1.9}$$

and R^a_{bcd} is given as

$$R^a_{bcd} = \Gamma^a_{\ b\ c,d} - \Gamma^a_{\ d\ b,c} + \Gamma^a_{\ d\ f}\Gamma^f_{\ c\ b} - \Gamma^a_{\ c\ f}\Gamma^f_{\ d\ b}. \tag{1.10}$$

This is known as the *Riemann curvature tensor* that measures the curvature of spacetime. If $R^a_{bcd} = 0$ then it is locally flat in certain regions representing the *Minkowski spacetime*. Contracting the first and third indices of Riemann curvature tensor gives the *Ricci tensor*. By Contracting the Ricci tensor gives the *Ricci scalar*, we have

$$R_{bd} = R^a_{bad}, \tag{1.11}$$

$$R = g^{bd} R_{bd}. \tag{1.12}$$

The properties of Riemann curvature tensor are:

1. If the two pairs of indices interchange, then R_{abcd} is *symmetric*

$$R_{abcd} = R_{cdab}. \tag{1.13}$$

2. If the first two or last two indices interchange, it is *skew-symmetric*

$$R_{abcd} = -R_{bacd} = -R_{abdc}. \tag{1.14}$$

3. The *first Bianchi identity* is given as

$$R_{abcd} + R_{acdb} + R_{adcb} = 0. \tag{1.15}$$

4. The *second Bianchi identity* is given as

$$R^a_{bcd;e} + R^a_{bec;d} + R^a_{bde;c} = 0. \tag{1.16}$$

1.4 The Geodesic Equation

Geodesic is the shortest available path on a curved space. The shortest path is the straightest path, but the straightest path is not necessarily the shortest path globally, locally it can be. We can see this by looking at the equation of geodesic [19]. The shortest path between two points is given by

$$S_{AB} = \int_A^B ds, \tag{1.17}$$

$$S_{AB} = \int_A^B 1.ds, \tag{1.18}$$

$$S_{AB} = \int_A^B g_{ab}(x^c)\dot{x}^a\dot{x}^b ds, \tag{1.19}$$

where 'S' is the arc length between two points. Take $L[x^c, \dot{x}^c] = g_{ab}(x^c)\dot{x}^a\dot{x}^b$, we have

$$S_{AB} = \int_A^B L[x^c, \dot{x}^c]ds. \tag{1.20}$$

From the Euler-Lagrange equations

$$\frac{\partial g_{ab}}{\partial x^c} = g_{ab,c}, \ \frac{\partial g_{ab}}{\partial \dot{x^c}} = 0, \tag{1.21}$$

$$\frac{\partial L}{\partial x^c} = g_{ab,c}\dot{x}^a\dot{x}^b, \tag{1.22}$$

$$\frac{\partial L}{\partial \dot{x}^c} = g_{bc}\dot{x}^b + g_{ac}\dot{x}^a, \tag{1.23}$$

$$\frac{d}{ds}\left(\frac{\partial L}{\partial \dot{x}^c}\right) = g_{bc}\ddot{x}^b + g_{ac}\ddot{x}^a + g_{bc,d}\dot{x}^b\dot{x}^d + g_{ac,d}\dot{x}^a\dot{x}^d. \tag{1.24}$$

The equation will be

$$g_{bc}\ddot{x}^b + g_{ac}\ddot{x}^a + g_{bc,d}\dot{x}^b\dot{x}^d + g_{ac,d}\dot{x}^a\dot{x}^d - g_{ab,c}\dot{x}^a\dot{x}^b = 0. \tag{1.25}$$

Replacing the dummy indices we get

$$g_{cd}\ddot{x}^d + \frac{1}{2}(g_{ac,b} + g_{bc,a} - g_{ab,c})\dot{x}^a\dot{x}^b = 0. \tag{1.26}$$

This is the *geodesic equation.*

1.5 Parallel and Lie Transport

Parallel transport displaces a tensor parallelly in a coordinate system, it shifts along parallelly. We get the parallel transport by Taylor's theorem using an intrinsic derivative. Consider a vector $\mathbf{p}$ to be transported parallelly as

$$\mathbf{p}^{\parallel} = e^{D_t}\mathbf{p}, \tag{1.27}$$

where $D_t = t.\nabla$ and t is a unit tangent vector. Working on the manifolds is different, *Lie transport* displaces a tensor along a curve on the manifold. It is obtained by Taylor's theorem but we take the Lie derivative instead of the intrinsic derivative

$$\mathbf{p}^{L_t} = e^{L_t}\mathbf{p}. \tag{1.28}$$

Lie derivative is a method of taking the derivative of a tensor along a curve. A tensor is Lie transported along a curve if its Lie derivative is zero. Consider a vector $\mathbf{p}$ to be Lie transported along a vector field say t, Lie derivative on a manifold at point a is given as

$$L_t p_a = \partial_p t(a)\partial_t p(a). \tag{1.29}$$

1.6 Geodesic Deviation

If two objects move in a gravitational field that change spatially, then the geodesic deviation explains their ability to proceed or retreat from one another. Consider two observers A and B both moving on a geodesic with unit tangent vector $\mathbf{t}$, B looks at A moving on the geodesic and defines his position vector $\mathbf{p}$. He has velocity as the first derivative of position vector with respect to proper time, and acceleration as the second derivative. Both the observers are moving with a constant velocity but suppose B thinks A is accelerating. The reason is, going along the geodesic, the rate of change of position does not remain constant, so acceleration comes from there. If the position vector is Lie transported along the geodesic it will join the geodesics. Lie transport displaces a tensor along a curve in the manifold and a tensor is Lie transported along a curve if its Lie derivative is zero. The geodesic deviation A^a is given as

$$L_t p^a = 0, \tag{1.30}$$

$$t^d p^a{}_{;d} - p^d\, t^a{}_{;d} = 0, \tag{1.31}$$

$$t^d\, p^a{}_{;d} = p^d\, t^a{}_{;d}, \tag{1.32}$$

$$A^a = \frac{d^2 p^a}{ds^2}, \tag{1.33}$$

$$A^a = t^c\, [t^d\, p^a{}_{;d}]_{;c}, \tag{1.34}$$

$$A^a = t^c \, [p^d \, t^a{}_{;d}]_{;c}, \tag{1.35}$$

$$A^a = t^c pd \, {}_{;c} t^a{}_{;d} + t^c \, p^d \, t^a{}_{;d;c}, \tag{1.36}$$

$$A^a = p^c \, t^d{}_{;c} \, t^a{}_{;d} + t^c \, p^d \, t^a{}_{;d;c}, \tag{1.37}$$

$$A^a = p^c (t^d{}_{;c} t^a)_{;d} - p^c \, t^d \, t^a{}_{;d;c} + t^c \, p^d \, t^a{}_{;d;c}, \tag{1.38}$$

$$A^a = -p^c t^d t^a{}_{;d;c} + t^c p^d t^a{}_{;d;c}, \tag{1.39}$$

$$A^a = t^c p^d t^a{}_{;d;c} + p^c t^d t^a{}_{;d;c}, \tag{1.40}$$

interchange "c" and "d"

$$A^a = t^d \, p^c \, t^a{}_{;c;d} + p^c \, t^d \, t^a{}_{;d;c}, \tag{1.41}$$

$$A^a = R^a_{bcd} \, t^b \, p^c \, t^d. \tag{1.42}$$

We see that the acceleration is because of spacetime curvature. This is called the *geodesic deviation* [19].

1.7 The Stress-Energy-Momentum Tensor

The presence of matter causes a gravitational field and if this field provides acceleration, then it must provide the curvature. So the curvature tensor needs to be related to matter. The gravitational field depends on the distribution of matter in space and its evolution with time. Special Relativity tells that matter and energy are linked together, so the energy distribution is required as well. Relativistically, a tensor of rank 2 is required which incorporates kinetic and potential energy. Leaving out the stresses in the potential, we have

$$T^{ab} = \rho u^a u^b, \tag{1.43}$$

where u^a and u^b are the velocity 4-vectors. This is the *energy-momentum tensor* [20]. In a rest frame

$$T^{00} = \rho c^2. \tag{1.44}$$

Energy can be carried by matter or contained by the stress in a medium. For incorporating potential part, stresses are added. *Stress* is a generalized form of pressure in which the directions of vectors matter, along with their magnitudes. Such a medium is called *anisotropic*. To incorporate stresses, define

$$\delta^{ab} = \sigma^{ij}\delta^a_i\delta^b_j. \tag{1.45}$$

So in the rest frame, the stress-energy-momentum tensor is represented as

$$T^{ab} = \rho c^2(\delta^a_0\ \delta^b_0) + (\sigma^{ij}\delta^a_i\ \delta^b_j), \tag{1.46}$$

where ρc^2 is the *energy density* and σ^{ij} is the *stress tensor*, given as

$$\sigma^{ij} = \frac{dF^i}{dS_j}. \tag{1.47}$$

It has a skew part which gives rotation but here rotation part is not considered. dF^i is the force and ds_j is the area element such that

$$ds_j = \varepsilon_{jkl}\ dx_k dx_l. \tag{1.48}$$

For an arbitrary frame, the *stress-energy-momentum tensor* is represented as

$$T^{ab} = \rho u^a u^b + \sigma^{ij}\delta^a_i\delta^b_j. \tag{1.49}$$

This is also called the *matter-stress-energy tensor* [20].

1.8 The Einstein Field Equations

Einstein's equations are ten partial differential equations which are the second order non-linear equations published in 1915. The equations have been used to predict the expanding Universe, black holes, and gravitational waves. Einstein's field equations represent a relationship between spacetime and geometry and the distribution of matter in the Universe by relating the spacetime curvature with stress, energy, and momentum in spacetime. The acceleration we get from the geodesic deviation is related to the curvature of space and

time. From the classical interpretation, we understand that the acceleration is caused by gravitation, and gravitation is caused by matter. So, the relationship between the matter (or energy) and curvature is given by [18]

$$\varepsilon^{ab}[g_{cd}, R^{c}_{drs}] = \kappa T^{ab}, \tag{1.50}$$

where κ is the proportionality constant called the *Einstein gravitational constant* and ε^{ab} is the tensor function of metric and curvature tensor. Using the second Bianchi identity $R^{a}_{bcd;e} + R^{a}_{bec;d} + R^{a}_{bde;c} = 0$, from "$a$" and "$c$" contraction

$$R_{bd;e} - R_{be;d} + R^{a}_{bde;c} = 0. \tag{1.51}$$

From "b" and "d" contraction

$$R_{;e} - R^{d}_{e;d} + (-R^{a}_{e;a}) = 0, \tag{1.52}$$

$$R^{d}_{e;d} + R^{a}_{e;a} - R_{;e} = 0. \tag{1.53}$$

Interchange "d" with "a"

$$2(R^{ae} - \frac{1}{2}R\ \delta^{a}_{e})_{;a} = 0. \tag{1.54}$$

Integrating this will give

$$\varepsilon^{ae} = R^{ae} - \frac{1}{2}R\ \delta^{a}_{e}. \tag{1.55}$$

This is called the *Einstein tensor*.

$$\varepsilon^{ae} = R^{ae} - \frac{1}{2}Rg^{ae}, \tag{1.56}$$

substitute it in eqn.1.50, we get

$$R^{ab} - \frac{1}{2}Rg^{ab} = \kappa T^{ab}, \tag{1.57}$$

where $\kappa = \frac{8\pi G}{c^4}$. These are the *Einstein field equations* that were stated by Einstein himself. He later modified these equations when General Relativity included Cosmology which will be discussed in the second chapter.

1.9 The Schwarzschild Solution

The Einstein field equations are way too complicated to solve by using general solutions. The reason is a large number of functions (10), four independent variables which are reduced by choosing a proper coordinate frame and coordinate system, and by making different assumptions regarding the spacetime symmetries of the solution and matter tensor which is relevant enough.

The simplest case was considered by Karl Schwarzschild in 1916 [18]. He considered vacuum that is $T^{ab} = 0$ and spherical symmetry. $T^{ab} = 0$ means that there is no matter, stress, or energy in the area under discussion but there is matter present everywhere else. Only the gravitational effects are considered, without providing energy. Consider a point mass m at the origin with spherical symmetry and static spacetime. The charge and angular momentum are zero. A general metric that is spherically symmetric can be written as given in ref. [17]

In spherical polar coordinates, the non-static metric will be

$$ds^2 = e^{\nu(t,r)}c^2dt^2 - e^{\lambda(t,r)}dr^2 - R^2(t,r)d\Omega^2, \tag{1.58}$$

where R, ν, and λ are the arbitrary functions. If the metric is static then

$$ds^2 = e^{\nu(r)}c^2dt^2 - e^{\lambda(r)}dr^2 - R^2(r)d\Omega^2, \tag{1.59}$$

where $d\Omega^2 = d\theta^2 + \sin^2\theta d\phi^2$. If R^2 is a varying function, the metric will be

$$ds^2 = e^{\nu(r)}c^2dt^2 - e^{\lambda(r)}dr^2 - r^2d\Omega^2, \tag{1.60}$$

where $d\Omega^2$ is the solid angle and $R^2(r)d\Omega^2$ is the area subtending solid angle at the center. The christoffel symbols are given as

$$\Gamma^0_{0\ 1} = \frac{1}{2}\nu',\ \Gamma^1_{0\ 0} = \frac{1}{2}\nu' e^{\nu-\lambda},\ \Gamma^2_{1\ 2} = \frac{1}{r} = \Gamma^3_{1\ 3},\ \Gamma^2_{3\ 3} = -\sin\theta\cos\theta, \tag{1.61}$$

$$\Gamma^1_{1\ 1} = \frac{1}{2}\lambda',\ \Gamma^1_{2\ 2} = -re^{-\lambda},\ \Gamma^1_{3\ 3} = -r\sin^2\theta e^{-\lambda},\ \Gamma^3_{2\ 3} = \cot\theta. \tag{1.62}$$

The vacuum solution of the Einstein field equations give

$$R_{ab} = 0. \tag{1.63}$$

So we have

$$R_{00} = \nu'' + \frac{1}{2\nu'}(\nu' - \lambda' + \frac{2\nu'}{r}) = 0, \tag{1.64}$$

$$R_{11} = -\nu'' - \frac{1}{2\nu'}(\nu' - \lambda' - \frac{2\lambda'}{r}) = 0, \tag{1.65}$$

$$R_{22} = 1 - e^{-\lambda} + \frac{1}{2r}(\lambda' - \nu')e^{-\lambda'} = 0, \tag{1.66}$$

$$R_{33} = R_{22}\sin^2\theta = 0. \tag{1.67}$$

Add R_{00} and R_{11}

$$\nu' + \lambda' = 0. \tag{1.68}$$

Integrating the above equation

$$\nu(r) + \lambda(r) = constant. \tag{1.69}$$

Absorb the constant in units of measurement of time as

$$\nu(r) = -\lambda(r). \tag{1.70}$$

Put the value of $\nu(r)$ in R_{22}

$$(-re^{-\lambda})' + 1 = 0. \tag{1.71}$$

Integrate the above equation and divide by "r"

$$e^{-\lambda(r)} = e^{\nu(r)} = 1 + \frac{\alpha}{r}, \tag{1.72}$$

$$ds^2 = c^2(1 + \frac{\alpha}{r})dt^2 - dr^2(1 + \frac{\alpha}{r})^{-1} - r^2 d\Omega^2, \tag{1.73}$$

with $\alpha = -\frac{2GM}{c^2}$.

$$e^{\nu(r)} = 1 - \frac{2GM}{c^2 r}, \qquad e^{\lambda(r)} = (1 - \frac{2GM}{c^2 r})^{-1}, \tag{1.74}$$

$$ds^2 = c^2(1 - \frac{2GM}{c^2 r})dt^2 - (1 - \frac{2GM}{c^2 r})^{-1}dr^2 - r^2 d\Omega^2. \tag{1.75}$$

This is the *Schwarzschild solution* of the Einstein field equations.

1.9.1 Schwarzschild Interior Solution

After the exterior solution, Karl Schwarzschild presented the interior solution of the field equations. Consider a non-rotating sphere of isotropic perfect fluid at the center, with zero pressure at the surface and $p(r)$ otherwise, density $\rho(r)$, and radius a. The metric is spherically symmetric and static from equation 1.60 as given in ref. [18]. For $r > a$ also applied for $r = a$, we have

$$p = \rho = 0. \tag{1.76}$$

The stress energy tensor will be

$$T_a^b = [\rho(r) + \frac{p(r)}{c^2}]u^b u_a - \delta_a^b \frac{p(r)}{c^2}, \tag{1.77}$$

where $\sigma_j^i = \delta_j^i \frac{p(r)}{c^2}$ is the stress tensor. From the energy conservation

$$T_{a;b}^b = 0. \tag{1.78}$$

Solving this we get

$$\frac{1}{2}\left[\rho(r)c^2 + p(r)\right]\nu'(r) + p'(r) = 0. \tag{1.79}$$

The *Schwarzschild interior solution* is written as [18]

$$ds^2 = \left[\sqrt{1 - \frac{2GM}{c^2 a}}(1 + A) - \sqrt{1 - \frac{2GMr^2}{c^2 a^3}}\right]^2 c^2 dt^2 - \frac{dr^2}{1 - \frac{r^2}{p^2}} - r^2 d\Omega^2, \tag{1.80}$$

where

$$e^{\nu(r)} = \left[\sqrt{1 - \frac{2GM}{c^2 a}}(1 + A) - \sqrt{1 - \frac{2GMr^2}{c^2 a^3}}\right]^2, \tag{1.81}$$

$$e^{\lambda(r)} = 1 - \frac{8\pi G\rho_0 a^2}{3c^2}. \tag{1.82}$$

A is determined by certain physical considerations.

1.10 Black Holes

The General Theory of Relativity tells about the existence of *black holes* [21,22]. They were first proposed by John Michell in 1783 calling them "*dark stars*". The word black hole was first used by John Wheeler. Classically, an object whose escape velocity is greater than or equal to the speed of light at the surface is called a black hole. Such objects are dark, invisible, and due to gravitational attraction they pull things inside. The *escape velocity* is

$$\nu_{esc} = \sqrt{\frac{2GM}{r}}. \tag{1.83}$$

The boundary of a black hole is called the *event horizon*. To escape the event horizon, velocity must be greater than the speed of light which means it is impossible to escape a black hole, trapped in forever. There is a singularity at the center of a black hole, it is infinitely dense with zero volume which means that all of its mass is concentrated in space with infinite gravity. All the laws of Physics including General Relativity fail there. Whatever gets too close, gets rip into its elementary particles. Light being the fastest of all cannot escape from this, that is why they are all dark. The distance from the center of a black hole to its boundary that is the event horizon is called the *Schwarzschild radius* which is given by

$$r_s = \frac{2GM}{c^2}, \tag{1.84}$$

where G is the gravitational constant, M is the mass of a black hole, and c is the speed of light. Black holes are discussed in detail in chapter 3.

Chapter 2

Cosmology and Dark Matter

Cosmology is the study of the Universe which includes how it came into being, its structure, changes occurring with time after the Big Bang, evolution with time, and future, with every phase full of mysteries yet to be unveiled. A commonly accepted idea is that the Universe came into being with the Big Bang, about ∼13.8 billion years ago from a single point where everything was concentrated. The Universe for scientists, many years ago, included the Sun and a few planets including our Earth. With time, our knowledge of the Cosmos expanded to the other stars, galaxies, and clusters of galaxies full of mysterious objects. We will start looking into Cosmology when Einstein applied General Relativity to it in 1917 in his paper.

2.1 Cosmological Principle

The principle of Cosmology can be stated as:
"The Universe looks the same to the observers everywhere".

The Universe is said to be isotropic, this observation may not be exactly correct but is approximately correct. *Isotropic* means that looking far away as a whole, the Universe looks almost the same in every direction. If it is isotropic then we can say, it is homogeneous. *Homogeneous* means moving away to the farther galaxies and looking back, we will see the same Universe as we see from here. There are about 10^{12} galaxies in the observable Universe and each galaxy has about 10^{11} stars. If these galaxies are uniformly distributed then we see the same Universe in every direction we look, also it looks the same from place to place. This is what we call the *cosmological principle* [23].

2.2 Einstein's Static Universe

Einstein applied his Theory of General Relativity to Cosmology [24] in 1917. When he applied his equations to the Universe, he found that it was stretching and contracting but assumed that it was static. He also assumed that the Universe has a uniform distribution of matter everywhere and the density is constant. As a result, the Einstein field equations reduced to two equations: the first one says that the curvature of spacetime is proportional to density which means, the more the density the more will be the curvature, the other one shows that the density is zero which is not possible. So to overcome this problem, Einstein modified his field equations by adding a constant of integration "Λ" which is called the *cosmological constant*, it gave an outward push to the effects of gravity. Now the density became proportional to Λ and the result was a *Static Universe* [25, 26], we have

$$\varepsilon^{\mu\nu} - \Lambda g^{\mu\nu} = \kappa T^{\mu\nu}, \tag{2.1}$$

$$R^{\mu\nu} - \frac{1}{2} R g^{\mu\nu} - \Lambda g^{\mu\nu} = \kappa T^{\mu\nu}. \tag{2.2}$$

The Einstein equations can also be written as

$$R^{\mu\nu} = \kappa \left[T^{\mu\nu} - \frac{1}{2} T g^{\mu\nu} \right] - \Lambda g^{\mu\nu}. \tag{2.3}$$

The cosmological constant then becomes

$$\Lambda \propto \frac{1}{R^2}. \tag{2.4}$$

So the general *Einstein Universe model* is given as

$$ds^2 = c^2 dt^2 - \frac{dr^2}{1 - r^2/R^2} - r^2 d\Omega^2, \tag{2.5}$$

where $e^{-\lambda} = C - \Lambda r^2$. For the Einstein Universe model $r = 0$ and $C = 1$. Galaxies are electrically neutral, so the only force acting is the gravitational force which is essential at large enough scales. If a galaxy is considered somewhere in the Universe, an equal amount of matter is present in every direction, if there was an excess of matter in one direction, it would accelerate towards that direction. This shows that the Universe might be static but this is not true.

2.3 Hubble's Law

In 1929, Edwin Hubble observed at the Mount Wilson observatory that the Universe is expanding [23]. He found the red-shift of galaxies, which means that they are moving away from us. To better understand this, consider a grid as a coordinate system. The distance between two lattice points on the grid is considered to be proportional to $d\chi$, such that the grid points pass through the same galaxies. In other words, if the galaxies move away or closer to each other the grid moves along with them. So the distance will be

$$dr = a(t)d\chi, \tag{2.6}$$

where 'a' is the scale factor, it may or may not be a constant. Consider that it is time-dependent. If it is a constant then the distance between two galaxies will remain constant with time. The relative velocity between two galaxies will be a time derivative of the distance.

$$dv = \dot{a}(t)d\chi, \tag{2.7}$$

where $\dot{a} = \frac{da(t)}{dt}$ and $d\chi$ remains the same because galaxies are frozen in the grid. The velocity-distance ratio is given as

$$\frac{dv}{dr} = \frac{\dot{a}(t)d\chi}{a(t)d\chi}, \tag{2.8}$$

$$v = \frac{\dot{a}(t)}{a(t)}r. \tag{2.9}$$

This shows that the ratio does not depend on the fact that which galaxies are considered. It could be any pair of galaxies regardless of how far or close they are.

$$\frac{\dot{a}(t)}{a(t)} = H(t), \tag{2.10}$$

where '$H(t)$' is *Hubble's constant.*

$$v = Hr. \tag{2.11}$$

This is called *Hubble's law.*

2.4 The Friedmann Equations

In 1922 Alexander Friedmann gave a solution to the Einstein field equations showing that the expanding Universe, homogeneity, and isotropy are the basic assumptions of the Friedmann Universe model. The following equation gives the model, given in ref. [23]

$$ds^2 = c^2dt^2 - a^2(t)\ [d\chi^2 + f^2(\chi)d\Omega^2], \tag{2.12}$$

where $d\Omega^2 = d\theta^2 + \sin^2\theta d\phi^2$. κ stands for the curvature, if $\kappa = 1, f(\chi) = \sin(\chi)$ it is the *positively curved space* or *spherical space*, if $\kappa = 0, f(\chi) = \chi$ this is called the *flat space*, and if $\kappa = -1, f(\chi) = \sinh(\chi)$ it represents the *negatively curved space* or *hyperbolic space*. The metric is called the *Friedmann-Lemaitre-Robertson-Walker* or *FLRW metric* which is an exact solution of the Einstein field equations [17, 23].

If Einstein's field equations are linked to Cosmology, all the matter and energy in the Universe become way too complicated to solve the equations. So a possibility is considered to assume the density to be constant everywhere and in every direction. Consider that $a(t)$ is a separation between two galaxies, the equations reduce to two equations, one is called the *Friedmann acceleration equation*, given as

$$\frac{\ddot{a}}{a} = -\frac{4\pi G}{3}\left(\rho + \frac{3P}{c^2}\right) + \frac{\Lambda c^2}{3}, \tag{2.13}$$

where G is the gravitational constant, c is the speed of light, ρ is the energy density of matter and if the Universe has matter it is non zero, P is the pressure of that matter and is considered to be zero, $a(t)$ is the scale factor which gives the rate at which the spacetime evolves, $\ddot{a}(t)$ is the acceleration term, this shows that the equation depends on density that is why it holds for every galaxy no matter where it is. The equation is a differential equation telling how a changes with time. So it can be seen that it is impossible to have a static Universe unless the Universe has no matter that is $\rho = 0$, if so $\dot{a} = \ddot{a} = 0$. The static Einstein Universe is shown in fig. 2.1

So this shows that the Universe is not static. The other equation is

$$\left(\frac{\dot{a}}{a}\right)^2 = \frac{8\pi G\rho}{3} - \frac{\kappa c^2}{a^2} + \frac{\Lambda c^2}{3}, \tag{2.14}$$

where $\left(\frac{\dot{a}}{a}\right)^2$ is the *Hubble parameter*. This is the *Friedmann equation*. In Cosmology, the relation between pressure and density is known as the *equation of state* which is given as

$$P = w\rho c^2, \tag{2.15}$$

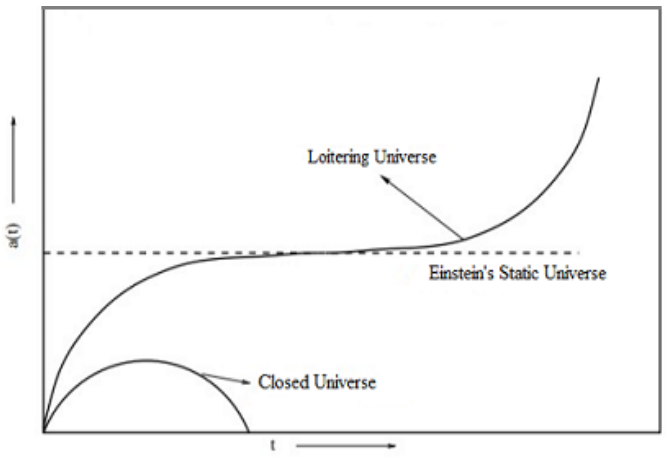

Figure 2.1: A spacetime plot of the static Einstein Universe model along with the other types of the Universe models are shown, with time along the x-axis and scale factor along y-axis. According to the static Einstein Universe theory, $\dot{a} = \ddot{a} = 0$ which means that the scale factor must be constant [1].

where 'w' is a constant. This gives the solution for scale factor as

$$a(t) \propto t^{\frac{2}{3(w+1)}}. \tag{2.16}$$

To understand the expansion rate with respect to time, various models were studied like the *matter dominated model* for which $w = 0$, the expansion of the Universe is given as

$$a(t) \propto t^{2/3}. \tag{2.17}$$

For *radiation dominated model* $w = 1/3$, so the rate of expansion of the Universe will be

$$a(t) \propto t^{1/2}. \tag{2.18}$$

2.5 Friedmann Universe Models

Consider time $t = t(\eta)$ such that the *cosmic time* is converted into the *conformal time*

$$cdt = a(\eta)d\eta. \tag{2.19}$$

Integrating this, gives the proper time elapsed since the start of expansion of the Universe. The metric then becomes

$$ds^2 = a^2(\eta)[d\eta^2 - d\chi^2 - f^2(\chi)d\Omega^2]. \tag{2.20}$$

This gives the three *Friedmann models of the Universe* [23] depending on the values of κ. All the three models have a starting point but not necessarily an endpoint.

2.5.1 Open Friedmann Universe Model

The *open Friedmann Universe model* [23] starts from the Big Bang at $\eta = 0$, such that $a(0) = 0$ and goes on expanding, has no end. It has a curvature $\kappa = -1$ as shown in fig. 2.2, the metric for the open Universe will be

$$ds^2 = a^2(\eta)[d\eta^2 - d\chi^2 - \sinh^2(\chi)d\Omega^2]. \tag{2.21}$$

It corresponds to a *3-hyperboloid*.

2.5.2 Flat Friedmann Universe Model

The *flat Friedmann Universe model* from $\eta = 0$, such that $a(0) = 0$, represents the Universe expanding forever with no end [23]. It has a curvature $\kappa = 0$ shown in fig. 2.2, the metric for this Universe is given as

$$ds^2 = a^2(\eta)[d\eta^2 - d\chi^2 - \chi^2 d\Omega^2]. \tag{2.22}$$

It represents the geometry of a *3-cone*.

2.5.3 Closed Friedmann Universe Model

The *closed Friedmann Universe model* [23] has a starting time $\eta = 0$ and $a(0) = 0$ like the two other models at which the Big Bang happened. It has a curvature $\kappa = +1$ and then expands to a certain maximum size, then starts to shrink and finally collapses at $\eta = 2\pi$ that is the spacetime curves back into itself as shown in fig. 2.2. Such a model of the Universe has a finite lifetime unlike the two others given by the metric

$$ds^2 = a^2(\eta)[d\eta^2 - d\chi^2 - \sin^2(\chi)d\Omega^2]. \tag{2.23}$$

Its geometry corresponds to a *3-sphere*.

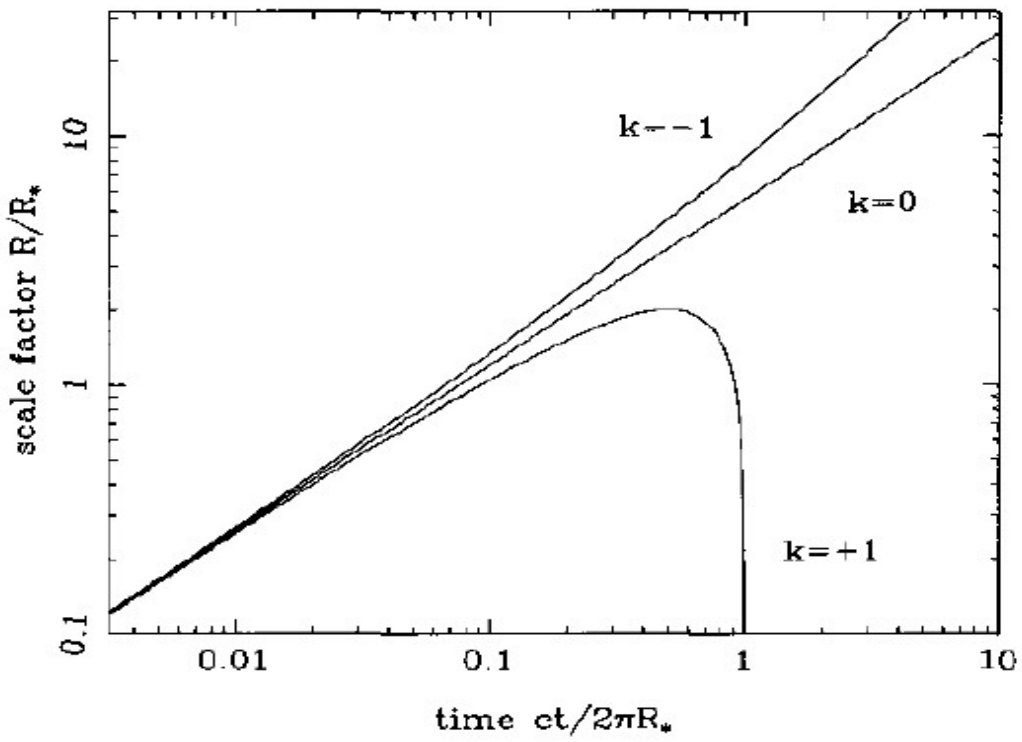

Figure 2.2: The first plot is for $\kappa = -1$, it is seen to expand continuously, representing the open Friedmann Universe model. The second plot is for $\kappa = 0$, expanding continuously, representing the flat Friedmann Universe model. The third plot is for $\kappa = +1$, initially expanding and then collapsing, it represents the open Friedmann Universe model [2]

.

2.6 The Big Bang

The *Big Bang* is a model of the Universe that describes how it began, expanded from a singularity of extremely high density and temperature at which the laws of Physics no longer hold, and inflated for about 13.8 billion years which is considered as the age of the Universe [23]. The Big Bang was not an explosion it was just the space expanding with time. The theory is in favor of Hubble's law that is the greater the distance of a galaxy, the faster it moves away from the Earth. There is absolutely no instrument to look back at the birth time of the Universe, the only sources of information are Mathematics, models, and the cosmic microwave background. After the very beginning when the Universe cooled a little, subatomic particles were formed, resulting in the formation of atoms and then hydrogen, helium, and traces of lithium were formed. Then gravity resulted in the formation of stars and galaxies. After the Big Bang, there were different stages in which the Universe evolved. Initially, the radiation density was greater than the matter density which means that it was a radiation-dominated era but with the expansion, many years after, the Universe became matter-dominated. Astronomers observed some gravitational effects of the dark matter and they found out that the accelerating expansion of the Universe is probably due to the dark energy [27, 28].

2.7 Chronology of the Universe

The *chronology of the Universe* consists of 5 stages in which the Universe expanded and evolved over about 13.8 billion years and is still evolving.

1. The very early Universe (all the epochs took place)
2. The early Universe, a period from 1 second after the Big Bang
3. The dark ages
4. The present Universe
5. The future Universe

2.7.1 The Radiation Era

In the time from 0 to 10^{-43} seconds of the expansion, the temperature of the Universe was approximately 10^{40} K, the four forces namely the gravitational force, strong nuclear force, weak nuclear force, and electromagnetic force, all were unified as a super force. There was no matter present at that time, only energy was there, this was the *Planck epoch* [23]. At the end of this epoch, the gravitational force separated from the other forces. At about 10^{-43} seconds, the *grand unification epoch* took place, now the three forces were left unified excluding gravity, and the temperature was about 10^{36} K, too hot that no particles were created. At the end of this epoch, the strong nuclear force separated, leaving behind the two forces unified. At about 10^{-37} seconds, when the temperature was about 10^{33} K, the Universe expanded exponentially, and then the temperature fell rapidly, this is called the *inflationary epoch*, this epoch ended at about 10^{-32} seconds. At approximately 10^{-36} seconds, when the temperature was approximately 10^{20} K, the *electroweak epoch* occurred, in which the weak nuclear force separated from the electromagnetic force. When the temperature was suitable enough, the quark-gluon plasma formed along with the other elementary particles. The next stage is the *quark epoch* at approximately 10^{-12} seconds, and the temperature was about 10^{15} K, still too dense and hot for the quarks to combine, there was the quark-gluon plasma. It is assumed that the *baryogenesis* may have taken place at about 10^{-11} seconds of the Big Bang making the baryons dominant to the anti-baryons. At about 10^{-5} seconds was the *hadron epoch*, and the temperature was approximately 10^{10} K, cold enough to combine the quarks to make hadrons that are protons and neutrons. By the end of the hadron epoch, majority of the hadrons and anti-hadrons annihilated with each other [23].

At about 1 second of the Big Bang was the *lepton epoch*, the Universe cooled down to 10^{9} K but still not cool enough to make the electron-positron pairs. Neutrinos decoupled and stopped interacting with the baryonic matter forming the cosmic neutrino background. Before decoupling these neutrinos were in thermal equilibrium with protons, electrons, and neutrons. After about 10 seconds of the Big Bang was the *photon epoch*, the temperature was favorable for the electron-positron pairs to annihilate, and the Universe became dominated by photons. At about 100 seconds, atomic nuclei were created in the process of the Big Bang. These were the last stages of the *radiation era* in which after about 3 minutes of the

Big Bang, protons and neutrons fused to make different nuclei, creating helium, lithium, and deuterium. At about 20 minutes, nuclear fusion stopped because the Universe was not hot enough for this process [23].

2.7.2 The Matter Era

After about 47,000 years of the Big Bang, the Universe became *matter dominated* and after about 370,000 years, the *dark ages* started. Neutral atoms, mostly hydrogen and helium were formed by combining nuclei with electrons in the process of *recombination*, the Universe became transparent because photons were not in thermal equilibrium with the matter anymore, and the temperature was dropped to 3000 K. Atoms which were newly formed, released the photons by reaching their ground state, this is the *photon decoupling* [23]. These are the photons that are detected today as the cosmic microwave background. From about 10 to 17 million years, the temperature became $273\ K - 373\ K$, suitable for the liquid water. After about 200 million years, stars and galaxies started forming and with the years passing, they evolved into the clusters of galaxies and superclusters. The elements present today were formed in the cores of those stars. The *reionization* process started after about 250-500 million years till 1 billion years [23].

After about 1 billion years, the dark ages ended and from that until now the Universe has looked almost the same. After approximately 9.8 billion years, the slowly expanding Universe started to accelerate.

In the future, a time will come when there will be no new stars born and local galaxies will be left only in the observable Universe. There are different theories regarding the future prediction of the Universe and how it would end.

2.8 Cosmic Neutrino Background Radiation

The *Cosmic neutrino background* is a background radiation of the Universe which is composed of neutrinos. These radiations were produced after about 1 second of the Big Bang when they decoupled from the matter and the temperature was about $10^{10}\ K$. Initially, they were in thermal equilibrium with the electrons, protons, and neutrons. Today the approximate temperature of the cosmic neutrino background is $1.95\ K$. Neutrinos have a very low energy that is why it is very hard to detect them and the cosmic neutrino background has an energy about 10^{10} times smaller than the ordinary neutrinos, so practically it is hardly possible to detect them. The weakly interacting neutrinos are a source of information from the earlier Universe [23, 29].

2.9 Cosmic Microwave Background Radiation

The *cosmic microwave background* is a background electromagnetic radiation of the Universe which comes from the very early stage of the Universe after the Big Bang. It is an important data source leading back to the initial phase of the Universe. It was discovered by Arno Penzias and Robert Wilson in 1964 [23]. The radiation strictly followed Planck's black body radiation law which is

$$\epsilon(f)df = \frac{8\pi h}{c^3}\frac{f^3 df}{\exp(hf/k_B T_0) - 1}, \tag{2.24}$$

where k_B is the Boltzmann constant, h is Planck's constant. In the recombination process, when the neutral atoms were formed, electrons transitioned to the ground state by emitting photons, called the *photon decoupling*. These photons after decoupling from the matter freely moved through the space not interacting with matter, are a source of the cosmic microwave background radiation. Today they have an estimated temperature of about 2.7 K. These photons have been traveling through the space since decoupling, losing the energy with an increase in wavelength due to the expansion of space.

2.10 High Energy Physics

While studying Cosmology and Astrophysics, many phenomena could only be explained in terms of Particle Physics. Currently, out of many unsolved problems of Astrophysics, a major problem is the characterization of the dark matter and dark energy which relates High Energy Physics (HEP) to Astrophysics and Cosmology. High Energy Physics explores what the world is made of and how it works. So, we briefly discuss the fundamental constituents of matter of the Standard Model which is a well tested model so far. Furthermore, we study various candidates of dark matter which relate to beyond the Standard Model particles such as the sterile neutrinos, Weakly Interacting Massive Particles (WIMPs), Gravitationally Interacting Massive Particles (GIMPs), supersymmetric particles, etc. Matter consists of atoms, atoms have electrons and nuclei which consist of protons and neutrons. Each proton and neutron is made up of three quarks which are the up and down quarks (labeled as u and d). Quarks are never seen existing freely, they are seen in a group of three quarks together or in a pair of quark and anti-quark.

Particles can be of two types: elementary particles and composite particles. *Elementary particles* are further categorized as: elementary fermions and elementary bosons.

2.10.1 Fermions

Fermions can be of two types: elementary fermions and composite fermions [30]. Fermions are the particles following the Fermi-Dirac statistics and obeying Pauli's exclusion principle which means only one fermion can occupy a quantum state at one time. These particles are the spin half particles. Quarks, anti-quarks, leptons, and anti-leptons are the *elementary fermions* which are matter and anti-matter particles. *Quarks* have six flavors: up, down, top, bottom, strange, and charm quarks, interacting via strong interaction. Up, charm, and top quarks have a charge "2/3" and down, strange, and bottom quarks carry a charge "-1/3", their respective anti-particles have the same properties as the original particles except for the charge which is opposite. Electron, muon, tau, electron neutrino, muon neutrino, and tau neutrino are the *leptons* and they do not interact via strong interaction. Electron, muon, and tau have a charge "-1"and their anti-particles have a charge "+1". Electron neutrino, muon neutrino, tau neutrino, and their anti-neutrinos have a charge "0", they are neutral. Each fermion has an anti-particle making the total fundamental fermions "24". Quarks and leptons with the same electric charge have different masses.

2.10.2 Bosons

Bosons are categorized as: elementary bosons and composite bosons [30]. Bosons follow the Bose-Einstein statistics and do not obey Pauli's exclusion principle which means one or more bosons can occupy a quantum state at one time. These particles have an integer spin. *Elementary bosons* are further divided into gauge bosons or vector bosons whose spin is "1" and scalar bosons with a spin "0". Photons, Z bosons, and gluons with a charge "0" and W bosons with a charge "$\pm$1" are the *gauge bosons*. Higgs boson is a *scalar boson* with spin/charge "0". Bosons are the force carriers. *Mesons* are the composite bosons which are made up from a quark and anti-quark pair.

2.10.3 Hadrons

The composite particles based on quarks, forming heavier particles are called the *hadrons*. They interact via strong interaction. This includes mesons and baryons excluding the leptons, which do not interact via strong force. Hadrons are composed of quarks either as the quark-antiquark pairs called mesons or as three quarks called the baryons. Baryons are the *composite fermions* made up of three quarks and mesons are the *composite bosons* made of a quark and anti-quark pair. The two up quarks in a proton are not the same because fermions obey Pauli's exclusion principle, the six flavors of quarks are further divided into three colors each.

2.10.4 Baryons

Baryons are the composite fermions that are made of three quarks and experience the strong nuclear force. The most common baryons are protons and neutrons. *Protons* are made up of two up quarks and one down quark (uud) and *neutron* is made up of two down quarks and one up quark (ddu). Baryons make most of the visible matter of the Universe. For example when two down quarks and one up quark combine they make a neutron which is a baryon. There is another type of baryons which have pentaquarks called the *exotic baryons* with four quarks and one anti-quark. But this type of baryons has not yet been observed.

2.10.5 Neutrinos

Neutrinos were postulated by Pauli in the 1930s, when the astronomers were unable to figure out what was causing the violation of energy and momentum conservation in β-decay? It was hypothesized to be a ghostly particle that barely interacts with matter. Many years later Cowan and Reines set up a detector to detect neutrinos and they were able to catch a few, confirming the existence of neutrinos [30]. Neutrinos are the leptons that interact via weak force and gravity. They were first formed after just 1 second of the Big Bang and are also being produced during the nuclear fusion reactions inside the cores of stars, just like our Sun. They are electrically neutral and have a very small rest mass which was earlier considered as zero. Neutrinos pass through the normal matter without being detected.

Neutrinos are of three types: electron neutrino, tau neutrino, and muon neutrino. All the three neutrinos are left-handed and every neutrino has an anti-neutrino. Neutrinos can be detected by looking for their interactions with atomic nuclei in enormous amount of matter but still, it is very rare to catch a neutrino in the detector. When neutrinos travel through a distance they oscillate between their flavors, like electron neutrino becomes tau neutrino or muon neutrino, since anything cannot oscillate without having a mass so the astronomers came to a conclusion that the neutrinos have a mass. Their masses are not known exactly.

2.10.6 Sterile Neutrinos

Sterile neutrinos [31–34] are the hypothetical spin "1/2", electrically neutral particles that only interact via gravity. They do not interact via any of the interactions of the Standard Model, that is why they are called sterile neutrinos and this is how they are different from the other neutrinos. The other neutrinos are left-handed particles while sterile neutrinos are assumed to be right-handed particles. Their mass is still unknown and there is no direct evidence of the existence of such neutrinos. Massive sterile neutrinos are a possible candidate for the dark matter. Neutrinos have a property called the *helicity*, if the spin of moving particles is along their direction of motion then they have a *right-handed helicity* and if they have an opposite spin to the direction of motion then they have a *left-handed helicity*. The helicity of the observed neutrinos is always left-handed. It is predicted that

the right-handed neutrinos which have not been observed yet, would only interact with the matter gravitationally known as sterile neutrinos.

Sterile neutrinos are produced at a temperature higher than the decoupling temperature of the active neutrinos, $T_{dec} \sim 1\ MeV$. Therefore, for the masses in keV range, sterile neutrinos are born relativistic [35]. The dark matter having candidates with such properties is the warm dark matter. Heavy sterile neutrinos could be discovered by the radioactive decay because heavier particles decay into lighter particles over time, similarly, sterile neutrinos can decay into their lighter particles and emit x-ray photons. Data from the Chandra X-Ray Observatory was studied to discover these x-ray photons but no evidence was found.

2.11 Dark Energy

Dark energy [27,28] is a form of energy assumed to fill most of the space. It is considered to be responsible for the accelerated expansion of the Universe. Approximately 68 *percent* of the Universe is dark energy, 27 *percent* is the dark matter, and both are invisible, the rest is all normal matter. During the early 1990s, there were many views regarding the expansion of the Universe, like the Universe might stop expanding one day and recollapse because of the enough energy density, or it might always expand without stopping with so little energy density but gravity would definitely slow down the expansion. Contrary to this, the Universe was seen expanding at an accelerated rate in 1998 by the Hubble Space Telescope, observing a distant supernova, it was from a dying giant star. So, it was thought that there must be something causing the expansion. Different explanations were made, it was thought to be a result of Einstein's equations with a cosmological constant, or some kind of energy fluid filling the space was causing it, or the theory itself was wrong which was not explaining the expansion. Astronomers gave it the name 'dark energy' which was causing the expansion.

Dark energy cannot be seen, no one knows what it is and what is it composed of, just the effects have been observed on the other bodies. It acts as a counter gravity force which does not allow gravity to squeeze the Universe with all the matter it has. That is why it is considered that dark energy has characteristics similar to Einstein's cosmological constant. If the energy is a property of space then this means empty space has its own energy, now with the expansion, more energy appears, and this would result in the expansion. For the space having energy, the astronomers came up with another idea that according to the quantum theory of matter, space is full of virtual particles that are constantly being produced and then disappear. They calculated the value of energy but the results were so wrong.

It is also assumed that dark energy may be the fifth fundamental force called the *quintessence*, filling the space as a fluid. Whose effects are opposite to those of gravity. But still, nothing is known about it.

2.12 Baryonic Matter

Ordinary matter made of electrically charged particles radiate when it is accelerating or something collides with it and it can be seen and observed. It is called the *baryonic matter* or luminous matter, made up of baryons, like protons and neutrons but it also has electrons which are leptons. Baryonic matter is studied by the Fermi-Dirac statistics and obeys Pauli's exclusion principle. The stars, planets, humans, and all the things seen or touched are made up of baryonic matter, we observe it through the direct telescopic observations. Whatever we see or touch is about ~ 5 *percent* of the matter of this entire known Universe and the rest is just a mystery. Earlier, it was thought that the whole Universe was made up of ordinary matter, but later when different galaxies were studied, observations were made which showed that there were the other forms of matter that actually dominate the Universe with about ~ 95 *percent* which are the dark matter and dark energy.

2.13 Dark Matter

One of the most intriguing problems these days that has taken the attention of most of the astronomers is the existence of *dark matter*. It is not visible on the electromagnetic spectrum that is why called "dark matter". It does not radiate like the normal baryonic matter, that is why also known as non-luminous matter. Its nature and composition is not known yet. Dark matter does not interact with normal matter via any of the interactions of the Standard Model, its effects can be seen only through gravity on the visible matter. The idea of dark matter hit the astronomers when the standard Newtonian gravity was applied to the known baryonic components in different galaxies, and discrepancies were seen between the observations and predictions. More evidence came in with the observations on the formation and structure of the Universe, formation and rotation of galaxies and clusters of galaxies, cosmic microwave background, gravitational lensing, and the other phenomena.

Many attempts have been made to describe dark matter by presenting different cosmological models, like the cold dark matter (CDM) model and ΛCDM model. The ΛCDM model successfully explained the Universe at large scales, but it seemed to fail at small scales. Problems such as the lost satellites problem and the core-cusp discrepancy were seen. So, the warm dark matter (WDM) model was proposed that predicts a lower bound in the keV regime for the dark matter particles. According to the ΛCDM model, baryonic matter is just about 5 *percent* of the matter this Universe has. The rest is assumed to be dark matter and dark energy which are collectively about 95 *percent* for the large and diluted galaxies, and about 99.99 *percent* for the dwarf galaxies [36]. Most of the matter in galaxies is considered to be dark, present in large halos around the galaxies, there is also a component of it in the galactic disk. Different assumptions were made for the existence of dark matter. Initially, it was assumed that there is matter that is too faint to be detected, so baryonic matter was the only dark matter candidate at that time. This idea was changed in the 1980s, when Particle Physics was applied to Astrophysics, the outcome was that the dark matter was made up

of a subatomic particle which is not known yet. Many experiments are being conducted to detect these particles but are unsuccessful till date.

We will discuss baryonic and non-baryonic dark matter along with the evidence for dark matter in the following sections.

2.13.1 Baryonic Dark Matter

Dark matter is considered to be baryonic or non-baryonic [37–41]. The *baryonic dark matter* is composed of baryons, with many different suggestions regarding its existence. One idea is that it is an ordinary baryonic matter which was unable to form the large clouds that collapse to make stars and not enough mass for the fusion reaction, hence stayed dark. Such objects are called the *Massive Compact Halo Objects* or *MACHOs* like the neutron stars, brown dwarfs, black holes, and some planets but it only accounts for a small percentage of the dark matter. Observations show that the mean mass of MACHOs lies between $0.15M_{\odot} < M < 0.9M_{\odot}$, which means that it only gives 20 *percent* of the dark matter in a halo.

There is another suggestion by Asghar Qadir and Francesco De Paolis of cold diffuse clouds that are propped up by the cosmic microwave background, calling them *virial clouds*. These are the interstellar gas clouds at the cosmic microwave background temperature, stabilized by the radiation coming from the cosmic microwave background balancing the radiation it would emit due to the virial theorem. The prediction to test that has been confirmed.

2.13.2 Non-Baryonic Dark Matter

Dark matter is generally assumed to be *non-baryonic*, the possible candidates are axions, sterile neutrinos, WIMPs, GIMPs, and supersymmetric particles [37, 38, 42]. The Standard Model being the most authentic model does not give a particle that can describe its nature. It gives a stable, weakly interacting, and electrically neutral particle that is neutrino but it was observed to be not responsible for the dark matter. An assumption for finding the dark matter particles includes the extension of the Standard Model which is called the *supersymmetry (SUSY)* that is beyond the Standard Model. In the supersymmetry theory, there are the supersymmetric partners of particles from one of the two groups of particles: fermions and bosons. Every particle from one group has a superpartner from the other group like electron, graviton, and neutrino might have supersymmetric partners called selectron, gravitino, and sneutrino from the bosonic group, there is no evidence of such particles yet. Sterile neutrinos and neutralinos which have not yet been observed are also considered to be the dark matter candidates. *Neutralinos* are the lightest supersymmetric particles, assumed to be stable, and least massive among the family of supersymmetric partners. If neutralinos are neutral, they make a good dark matter candidate. To determine the nature of dark matter particles, many experiments are being performed, just like those at the Large Hadron Collider.

2.13.3 Evidence of Dark Matter

Galaxies in our Universe rotate with such high speeds that the gravity generated by their observable matter could not possibly hold them together or they would not have formed at the first place. Scientists think that something is giving these galaxies extra mass which generates the extra gravity that they needed for their formation process, or to stay together without drifting apart. This unusual and unknown matter was called the dark matter.

In 1932, Jan Oort predicted the dark matter when he was studying the motion of stars in the nearby galaxies, but his estimates for this matter were not reliable. In 1933, Fritz Zwicky studied the clusters of galaxies and he obtained the evidence of an unknown matter, while applying the virial theorem to the Coma Cluster. He estimated the mass of this unknown matter, it came out to be about 400 times more than the mass visually observed. Zwicky found out that the effects of gravity for such galaxies were small as compared to the faster orbits, so he concluded that there must be some invisible mass holding the clusters together. Though his calculations were not exactly correct but the observations were right.

In the 1970s, Vera Rubin and Kent Ford studied the rotation curves of the Andromeda galaxy. They extended their work to the other spiral galaxies and concluded that most of the galaxies should have about six times more mass than the visible mass. They studied the optical rotation curves using the radio telescopes, the HI rotation curves showed a different behavior than the normal expected *Keplerian behavior*. Further, when more sensitive instruments were used, the rotation curves were observed to be flat in the outer regions of galaxies. The arms of spiral galaxies rotate around their centers. Going from the center to the outer regions of these galaxies, mass density decreases. From *Kepler's law*, the rotation velocity must decrease with distance but the rotation curve is observed to be flat with increasing the distance. So it is concluded that a lot of invisible matter is present in the outer regions of galaxies.

Equating gravitational and centripetal force, we have

$$\frac{GM}{r^2} = \frac{v^2}{r}, \tag{2.25}$$

$$v^2 = \frac{GM}{r}. \tag{2.26}$$

So, the velocity is proportional to $1/\sqrt{r}$, which is Kepler's law. It means that an object away from the center should move slower because of less gravitational pull and the rotation curve should decline. But the observations show that the linear velocity is pretty much constant. The flat rotation curves were obtained with almost a constant circular velocity in the dark matter halo which indicated the existence of dark matter in galaxies. To account for this, it was assumed that there was more mass in the outer regions. So mass as a function of distance was considered, given as

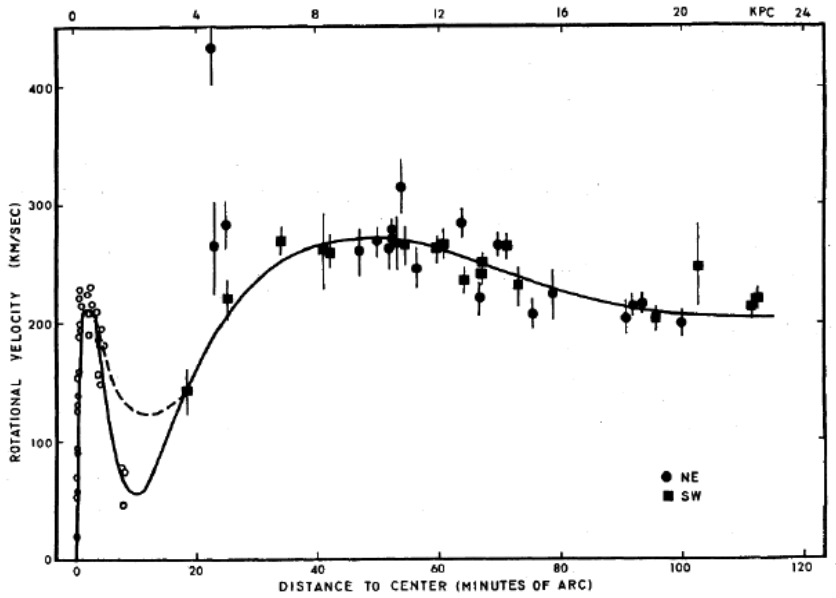

Figure 2.3: Rotational velocities of M31 [3] as a function of distance from the center showing flat behavior at large radii ($r > 20\ kpc$).

$$v^2 = \frac{GM(r)}{r}, \tag{2.27}$$

where $M(r)$ is the total mass within the distance r. If v is constant then

$$M(r) \propto r, \tag{2.28}$$

which tells that $M(r)$ increases almost linearly as we move away from the center to the outer boundary of the galaxy or beyond that.

Initially, it was thought that galaxies were made up of luminous matter and the mass of a galaxy gave the mass of luminous matter. In galaxies, large velocity dispersion was observed which indicated the presence of dark matter. Stars in the systems like elliptical galaxies, obey the virial theorem. The velocity distribution and virial theorem give the mass distribution in galaxies. The observed velocity dispersion in the elliptical galaxies does not match the predicted velocity dispersion. So it was seen that galaxies and clusters of galaxies do not behave gravitationally correct according to Newton's laws or the laws of Relativity [23]. Another way to predict dark matter was the *gravitational lensing*, which is the bending of light around a high concentration of dark matter. It was found that most of the luminous matter was present at the center of a galaxy [40], its outer parts moving under the influence of a central force was due to the central mass.

We do not know what the dark matter could be but we know that it cannot be baryonic beyond a very small amount because we know how much the total matter is and it is much

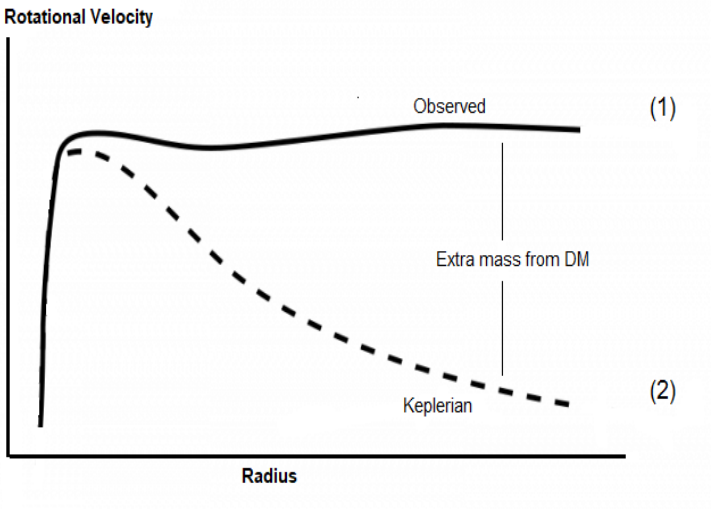

Figure 2.4: The galaxy rotation curves showing discrepancy between the observed and predicted curves, (1) shows the rotation curve of stars, which was obtained from the observations and (2) shows the predicted Keplerian rotation curve [4].

more than is allowed by the nucleosynthesis. One way to avoid it is by having a change in the law of gravity. The earliest attempt was with *modified Newtonian dynamics*, but we know that Newtonian dynamics does not work. So it was modified relativistically, Dr. Asghar Qadir worked on the *modified relativistic dynamics*. Otherwise, people normally look for supersymmetric particles and all evidence seem to be there are no supersymmetric particles and no supersymmetry. LHC does not show any supersymmetry, any signature of supersymmetric particle is missing. Expectations were that they should have already been observed at about 1 TeV, but they are now at about 14 TeV, still nothing observed. That is why Remo Ruffini, Carlos Argüelles, and Jorge Rueda went for degenerate fermionic cores which will be providing halo as well, that would be dark matter. They say that the core with mass above a certain scale gives a black hole. But there is no evidence of this. There must be some predictions made to check this, we will discuss that while concluding the thesis in future prospects.

Dark matter is divided into three categories based on the velocity of its particles rather than temperature as the names show:
1. Hot Dark Matter
2. Cold Dark Matter
3. Warm Dark Matter

2.13.4 Hot Dark Matter

Hot dark matter is assumed to be made up of light particles, like massive neutrinos with mass $\lesssim 1\ eV$ and speed close to the speed of light. They decouple very early in a relativistic environment. In the hot dark matter theory, it is considered that the largest structures were

made in the first place, and from them smaller structures emerged because of the relativistic velocities. Like from the superclusters our Milky Way was made, this structure is called the *top-down structure*. If this mystery gets solved, it would give the information of how the superclusters were formed after the Big Bang. Many solid arguments rule out the theory of hot dark matter [43].

2.13.5 Cold Dark Matter

Cold dark matter [44, 45] is hypothesized to be composed of heavy particles whose speed is less than the speed of light and masses $\gtrsim 2\ GeV$, they decouple non-relativistically. The possible candidates are axions, primordial black holes, and WIMPs [42]. The theory of cold dark matter was first presented in 1982, in which it is assumed that the smaller objects or structures collapse under their own gravity due to the non-relativistic velocities and then merge to make bigger structures, this structure is called the *bottom-up structure*. Predictions made by this theory almost agree with the Cosmology of structure formation in the Universe. There are issues with the predictions made by the cold dark matter theory and the observed data of galaxies like the cusp halo problem, missing satellites problem, and a few others. Many models have been presented to overcome the discrepancies.

2.13.6 Warm Dark Matter

Warm dark matter [46, 47] has characteristics of both, the hot dark matter and cold dark matter. Commonly accepted candidates for warm dark matter are the sterile neutrinos and gravitino, or the candidates with masses in the keV range. Predictions made for this type of dark matter are almost similar to those made for cold dark matter with lesser small-scale perturbations in the density. So, the predicted large number of dwarf galaxies is reduced and it leads to a very low dark matter density at the centers of large galaxies. The standard electroweak theory is the simplest model with a possible non-baryonic dark matter candidate, the right-handed or sterile neutrinos.

2.14 Degeneracy of Matter

If two or more eigenstates have the same energy eigenvalue, the system is said to be *degenerate* and if they have different energy eigenvalues then it is a *non-degenerate* system. The *degenerate matter* [48] is a fermionic matter in its extremely dense state and particles satisfy Pauli's exclusion principle. Like the dense stellar objects, where due to an extreme gravitational pressure the quantum mechanical effects become dominant. It is found in stars which are in the final evolution stages, like the white dwarfs and neutron stars where thermal pressure alone cannot avoid the gravitational collapse.

In the degenerate matter, from quantum mechanical view, particles in a finite volume may have discrete quantum states and Pauli's exclusion principle does not allow two fermions to occupy the same quantum state. When thermal energy is negligible, the lowest quantum states are filled. This is called a state of *full degeneracy*. If more particles are added, the volume is reduced, it will force the particles to move to higher quantum states even at low temperatures. Matter experiences thermal pressure and degenerate pressure. In degenerate matter, the degeneracy pressure is significant and the thermal pressure becomes negligible where the densities are extremely high and temperature has a negligible effect on the total pressure. Matter can become non-degenerate if there is an enormous increase in the temperature even without a decrease in density.

In a degenerate gas, quantum states are completely filled up to the Fermi energy. A fermion gas is called a *fully degenerate fermion gas* if all the quantum states below a given energy level are filled. The difference between this energy level and the lowest energy level is called the *Fermi energy*. Thermal pressure holds gravity from compressing the core of a star, if thermal pressure is not enough, atoms and electrons start getting closer and closer to each other but electrons cannot get closer than the quantum laws allow. If matter is compressed further, Pauli's exclusion principle generates the *degeneracy pressure* which is a counter pressure preventing the further compression of a star. Degeneracy pressure is not temperature dependent, like for normal matter, increasing the temperature increases the pressure. Further increase of pressure on the degenerate matter increases the speed of electrons but increasing the pressure to a certain point, electrons will approach the speed of light, at this point the degeneracy pressure no longer supports the pressure of matter and the core collapses. If the matter is dominant with electrons like in white dwarfs, the pressure comes from the electron degeneracy.

Chapter 3

Black Holes

Out of many bizarre objects floating around in the Universe, black holes are the incomparable ones, breaking down most of the laws of nature. They crush a huge amount of matter in a very small space making them extremely dense and compact objects. When a star reaches the end of its evolutionary life, it finally meets one of the three possible fates depending on its mass: if it is a very massive star, it ends up as a black hole, a mysterious yet fascinating object; if it is a less massive star then it ends up as a neutron star, and if it is a medium sized star like our Sun or still less massive, it becomes a white dwarf or brown dwarf. Before explaining what the black holes actually are, we look into the stars that black holes were once, not dark and dense as they are now. We will discuss different types of stars and the other two types of fates a star could possibly have if not ending up as a black hole [49–54].

3.1 Stars

From the Earth, many *stars* are seen twinkling in the sky at night. But looking closer, these stars are massive bodies with different colors, some are bright and some are faint. How bright a star is, depends mostly on its mass and age. Stars are born inside the *nebulae*, which are vast clouds of dust, hydrogen, and helium spread out everywhere. Nebula is either formed from the gas present in the interstellar medium, for example, the giant molecular cloud often called the *star nursery* which is a region of the new stars that are being born, or from the *supernova explosion* when a star dies, for example, the *planetary nebula*. With an increase in the size of a cloud, by feeding on the dust and gas from the surroundings, gravity increases and under the influence of this gravity, a cloud breaks into different clumps which flatten to form a disk.

There was no angular momentum at the time of the Big Bang. When the Universe became transparent the electrons were floating freely, the photons were then interacting with electrons, and the light was scattering back and forth. At that stage the electrons got pulled

into the hydrogen atoms, after which the Universe was mostly empty. The electrons got associated with the nuclei, got separated off, and there were large empty spaces, so the photons streamed through. This is the cosmic microwave background (CMB) radiation that we see. When this happened, the Universe was cool enough and there were sudden phase transitions. We are now able to get the photons coming through and they do not show any net angular momentum, so we say there was no angular momentum at that time. But where did it come from, if it was at the subatomic scales then there was no way to build it up into sizeable angular momentum. We can say that at the time when the Universe with uniformly distributed hydrogen and helium expanded, due to slight random density fluctuations in gravity, they caused extra density at some places and that caused gravitational collapse over there. With an increasing collapse, virial energy first gave out a temperature. After that, there were the stars which were about a thousand solar masses, when they started collapsing they became blue, burnt as blue giant stars, and then they exploded. This was a very fast process. If they would explode in a spherically symmetric form, then there would be just uniformly exploding all over. Now consider two such stars exploded, the ejectas from the two stars hit each other with one hitting the other from the above. For their common center of mass there would be a net impact parameter and an angular momentum, and the cloud would start rotating. The effects of gravity on the cloud would contract it, resulting in a decrease in the moment of inertia. So as to conserve the angular momentum, it would spin faster giving observable angular velocities. The rotating cloud has a very high temperature such that it collapses into a hot core forming a *protostar*. After this, when the temperature reaches about $10^7\ K$, the fusion reaction starts in the core fusing hydrogen into helium, and a young star is born. The leftover material from the disk forms planets, asteroids, etc. It takes millions of years for a star to form.

In less massive stars the fusion stops, not being able to fuse heavier elements. But in very massive stars, the fusion continues until it reaches iron, and then energy generation stops. When the fusion reaction stops, there is no energy left to inflate the star against gravity and its balanced state is disturbed. Gravity keeps on pushing the star inwards and compresses it.

Stars can be classified into different *spectral classes* based on the characteristics like frequency or the surface temperature. According to this, stars are divided into seven groups "OBAFGKM", ranging from the coolest stars to the hottest ones. Also the coolest stars are categorized as low mass stars and the hottest ones as high mass stars:

1. O group (the hottest normal stars), surface temperature $> 30,000\ K$
2. B group, surface temperature $\approx 10,000\ K - 30,000\ K$
3. A group, surface temperature $\approx 7500\ K - 10,000\ K$
4. F group, surface temperature $\approx 6000\ K - 7500\ K$
5. G group, surface temperature $\approx 6000\ K$
6. K group, surface temperature $\approx 5000\ K$
7. M group (the coolest stars), surface temperature $< 3500\ K$

These groups are subdivided into the groups with digits from 0 to 9, from the hottest to the coolest stars. Stars are also classified on the basis of light they emit, known as *luminosity*.

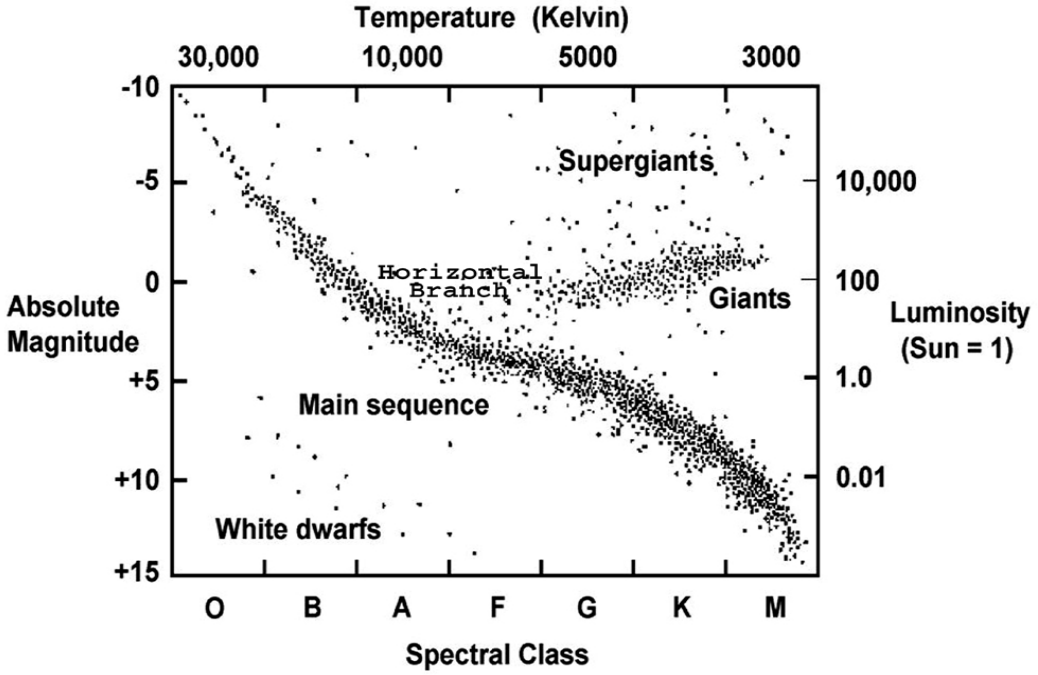

Figure 3.1: The Hertzsprung Russell diagram shows the detailed classification of stars on the basis of temperature, spectral classes, luminosity, and absolute magnitude.

These are called the *luminosity classes* represented by Roman numbers. Stars are also sorted out by colors from red to blue, the hotter stars are blue and the cooler stars are red, in between there are stars with orange and yellow colors. White stars are the hottest, like white dwarfs are the hottest stars with temperature about $100,000\ K$ but they are degenerate stars.

3.1.1 Stellar Structure

The *stellar structure* describes the internal structure of a star with the help of different models. Stars belonging to different classes have different internal structures, described by a set of equations. If the stellar structure is spherically symmetric and the star is in a steady state, we have a set of four first order differential equations which give mass, pressure, temperature, and luminosity that vary with radius, given by

$$\frac{dM}{dr} = 4\pi r^2 \rho, \tag{3.1}$$

where ρ is the density. This is known as the *equation of mass conservation.*

$$\frac{dP}{dr} = -\frac{GM\rho}{r^2}. \tag{3.2}$$

This is known as the *equation of hydrostatic equilibrium.* For a star in hydrostatic equilibrium, its gravity is balanced by pressure.

$$\frac{dL}{dr} = 4\pi r^2 \rho \epsilon, \tag{3.3}$$

where ϵ is the rate of energy generation per unit mass. Luminosity gives the energy that leaves the surface of a star. This is the stellar structure *equation for luminosity.*

$$\frac{dT}{dr} = -\frac{3\kappa\rho L}{16\pi acr^2 T^3}, \tag{3.4}$$

where κ is the coefficient of radiative opacity, a is the radiation constant whose value is $a = 4\sigma/c = 7.56 \times 10^{-16}\ Jm^{-3}K^{-4}$, and σ is the Stefan-Boltzmann constant whose value is $\sigma = 5.67 \times 10^{-8}\ Wm^{-2}K^{-4}$. This is the *equation of energy transport* through radiation which describes how energy is transported through different layers of a star. Heat is transported in three different ways: conduction, convection, and radiation. In stars energy is mostly transported through convection and radiation.

In order to solve these differential equations, the boundary conditions are given as: $M(r = 0) = 0$ and $L(r = 0) = 0$ and the surface boundary conditions are approximated as: $\rho(r = r_s) = 0$ and $T(r = r_s) = 0$. This set of equations has the space component at fixed time. To make the equations more convenient, we use mass as the space-like independent variable instead of r because in the lifetime of a star there is a significant change in its radius but the mass is relatively constant, we have

$$\frac{dr}{dM} = \frac{1}{4\pi r^2 \rho(r)}, \tag{3.5}$$

$$\frac{dP}{dM} = \frac{GM}{4\pi r^4} - \frac{1}{4\pi r^2}\frac{d^2 r}{dt^2}. \tag{3.6}$$

For pulsating stars, the force of gravity does not balance the pressure and we get an acceleration term. If the time derivative vanishes, we get the hydrostatic equilibrium equation.

$$\frac{dL}{dM} = \epsilon, \tag{3.7}$$

$$\frac{dT}{dM} = -\frac{3\kappa L}{64\pi^2 acr^4 T^3}. \tag{3.8}$$

If the time derivative vanishes, the star is in thermal equilibrium. These equations explain the evolution of a spherically symmetric star. The boundary conditions are: $r(M = 0) = 0$

and $L(M = 0) = 0$, at surface, $\rho = 0$ and $T = 0$. The energy of a star is due to the fusion reaction taking place inside it, depending on the mass of the star [55].

3.1.2 Main Sequence Stars

A star that does not have enough mass and temperature after its birth to start the fusion reaction to become a main sequence star is called the *brown dwarf*. The electron degeneracy pressure and gravity are in a balanced state, not letting hydrogen to start burning. Brown dwarf is a very faint star having mass less than about 8 *percent* of the mass of the Sun. It is quite difficult to spot the brown dwarfs because they are left with a very low residual luminosity, after the energy loss in about 10^8 years. Today they are being searched in the clusters of young stars but it is hard to differentiate between the young brown dwarf stars and very low mass stars. The stars with mass greater than 0.015 $M_\odot$ burn deuterium and those with mass greater than 0.065 $M_\odot$ burn lithium, the presence of deuterium and lithium identifies them as stars [56, 57].

The stars having enough mass and temperature more than 10^7 K start to fuse hydrogen into helium which takes place inside their cores. In the fusion reaction, hydrogen atoms fuse into helium and the other heavier elements releasing an enormous amount of energy. Gravity which pushes a core inwards to shrink is balanced by the energy released as a result of the fusion reaction, this is why a star shines. As long as the fusion continues, a star remains in its stable state. Most of the stars in the Universe like our Sun are *main-sequence stars*. These stars are of colors: blue, white, yellow, and red.

Blue stars are hot, very bright, and big with mass about 200 solar masses, known as the *blue dwarfs*. *Red dwarfs* have low luminosity, less than about one tenth of our Sun. They are cooler as compared to the blue dwarfs and have a small mass of about 0.1 $M_\odot$ with an extremely high density. These stars burn their fuel slowly, live for trillions of years and finally, become blue dwarfs. Then their cores collapse into white dwarfs without turning into the red giants. Most of the stars in our Galaxy are red dwarfs. *Yellow stars* are in between the red and blue stars, their size is about $80 - 100$ *percent* the size of our Sun, which is a yellow star. Their surface temperature is in between $5300 - 6000$ K. Nuclear fusion in such stars continues for about 10 billion years [58].

3.1.3 Red Giants and Red Supergiants

A star remains a main sequence star until all of its hydrogen is fused into helium. When it is left with just a small amount of hydrogen, the process of fusion speeds up, releasing a large amount of energy which results in expanding the outer layers of the star and shrinking its core. After that, the core is left with helium with no energy to balance the force of gravity, so gravity starts compressing the core and it heats up, if the star is big enough, helium starts fusing into carbon and oxygen. Outside the core, hydrogen is still available so it starts fusing in the shell outside the core. As a result the extremely hot core pushes the outer layers of the

star outwards, expanding the outer layers forming the star to be a *red giant* by increasing its size 100 times its original diameter. A main sequence star takes billions of years to fuse hydrogen into helium. Stars with mass $0.6 - 10\ M_{\odot}$ become red giants. On the HR diagram, they are seen at the right edge [58–60].

If a star is massive, it takes just a few million years to fuse hydrogen into helium and it becomes a *red supergiant* with a helium core. After this, helium starts fusing into carbon, it keeps on fusing into heavier elements until it reaches iron. The star cannot further fuse into heavier elements and the fusion stops.

3.1.4 Hypergiants and Supergiants

Hypergiant is a very rare star with an enormous mass of about more than 100 times the mass of our Sun. It has a surface temperature of more than about $30,000\ K$ with luminosity class $Ia0$ or Ia^{+}, at the top of the HR diagram. Hypergiants emit thousands of times more energy than our Sun and that is why they have short lifetimes.

Supergiant is also a star with huge mass but less than the mass of a hypergiant. It lies at the top of the HR diagram, just below the hypergiant. Supergiants belong to the class Ia and Ib with temperature up to $20,000\ K$. Similarly, there are bright giants with luminosity class II, they are in between the normal giants and supergiants [59, 60].

3.1.5 White Dwarfs

The fate of a star depends on its mass and majority of the stars in the observable Universe will become white dwarfs eventually. Very small stars, like the red dwarfs burn their fuel in trillions of years and finally turn into white dwarfs. Medium sized stars, like our Sun become red giants after the hydrogen fusion ends. During their red giant phase, they fuse helium into carbon and oxygen in their cores. If a star has not enough mass to carry on the fusion reaction, carbon and oxygen start building up in the core and the fusion stops. After this, the star sheds all of its outer layers in a planetary nebula and gravity shrinks the core to a size of our Earth. This is called a *white dwarf* [61–63]. Some white dwarfs are made up of carbon and oxygen, with masses in between about 8 and 10 $M_{\odot}$, the core temperature will be enough to fuse carbon, now the white dwarfs will be made up of oxygen and neon.

When there is no energy left to balance gravity after the fusion stopped, the electron degeneracy pressure comes in, not allowing gravity to further compress the core because of Pauli's exclusion principle. It makes the star extremely dense and the electron degeneracy pressure holds the core against gravity from further compressing it. The temperature reaches about $100,000\ K$, due to extreme heat inside it trapped, it glows. After billions of years, it cools down and stops glowing, hence becomes a *black dwarf* [51].

3.1.6 Neutron Stars

Massive stars which are about 8 to 20 times the mass of our Sun, things are different for them after the fusion stops. When a massive star becomes a red supergiant, it explodes in a supernova explosion, leaving behind a dense core. Since there is no fusion going on, gravity keeps on pressing the core so tightly that the electrons and protons combine, forming neutrons and neutrinos in the reaction, given by

$$p + e^{-} \longrightarrow n + \nu, \tag{3.9}$$

where the neutrinos scatter out in the space. The core is left with 90 *percent* neutrons packed together, there is a limit after which gravity cannot further squeeze the core. *Neutron stars* are the stars with mass about 1.4 times the mass of our Sun, squeezed to the size of a city, being such dense objects. In a neutron star, the core collapse is stopped by the neutron degeneracy pressure or by the repulsive nuclear forces, if the object is greater than about $0.7\ M_{\odot}$. If the mass of a star is about $1\ M_{\odot}$, it becomes a white dwarf. If the mass is increased to approximately $1.4\ M_{\odot}$, it becomes a neutron star. This limit is called the *Chandrasekhar limit*. The surface temperature of neutron stars is more than about $600,000\ K$.

Gravity on the surface of a neutron star is so strong which is approximately 2 billion times stronger than that on the Earth. Some neutron stars have extreme magnetic field, thousands of times more than the magnetic field of ordinary neutron stars which is about a trillion times that of the Earth's. Such objects are called the *magnetars*. A neutron star rotates in the space after it is formed, as the core is compressed its spinning speeds up to conserve the angular momentum. The spinning neutron star has pulses of radiations at regular intervals. That is why it is known as a *pulsar*. After many years, the pulsars stop spinning and become normal neutron stars after draining all the energy [64–66].

A neutron star is divided into the inner core, outer core, crust, envelope, and atmosphere. The envelope and atmosphere have a negligible mass but the former takes an essential part in the release and transportation of the thermal energy. The outermost layers are made up from the left over iron from the supernova explosion. These layers are squeezed together to form a crystal lattice, with electrons flowing through them. In the crust, neutrons start getting out of the nuclei at certain densities where the neutron chemical potential becomes zero making neutron fluid. Gravity squeezes nuclei closer with very few protons, as most merged to form neutrons. Reaching the lowest part of the crust, nuclei are tightly squeezed together such that they start touching and the dimensionality of matter changes. Neutrons rearrange from 3-dimensional structures to 2-dimensional long cylinders shaped like spaghetti and 1-dimensional lasagna, then to 2 and 3-dimensional structures known as nuclear pasta, beneath this is the core which is assumed to have the exotic particles in abundance.

Neutron stars may exist alone or in binary systems, they radiate energy as the gravitational waves. They come closer while orbiting and finally crash into each other in a kilonova explosion. This creates heavier nuclei than iron.

3.2 Black Holes

Black holes are such strange objects where the laws of Physics are seen violated inside them. The gravity of a black hole is so intense that anything including light once getting inside its boundary that is the event horizon, there is no way of escape. According to the General Theory of Relativity, when a star with mass M shrinks to a size less than $2GM/c^2$, it becomes a black hole. If a star is massive enough, it undergoes gravitational collapse forming a stellar-mass black hole. A stellar-mass black hole has a mass range of roughly 10-100 solar masses. Different compact objects are identified as black holes on the basis of their mass and on a limit, that is the maximum mass a neutron star can have before undergoing a gravitational collapse. If the mass of a neutron star is increased between 1.5 to 3 solar masses, it collapses into a black hole. This is known as the *Tolman-Oppenheimer-Volkoff limit*. There is a *Christodoulou-Fang-Ruffini* mass limit of 3.2 solar masses for a neutron star to become a black hole.

Black holes can be big called the supermassive black holes with weaker gravity or they can be small with stronger gravity, mostly found at the center of galaxies. Latest studies show that the mass of supermassive black holes ranges from a few million to a few billion solar masses. The most massive black hole known is ESO 444-46 with a mass of $\sim 7.8 \times 10^{10}\ M_\odot$. No matter what size a black hole is, it keeps growing by feeding on gas, dust, and other objects that lurk in its vicinity [51]. Some of the supermassive black holes are thought to have formed about 600 million years after the Big Bang, when the Universe was at its very early stage of formation. The oldest known black hole is in the quasar J0313-1806, with a mass of about $1.6 \times 10^9\ M_\odot$, formed about 670 million years after the Big Bang. There is no good explanation available for such black holes forming so soon via the normal channel of solar mass black holes coalescence, as there was not enough time. They are thought to have formed from the intermediate-mass black holes. The mass of intermediate-mass black holes is roughly between 100 and 100000 solar masses that is in between the stellar-mass black holes and the supermassive black holes. That is why they are known as the missing links between the supermassive and stellar-mass black holes. But many years of research has given a few evidence on such black holes, so a problem of the missing black holes in the intermediate mass range exists. This would explain the formation of supermassive black holes, formed shortly after the Big Bang.

Since the black holes do not reflect any light, they are completely dark, and cannot be seen directly. Their presence can be determined by seeing their interactions with the other matter or light present in their vicinity. The matter in the vicinity of a black hole falls into it, forming an accretion disk which can be observed. Their masses can be determined by looking into the orbits of the other stars orbiting the black holes. Also, when a black hole is in a binary system with some other star or a black hole, they merge and emit gravitational waves. Recently, LIGO (LASER Interferometer Gravitational Wave Observatory) directly detected the first ever gravitational waves produced by a black hole merger with two black holes of masses 36 $M_\odot$ and 29 $M_\odot$.

3.2.1 Outside a Black Hole

The gravitational field warps the space as well as time. In the vicinity of a black hole, gravity is so strong that an observer A who is watching a person B going inside a black hole from far away, would not see him fall into it quickly, A would see B approach the black hole, slow down until he reaches the event horizon, if this is crossed then there is no coming back. To observer A this is the point where the journey of B ended, he would seem frozen in the space, redder due to the gravitational red-shift, and then fade away. A would never see B crossing the event horizon but B would continue and pass the event horizon. When he hits the singularity no one knows what would happen, either he would completely disappear or may reappear somewhere else in the Universe through a *wormhole*. It is thought that a wormhole might be formed from a moving or spinning black hole.

The area, volume, and density of a black hole are given as

$$A = \frac{16\pi G^2 M^2}{c^4}, \tag{3.10}$$

$$V = \frac{32\pi G^3 M^3}{3c^6}, \tag{3.11}$$

$$\rho = \frac{3c^6}{32\pi G^3 M^2}. \tag{3.12}$$

At the surface of a black hole, the maximum tidal acceleration of an object is given as

$$A = \frac{2GMx}{r_s^3}, \tag{3.13}$$

where x is the length of the object and r_s is the Schwarzschild radius given in equation 1.84.

There is no way to directly measure the mass of a black hole but if a black hole has a company of another star both orbiting each other, then using the formula for the universal gravitation, their masses can be determined. It is computed by finding the distance between both the objects and orbital velocity using mathematics and instruments [51].

3.2.2 Inside a Black Hole

No one can tell what is inside a black hole because once getting in, there is no turning back. But there are a few ideas about what would happen there. If a person continues falling freely inside a black hole, he would feel being torn apart due to the tidal forces. Gravity becomes greater at his feet than his head, so the feet start falling faster than the head does. The tidal

forces become greater than the intermolecular forces that bind the body and a point comes when he is snapped into two pieces, which further feel the tidal forces, and the bifurcation keeps going on until he becomes a stream of atoms. It does not end here, the space that he occupied earlier was larger, while falling it gets narrower. So along with stretch, he gets squeezed, this is called the *Spaghettification*. Further, if there is any angular momentum involved, either in the black hole or the incoming object, it will get twisted up [51].

Theoretical black holes like the Schwarzschild black hole, Reissner-Nordstrom black hole, Kerr, and charged Kerr black hole are given next.

3.3 The Schwarzschild Black Hole

The Schwarzschild solution to the Einstein field equations has been already discussed which gave a vacuum solution to the field equations by explaining the gravitational field outside a sphere given by the equation 1.75. So the *Schwarzschild black hole* is a spherically symmetric and static black hole with a mass and no angular momentum and charge. Two Schwarzschild black holes can only be differentiated by mass. Such black holes are explained by the Schwarzschild metric given in equation 1.60. $r = r_s = \frac{2GM}{c^2}$ is the radius of a black hole called the *Schwarzschild radius*. It is called the *event horizon* of the Schwarzschild black hole [17].

The metric reduces to the Minkowski spacetime in the limit as $r \to \infty$. At $r = r_s$ there is a *coordinate singularity*, we have

$$g_{00} = 1 - \frac{2GM}{c^2 r} \to 0, \tag{3.14}$$

$$g_{11} = \frac{1}{1 - 2GM/c^2 r} \to \infty, \tag{3.15}$$

and we check the curvature invariance to see whether there is a *curvature singularity* or not. Also, we look for a *genuine singularity*, this singularity is where the curvature is infinite and where the curvature is infinite, acceleration becomes infinite. This is also called a *crushing singularity*. We consider the following invariants

$$R_1 = 0, \tag{3.16}$$

$$R_2 = \frac{48G^2M^2}{c^4 r^6}, \tag{3.17}$$

$$R_3 = \frac{64G^3M^3}{c^6r^6}. \tag{3.18}$$

At $r = r_s$ we have a coordinate singularity but no curvature singularity. At $r = 0$ there is a genuine singularity. Consider a radial geodesic

$$\nu^\alpha = (\nu^t, \nu^r, 0, 0), \tag{3.19}$$

$$\nu^\alpha\nu^\beta = 0 = e^\nu(\nu^t)^2 - e^{-\nu}(\nu^r)^2, \tag{3.20}$$

$$\frac{dr}{dt} = \frac{\frac{dr}{d\tau}}{\frac{dt}{d\tau}} = \frac{\nu^r}{\nu^t} = e^\nu = 1 - \frac{r_s}{r}. \tag{3.21}$$

At $r = r_s$, $\frac{dr}{dt} = 0$. This is a*null hypersurface*, *infinite red shift horizon*, *infinite time delay horizon*, and a *trapped surface*. To remove the singularities different coordinate systems are introduced for instance, Eddington-Finkelstein coordinates, Kruskal coordinates, Kruskal-Szekeres coordinates, and the others.

3.3.1 Carter-Penrose Diagram for Schwarzschild Black Hole

To avoid the singularity at $r = r_s$, consider a new space coordinate $dr' = \frac{dr}{1-r_s/r}$, we get the following metrices

$$ds^2 = 2(1 - r_s/r)du^2 + 2\sqrt{2}dudr - r^2d\Omega^2, \tag{3.22}$$

$$ds^2 = 2(1 - r_s/r)dv^2 - 2\sqrt{2}dvdr - r^2d\Omega^2, \tag{3.23}$$

where $u = \frac{1}{\sqrt{2}}(ct - r)$ is the *retarded time* and $v = \frac{1}{\sqrt{2}}(ct + r)$ is the *advanced time*. $u = \frac{1}{\sqrt{2}}(ct - \frac{dr}{1-r_s/r})$ and $v = \frac{1}{\sqrt{2}}(ct + \frac{dr}{1-r_s/r})$ are the *Eddington-Finkelstein coordinates*. The metric shows that $g_{00} = 0$ but the determinant is non zero. Writing them simultaneously, we have

$$ds^2 = 2(1 - r_s/r)dudv - r^2d\Omega^2. \tag{3.24}$$

This gives a singularity at $r = r_s$. To fix this, we have the following metric

$$ds^2 = \frac{4r_s^3}{\alpha^2 r}e^{-r/r_s}dudv - r^2d\Omega^2, \tag{3.25}$$

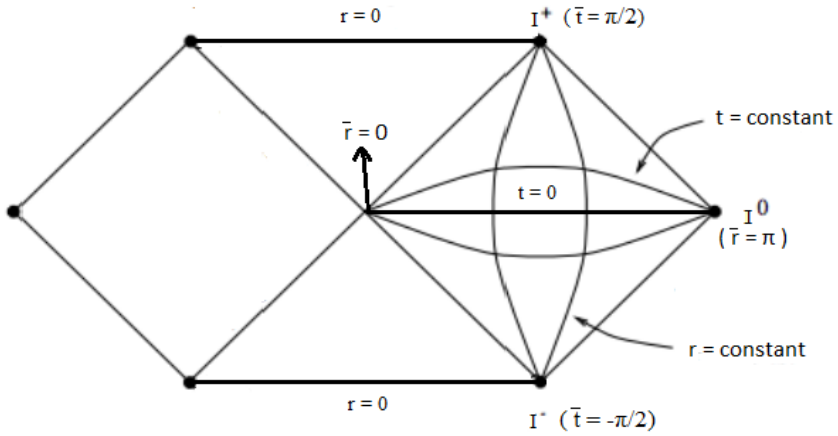

Figure 3.2: The Carter-Penrose diagram for compactified Schwarzschild black hole. The boundaries above and below are at $r = 0$. There is a past time-like and future time-like infinity on the top and bottom vertices, and the side vertex is space-like infinity. Compactified coordinates change the range to $-\pi/2$ to $+\pi/2$ and 0 to π.

where $U = -\alpha e^{-u/\beta}$, $V = \alpha e^{v/\beta}$, and $\alpha = 2r_s$, $\beta = \sqrt{2}r_s$. These are the *Kruskal coordinates*. At $r = r_s$ there is no singularity and the determinant is non zero. We have another coordinate system whose metric is given by

$$ds^2 = \frac{2r_s}{r}e^{-r/r_s}(dT^2 - dR^2) - r^2 d\Omega^2, \tag{3.26}$$

where $T = \frac{V-U}{\sqrt{2}}$, $R = \frac{V+U}{\sqrt{2}}$, and $T = \sqrt{2}|\frac{r}{r_s}-1|^{1/2}e^{r/2r_s}\sinh(\frac{t}{2r_s})$, $R = \sqrt{2}|\frac{r}{r_s}-1|^{1/2}e^{r/2r_s}\cosh(\frac{t}{2r_s})$. These are the *Kruskal-Szekeres coordinates* for which T goes from $-\infty$ to $+\infty$ and R from 0 to ∞. For more convenience, *compactified coordinates* are used in which $-\infty$ and $+\infty$ are mapped to $-\pi/2$ and $+\pi/2$ respectively, the metric will be

$$ds^2 = \frac{4r_s^3}{r\cos^2\bar{v}\cos^2\bar{u}}e^{-r/r_s}(d\bar{u}d\bar{v}) - r^2 d\Omega^2, \tag{3.27}$$

where $\bar{u} = \tan^{-1}U$ and $\bar{v} = \tan^{-1}V$. The metric is singular at r=0 [17].

3.4 Reissner-Nordstrom Black Hole

The Reissner-Nordstrom metric is a simple solution to the Einstein field equations determined by Reissner and Nordstrom, if a charge is there on the mass. *Reissner-Nordstrom black hole* is spherically symmetric and static, with mass M and a charge Q but no angular momentum. The Reissner-Nordstrom metric is given by

$$ds^2 = (1 + \frac{\alpha}{r} + \frac{GQ^2}{c^4 r^2})c^2 dt^2 - (1 + \frac{\alpha}{r} + \frac{GQ^2}{c^4 r^2})^{-1} dr^2 - r^2 d\Omega^2, \tag{3.28}$$

where

$$e^{\nu(r)} = 1 + \frac{\alpha}{r} + \frac{GQ^2}{c^4 r^2}, \qquad e^{\lambda(r)} = (1 + \frac{\alpha}{r} + \frac{GQ^2}{c^4 r^2})^{-1}, \tag{3.29}$$

where $\alpha = -\frac{2GM}{c^2}$. This metric has a singularity when

$$e^{\nu(r)} = 1 + \frac{\alpha}{r} + \frac{GQ^2}{c^4 r^2} \to \infty, \tag{3.30}$$

or

$$e^{\nu(r)} = 1 + \frac{\alpha}{r} + \frac{GQ^2}{c^4 r^2} \to 0. \tag{3.31}$$

This occurs at $r = 0$.

$$e^{\nu(r)} = (r^2 - \frac{2GMr}{c^2} + \frac{GQ^2}{c^4})/r^2, \tag{3.32}$$

$$r = r_\pm = \frac{GM}{c^2} \pm \sqrt{\frac{G^2M^2}{c^4} - \frac{GQ^2}{c^4}}. \tag{3.33}$$

At $Q^2 = GM^2$ and $0 < Q^2 < GM^2$, there are singularities. If $Q = 0$, the metric reduces to the Schwarzschild metric. $r = r_\pm$ are the coordinate singularities and $r = 0$ is an essential singularity [53].

Compactified coordinates for Reissner-Nordstrom black hole are $(\bar{u}, \bar{v})$, $U = \tan \bar{u}$, and $V = \tan \bar{v}$. Here we need two coordinates patches with $-\pi/2 < \bar{u_1}, \bar{v_1} < \pi/2$ for $(r_- < r < \infty)$ and $-\pi/2 < \bar{u_2}, \bar{v_2} < \pi/2$ for $(0 < r < r_+)$. The Carter-Penrose diagram is given as

In equation 3.32, if $Q^2 > GM^2$ then

$$1 - \frac{2GM}{c^2 r} + \frac{GQ^2}{c^4 r^2} > 0. \tag{3.34}$$

No event horizon, hence there is a *naked singularity*. In General Relativity, any singularity occurring naturally must possess an event horizon around it. This is known as the *cosmic censorship conjecture*. It is also assumed that the naked singularities might exist, that are the

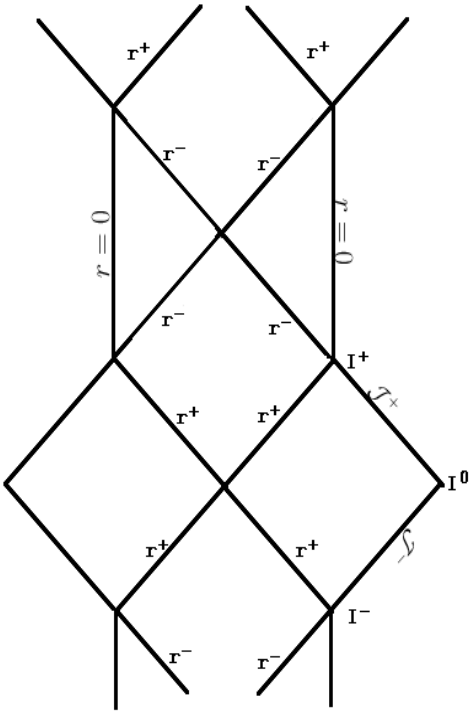

Figure 3.3: The Carter-Penrose diagram for compactified Reissner-Nordstrom black hole. There is a past time-like infinity, future time-like infinity, and space-like infinity. The singularity is time-like.

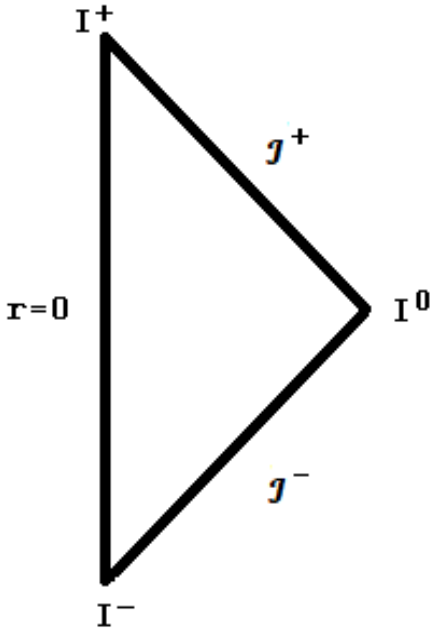

Figure 3.4: The Carter-Penrose diagram for Reissner-Nordstrom naked singularity for $Q^2 > GM$. There is a time-like singularity.

singularities without an event horizon, or in an alternative case both would be present [49]. The Carter-Penrose diagram for the naked singularity is given in fig. 3.4

3.5 The Kerr and Charged Kerr Black Hole

The Kerr metric is a solution obtained by Roy Patrick Kerr for a rotating and an uncharged *Kerr black hole* with mass M and angular momentum, given by the metric [17]

$$\begin{aligned} ds^2 &= \left(1 - \frac{2GMr}{\rho^2 c^2}\right) c^2 dt^2 - \frac{\rho^2}{\Delta} dr^2 - \rho^2 d\theta^2 \\ &- \left[(r^2 + \frac{a^2}{c^2}) \sin^2\theta + \frac{2GMra^2 \sin^4\theta}{\rho^2 c^2}\right] d\phi^2 + \frac{2GMra \sin^2\theta}{\rho^2 c^2} dt d\phi, \end{aligned} \tag{3.35}$$

where $a = \frac{L}{m}$ and L is the angular momentum.

$$\rho^2 = r^2 + \frac{a^2 \cos^2\theta}{c^2}, \tag{3.36}$$

$$\Delta = r^2 - \frac{2GMr}{c^2} + \frac{a^2}{c^2}. \tag{3.37}$$

The *charged Kerr black hole* or *Kerr-Newmann black hole* is given by the metric

$$\begin{aligned} ds^2 &= \left[1 - \frac{\left(\frac{2GMr}{c^2} - \frac{GQ^2}{c^4}\right)}{\rho^2}\right] c^2 dt^2 - \frac{\rho^2}{\Delta} dr^2 - \rho^2 d\theta^2 \\ &- \left[\left(r^2 + \frac{a^2}{c^2}\right) \sin^2\theta + \frac{2GMra^2 \sin^2\theta}{\rho^2 c^4}\right] d\phi^2 + \frac{2GMra \sin^2\theta}{\rho c^2} dt d\phi, \end{aligned} \tag{3.38}$$

where ρ^2 is the same as in equation 3.36 and Δ is given as

$$\Delta = r^2 - \frac{2GMr}{c^2} + \frac{a^2}{c^2} + \frac{GQ^2}{c^4}. \tag{3.39}$$

This metric explains that due to the angular momentum of a rotating body, inertial frames are dragged along with the rotation. The objects start rotating with the rotating mass, when they come closer due to the curvature of spacetime. For such black holes anything at a distance close enough, starts rotating with them, even light. Such a region is called an *ergosphere*. Roger Penrose and Roger Floyd showed that by sending a particle inside an ergosphere, the energy can be extracted from it. A particle breaks into two particles, one falls into the black hole and the other escapes. The one that escapes has a greater energy than the original particle, but classically energy cannot be extracted from the event horizon. So the rotational energy can be extracted from the ergosphere [17].

The charged Kerr metric gives the rotating and charged black holes 3.38. It is considered to be the most general and axisymmetric solution of the Einstein field equations which tells that a black hole can be completely described by mass, charge, and angular momentum. If two black holes have the same values for these properties, they are indistinguishable from one another. This is known as the *"no-hair theorem"* [51].

3.6 Types of Black Holes

With respect to mass, black holes are of three types:

1. Primordial black hole
2. Stellar-mass black hole
3. Intermediate-mass black hole
4. Supermassive black hole

3.6.1 Primordial Black Hole

Primordial black holes are hypothesized to have formed at the time of the Big Bang at the regions of high densities undergoing gravitational collapse, they have not yet been observed. The mass of primordial black holes is very less than the stellar-mass black holes, so they are not formed from the dying stars. They are also thought to be the candidates for dark matter belonging to a class of MACHOs. It is assumed that there might be millions of such black holes in the Universe, may be sooner or later one of them would come in the spotlight of observations by the astronomers [51].

3.6.2 Stellar-Mass Black Hole

Stellar-mass black holes are the most common of all the black holes, formed when the stars die due to the gravitational collapse. In the final evolutionary era of a red supergiant star, when all of the fuel of a star is fused into iron, and cannot be further fused into heavier elements, the fusion stops. Iron keeps on building up in the core and the balance between gravity and fusion energy is broken. Due to the increased pressure of gravity inwards, the star collapses in a supernova explosion. The result is a *stellar-mass black hole.*

A star with the size of our Sun ends as a white dwarf, if the mass of a white dwarf is increased, gravity gets stronger and the size gets smaller with an increased spin. At 1.39 solar masses, gravity becomes stronger, combining the electrons and protons making neutrons and neutrinos. This value is called the Chandrasekhar limit. Now the star ends as a neutron star. Further increasing the mass between 1.5 to 3 solar masses, gravity becomes even stronger and the star collapses into a black hole. This limit of mass is called the Tolman-Oppenheimer-Volkoff limit. Many stars observed in our Galaxy have mass greater than 1.5 solar masses, so many stars have ended up as black holes because the evolution time of massive stars is less than the age of the Universe. Their mass ranges from roughly 10-100 solar masses. Such black holes are small as compared to the other types, but very dense. The more a black hole is less in mass, the more deadly it is.

Black holes emit no light that is why they are not visible, so the stellar black holes are observed in close binary systems. In a closed binary system, when the matter from a star of such system transfers to the black hole, an enormous amount of energy is released which heats up the matter producing an accretion disk and X-rays are produced. The mass of the black hole can be observed by looking for the gravitational effects of that black hole on the companion star. Recently LIGO has detected the gravitational waves produced from a black hole merger [51].

3.6.3 Intermediate-Mass Black Hole

Intermediate-mass black holes have mass range in between the stellar and supermassive black holes, they are about 100-100000 solar masses. Such black holes are not formed by the gravitational collapse of stars because of being way more massive than the stellar black holes. The reason how they are formed is unknown. Two stellar black hole mergers could form an intermediate black hole or maybe it was formed at the time of the Big Bang, giving the problem of the missing black holes in the intermediate mass range. Another possibility is, smaller black holes feeding on gas and dust might grow into intermediate-mass black holes. It was considered that such black holes would be formed in a region where stars and gas are dense.

3.6.4 Supermassive Black Hole

The velocity dispersion of different stars in the areas near the centers of galaxies show that the expected characteristic velocity would vary as [50]

$$v^2 \sim \frac{GM}{r}. \tag{3.40}$$

If the central region of a galaxy has a mass domination due to a *supermassive black hole*, then it is assumed that going near to the center would increase the velocities of stars. This was found to be happening in many of the galaxies. So, by using the rate of increase of the velocity with radius, mass of the central part can be approximated with the mass of the bulge correlated. This shows that at the time of galaxy formation, half of the bulge mass might have collapsed at the center of the galaxy creating a supermassive black hole.

These monstrous black holes have masses equal to several millions even billions of Suns. Recent studies have shown that these black holes most likely reside at the centers of galaxies. Our Galaxy also has a supermassive black hole at its center. In the first place how were these giants formed is still not known because they are thought to have formed about 600 millions years after the Big Bang which is a very short time for the formation of such gigantic black holes. Maybe they were formed from the intermediate black holes right after the Big Bang or small black holes once formed, consuming gas and dust from the surroundings grew into bigger black holes. Another idea is the smaller black holes would have merged with the other black holes resulting in the bigger ones. Also, they might have formed when several stars collapsed all at once or the merger of galaxies may have formed such massive black holes, but nothing is known for certain. Some of the theoretical considerations include that these supermassive black holes might be a result of the gravitational collapse of fermion balls of massive neutrinos in the keV range which are supported by the degeneracy pressure. Tidal forces for supermassive black holes near the event horizon are weaker as compared to the smaller mass black holes. In a galaxy hosting a supermassive black hole, it plays a basic role in the distribution of stars, dust, and gas, playing a vital role in shaping a galaxy.

3.7 Galaxies

In the early Universe, huge clouds of gas and dust began to collect because of gravity, formed billions of stars which were gravitationally bound to one another making different *galaxies*. Other than stars, planets, dust, and gas, dark matter is also present in the galaxies. There are about 10^{12} galaxies in the observable Universe, these galaxies are further parts of clusters and superclusters. Our Galaxy Milky Way is in the *Local Group cluster* which is a part of the *Virgo supercluster*, it has about 100 billion stars. It has been observed that these galaxies have supermassive black holes at their centers. Some of these galaxies are surrounded by the accretion disks of gas and matter which fall into the black holes swirling around, making them the *quasars*. Galaxies have different sizes and shapes, some galaxies are dwarf galaxies with just 100 million or more stars and some are giant galaxies with billions of stars and even more.

While Vera Rubin was studying the galaxies, she discovered that our neighboring galaxy Andromeda was behaving strangely while rotating. She saw that the matter present at the outer edges of Andromeda, which was less concentrated as compared to the matter near the center, was moving as fast as the matter present at the center and there was a violation of Newton's and Kepler's laws. So she discovered that there is a huge dark matter halo.

Astronomers now know that the galaxies can change in the appearance over time which is because of the collisions, interactions, or mergers between the galaxies. In 1924, astronomer Edwin Hubble proved that the galaxies are distant objects with several billion stars bound together by gravity. So after a few years, he classified these galaxies into three categories: [67–69]

1. Elliptical galaxies
2. Spiral galaxies
3. Irregular galaxies
4. Lenticular galaxies

3.7.1 Elliptical Galaxies

Elliptical galaxies are spherical galaxies represented by the letter 'E'. They mostly contain the old population of stars formed in the very early Universe with very little gas and dust between these stars which are responsible for the star formation, so elliptical galaxies lack these ingredients of star formation. The formation of most of these galaxies is considered to be due to mergers of smaller galaxies or when the non-rotating gas collapses. These galaxies are further divided into different types depending on how spherical they are. For that, a number is added after E from 0 to 7, a completely spherical galaxy is E0 [68].

3.7.2 Spiral Galaxies

Spiral galaxy has a flat disk-like shape with its arms spiraling out from the center. It has a bulge at the galactic center with older stars that appear to be redder. It has a mixed ratio of the old and young stars with a lot of interstellar gas and dust in the disk, so new stars are created there. About 77 *percent* of the observed galaxies are spirals. Spiral galaxies are further divided into two types:

Regular spiral is denoted by the letter 'S' with arms that spiral inwards towards its center. Such galaxies are further divided into different types, depending on how tightly the spiral arms are wounded, like SA, SB, and SC. SA is the galaxy whose arms are very tightly wounded around the central bulge, SC with loose arms wounded around.

Barred spiral is denoted by 'SB', having a bar-like shape at the center, with the arms extending out. About 2/3 of all the spiral galaxies are barred, even our galaxy Milky Way is supposed to be a barred galaxy. Barred spirals are subdivided into SBA, SBB, SBC galaxies. These are the same as the types of regular spirals but with bar structure at the centers.

Both regular and barred spirals are defined by the spherical bulge of stars at their centers which is then surrounded by a thin rotating disk of stars containing spiral arms [68].

3.7.3 Irregular Galaxies

Any other galaxy that does not fit in the category of an elliptical or a spiral galaxy, is known as an *irregular galaxy*. Irregular galaxies lack a proper structure and are often very bright having young stars. When an elliptical or a spiral galaxy collides with another galaxy, both merge into a bigger galaxy with an irregular shape, becoming an irregular galaxy. It has no further subdivisions [68].

3.7.4 Lenticular Galaxies

Lenticular galaxy has a disc-like structure with a prominent bulge and disc but no spiral arms and very little dust, gas, and active star formation which are usually seen in the other types of galaxies. Because of the nearby spirals, it is assumed that these galaxies with time originated from them due to various reasons. Lenticular galaxies are represented by 'S0' and if they have bar then 'SB0' [68].

3.8 Components of a Galaxy

A galaxy is divided into many different components which are: a nucleus, central bulge, disc, spiral arms, and a massive halo. At the center of almost every galaxy is a supermassive black

hole. Our Milky Way has a supermassive black hole called *Sgr A**, its mass is estimated to be about $4 \times 10^6\ M_\odot$. A *central bulge* surrounds the black hole which consists of many stars, mostly the old ones that are tightly packed, also the bulge has less amount of gas and dust. *Disc* is a region around the bulge, it is a flattened region with mostly young stars along with some old stars, and more gas and dust is present as compared to the bulge. *Halo* is the largest part of a galaxy which contains a few stars and mostly the dark matter. Things are unclear about this component and its presence is understood by looking at the rotation curves of a galaxy.

Milky Way is a disk spiral galaxy with about 10^{11} stars, most of these stars are present in the thin disc moving in nearly circular orbits, disc is the most massive baryonic component of the Galaxy. Radius of the disc is about 10^4 *pc* and its mass is about $5 \times 10^{10}\ M_\odot$. Dust and gas clouds are also present there which are signs for the star formation, gas is mainly atomic and molecular hydrogen. Then there is a bar shaped bulge that contains old stars, it is smaller in size than the disc with radius about $1 - 2$ *kpc*, its mass is about $1.5 - 3 \times 10^{10}\ M_\odot$. At the center lies a supermassive black hole called the Sgr A* with mass approximately $4 \times 10^6\ M_\odot$. Then there is another component called the dark halo, it is the largest component whose composition is not known yet [68].

Chapter 4

The RAR Model

The structure of galaxies, their formation, components, especially the dark matter halos have always been a subject of curiosity for many astronomers. Problems regarding the nature, masses, and interactions of the dark matter particles are studied with deep interest these days. Initially, Newtonian gravity was applied to the baryonic components in different galaxies which showed a difference in the observations and predictions. These differences were understood when the rotation curves of different galaxies gave the idea of the existence of dark matter, abundantly present in the galactic halos. Thus a model named after the three scientists proposing it, the *Ruffini-Argüelles-Rueda* (*RAR*) *model* [5,13] was proposed with a set of equilibrium equations to explain the dark matter distribution in galaxies and the dark matter halos with central compact quantum cores by considering a self-gravitating system of massive fermions with certain fixed parameters.

4.1 Collisionless and Collisional Dynamics

When a physical process attains equilibrium after disturbances, erasing all the previous information of the initial conditions. This is known as the *relaxation process*. For a galactic halo, before it enters the steady state, the process of relaxation takes place. In the RAR paper [5]}, ignoring the previous relaxation process, quasi-relaxed state of a galactic halo is considered. The *Collisionless relaxation* (violent relaxation) is considered because it would give non-interacting dark matter in the halos [70], described by the Vlasov-Poisson equation for space and time variations in the gravitational potential. A collisionless system quasi-relaxes into a quasi-stationary state which can be explained in terms of the Fermi-Dirac distribution. In the dilute regime, the Fermi-Dirac distribution reduces to the Boltzmann distribution. There is another type of relaxation known as the *collisional relaxation* which gives stationary solutions, described by the Fokker-Planck equation, explained by the Maxwellian distribution [71,72]. The phase space distribution given in the AKRR paper [13] is obtained by considering the violent relaxation and evaporation (for cutoff).

4.2 The RAR Model

The dark matter distribution problem taken into account here is studied in terms of the *RAR model* [5]. This model is based on a system of self-gravitating massive fermions that include bare massive fermions known as "*inos*", the possible dark matter constituents. Initially, the fermions are assumed to be non-interacting (that is we do not assume weakly interacting particles), obeying quantum statistics. The model starts with specifying the phase space density and pressure of dark matter given by the Fermi-Dirac statistics. Then a set of equilibrium equations is given, these equations are to be solved numerically within the general relativistic limits with certain initial conditions for the core and boundary conditions for different types of galaxies for the halo. Also, in the model anti-fermions are not considered that is the temperature is considered to be $T \ll mc^2/k_B$. The *phase space density and pressure* of the fermion system with integration carried over the momentum space is given by [5]

$$\rho = \frac{gm}{h^3}\int_0^\infty f(p)\left[1+\frac{\epsilon(p)}{mc^2}\right]d^3p, \tag{4.1}$$

$$P = \frac{g}{3h^3}\int_0^\infty f(p)\left[1+\frac{\epsilon(p)}{mc^2}\right]^{-1}\left[1+\frac{\epsilon(p)}{2mc^2}\right]\epsilon d^3p, \tag{4.2}$$

where $g = 2s+1$ is the *spin multiplicity* of quantum states and for fermions $s = 1/2$, m is the mass of inos, h is the Planck constant, c is the speed of light, and $f(p)$ is the distribution function $f(p) = \frac{1}{\exp[(\epsilon-\mu)/k_BT]+1}$, ϵ is the kinetic energy of a particle which is $\epsilon = \sqrt{c^2p^2+m^2c^4} - mc^2$. μ is the chemical potential with the rest energy of particle subtracted off, k_B is the Boltzmann constant, T is the temperature. For a spherically symmetric metric

$$g_{\mu\nu} = diag(e^\nu, -e^\lambda, -r^2, -r^2\sin^2\Theta), \tag{4.3}$$

where ν and λ depend on the radial component r and Θ is the azimuthal angle, the *equilibrium equations* of the RAR model are

$$\frac{d\hat{M}}{d\hat{r}} = 4\pi\hat{r}^2\hat{\rho}, \tag{4.4}$$

$$\frac{dP}{dr} = \frac{(\frac{-G}{c^4})(p+\rho)(M+4\pi pr^3)}{r(r-2GM/c^2)}, \tag{4.5}$$

$$\frac{d\hat{\theta}}{d\hat{r}} = -\frac{1-\beta_0(\theta-\theta_0)}{\beta_0}\frac{\hat{M}+4\pi\hat{P}\hat{r}^3}{\hat{r}^2(1-2\hat{M}/\hat{r})}, \tag{4.6}$$

$$\frac{d\hat{\nu}}{d\hat{r}} = \frac{2(\hat{M} + 4\pi\hat{P}\hat{r}^3)}{\hat{r}^2(1 - 2\hat{M}/\hat{r})}, \tag{4.7}$$

$$\beta(r) = \beta_0 e^{\frac{\nu_0 - \nu(r)}{2}}. \tag{4.8}$$

For making the equations dimensionless, some *dimensionless quantities* are introduced, given as

$$\hat{\rho} = \frac{G\chi^2\rho}{c^2}, \quad \hat{P} = \frac{G\chi^2 P}{c^4}, \quad \hat{M} = \frac{GM}{c^2\chi}, \quad \hat{r} = \frac{r}{\chi}, \tag{4.9}$$

where $\chi = 2\pi^{3/2}(\hbar/mc)(m_p/m)$ and m_p the *Planck mass* is given as

$$m_p = \sqrt{\frac{\hbar c}{G}}. \tag{4.10}$$

The *thermodynamic equilibrium conditions of Tolman and Klein* are given as [73] [74]

$$e^{\nu/2}T = constant, \tag{4.11}$$

$$e^{\nu/2}(\mu + mc^2) = constant. \tag{4.12}$$

The two free RAR model parameters, the *temperature parameter* β and the *degeneracy parameter* θ are

$$\beta = \frac{k_B T}{mc^2} \qquad , \qquad \theta = \frac{\mu}{k_B T}. \tag{4.13}$$

By integrating this system of equilibrium equations for different values of m, θ_0, and β_0, variables like $M(r)$, $\theta(r)$, $\nu(r)$, $\beta(r)$ are obtained with the given *initial conditions* at $r = 0$ such that $M(0) = 0$, $\nu(0) = 0$, $\theta(0) = \theta_0$, $\beta(0) = \beta_0$ for core. The halo boundary conditions are given for different types of galaxies. The *boundary conditions* for spiral galaxies are

$$r_h = 25\ kpc, \quad M_h = 1.6 \times 10^{11}\ M_\odot, \quad v_h = 168\ km\ s^{-1}. \tag{4.14}$$

For big spiral galaxies, the boundary conditions are given as

$$r_h = 75\ kpc, \quad M_h = 2 \times 10^{12}\ M_\odot, \quad v_h = 345\ km\ s^{-1}. \tag{4.15}$$

For dwarf spheroidal galaxies the boundary conditions are

$$r_h = 0.6\ kpc, \quad M_h = 2 \times 10^7\ M_\odot, \quad v_h = 13\ km\ s^{-1}. \tag{4.16}$$

The galactic structures considered as a system of self-gravitating fermions in the classical regime and explained in terms of the Boltzmann distribution are not stable. The central degeneracy gives stabilization against the gravitational collapse and Pauli's exclusion principle stops the core from collapse just like the electron degeneracy in the white dwarfs and neutron degeneracy in the neutron stars [5].

4.2.1 Density Profiles

The *density profiles* and *degeneracy profiles* of the fermionic dark matter, plotted for different values of ino mass m, the degeneracy parameter θ_0, and the temperature parameter β_0 are shown in Fig.4.1a and 4.1b. The profiles show three different regimes: core, plateau, and halo. The first region is a *degenerate quantum core* of fermions with a constant density and positive degeneracy parameter such that $\theta_0 > 0$. The second region is the *transition region* for $r > r_c$, with a sharp decrease in the density followed by an extended plateau, the degeneracy parameter transitions from positive to negative values. The third region is the *classical Boltzmann regime* with $\rho \propto r^{-2}$ which gives the Newtonian isothermal sphere and the degeneracy parameter has negative values that is $\theta_0 \ll -1$ [5].

Some other models to describe the dark matter halos are: Navarro-Frenk-White (NFW), Einasto, Burkert, and non-singular isothermal sphere (NSIS). The *NFW model* describes the dark matter halos providing satisfactory results at large scales of the Universe but there are problems at the galactic scales. The NFW dark matter density profile shows a cuspy behavior through the center whereas the RAR model shows central cored structure, this would help in understanding the core-cusp discrepancy. In the inner region, density goes as $\rho \propto r^{-1}$ while in the halo part, density scales as $\rho \propto r^{-3}$. The density expression of this model is given as [6]

$$\rho_{NFW}(r) = \frac{\rho_0}{r/r_0(1 + r/r_0)^2}, \tag{4.17}$$

where ρ_0 is the central density and r_0 is the scale radius, both are the free parameters, such that $\rho(r_0) = \rho_0/4$. Another model to understand the distribution of matter in galaxies is the *Einasto model*, its density is given by

$$\rho_E(r) = \rho_{-2} \exp\left(\frac{-2}{n}\left[\left(\frac{r}{r_{-2}}\right)^n - 1\right]\right), \tag{4.18}$$

where ρ_{-2} is the density and r_{-2} is the radius at which $\rho(r) \propto r^{-2}$, and n is the Einasto index which determines the shape of the profile. It provides both cored and cusped distributions for different values of model parameters [7]. Another model is *Burkert model* whose density is defined as

$$\rho_{Bur}(r) = \frac{\rho_0}{[1 + (r/r_0)][1 + r/r_0]^2}, \tag{4.19}$$

where ρ_0 is the central density and r_0 is the scale radius. A dark matter density profile which gives the flatness of the rotation curves is represented by the *NSIS profile*

$$\rho(r) = \frac{\rho_0}{1 + (r/r_0)^2}, \tag{4.20}$$

where ρ_0 is the central density and r_0 is the scale radius.

In Fig.4.2 different profiles of density are plotted and combined together to see a visible difference between them. The RAR model density profile shows a cored behavior. The NFW dark matter density profile shows a cuspy core with an increasing density at small distances. The Einasto dark matter halo model shows both cusped and cored distributions [5].

4.2.2 Rotation Curves

The *circular velocity* is given by [5]

$$v = \sqrt{\frac{GM(r)}{r - 2GM(r)/c^2}}. \tag{4.21}$$

It is plotted as a function of r in fig. 4.3 for different values of m, θ_0, and β_0, giving the *rotation curve*. The *core radius* r_c is at the first maximum of the rotation curve. The second maximum of the rotation curve gives the *halo radius* r_h. The halo radius and mass here represent one-halo scalelength and mass. Just like the different regimes in density profiles and the degeneracy parameter profiles, there are also different regions in the rotation curves:

1. The first region is linearly increasing with the circular velocity $v \propto r$, it reaches the maximum when $r = r_c$, giving a degenerate core of almost constant density.

2. The second region is *Keplerian* where $v \propto r^{-1/2}$ and shows a transition from quantum degenerate to dilute region.

3. It then starts increasing with the circular velocity $v \propto r$ reaching a second maximum r_h, the halo size. This is also called one-halo scale length.

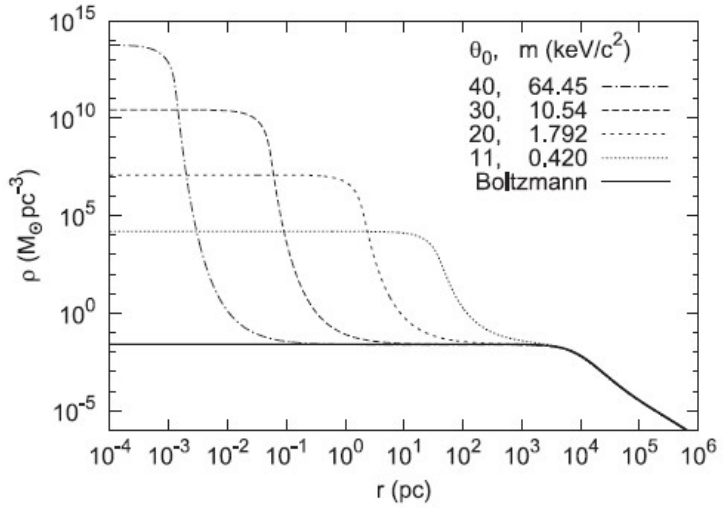

(a) Mass density

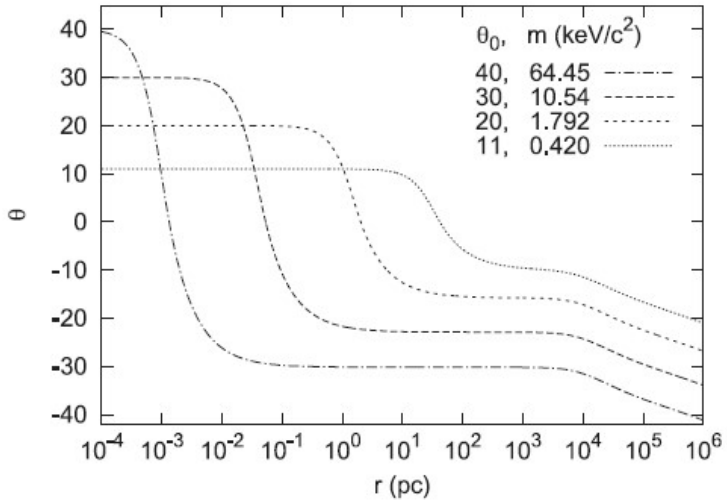

(b) Degeneracy parameter

Figure 4.1: Mass density and degeneracy parameter for different ino masses m, central degeneracy parameter θ_0, and temperature parameter β_0 from 10^{-4} pc to 10^6 pc. The plots clearly show three regimes: core, transition region, and halo. The density solutions for the RAR model are compared with the Boltzmannian profile. All the plots converge for $r \gtrsim r_h$ to the Boltzmannian distribution for any value of m and the model parameters. [5].

4. In the last regime, the solution becomes a Newtonian isothermal sphere with $\rho \sim r^{-2}$ which gives a flat rotation curve. For real systems, the flat area of the velocity curve cannot continue indefinitely, a cutoff in the momentum space is added which will be discussed later. For any value of θ_0, β_0, and corresponding m, the plots converge to the Boltzmannian isothermal distribution for $r \gtrsim r_h$.

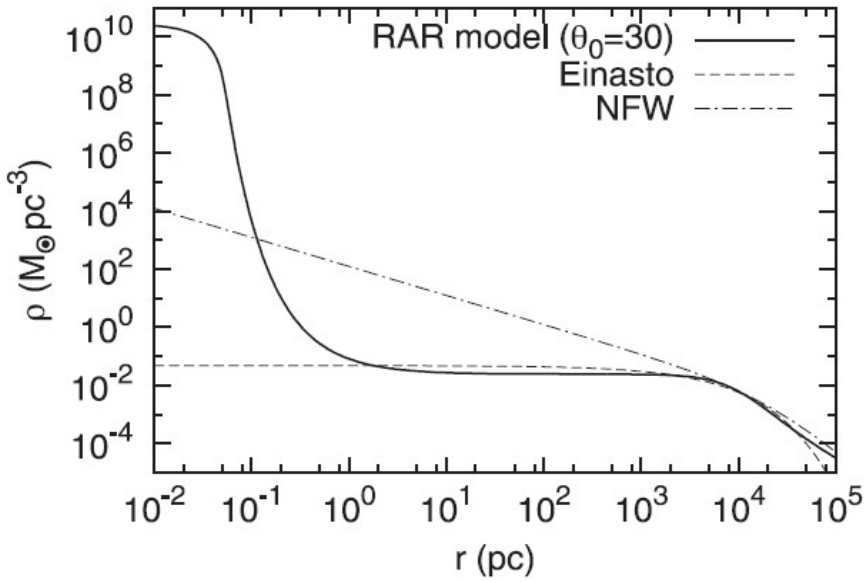

Figure 4.2: The RAR model density profile which shows cored behavior is compared with the cuspy NFW density profile [6] and cored Einasto profile showing a visible difference [7,8].

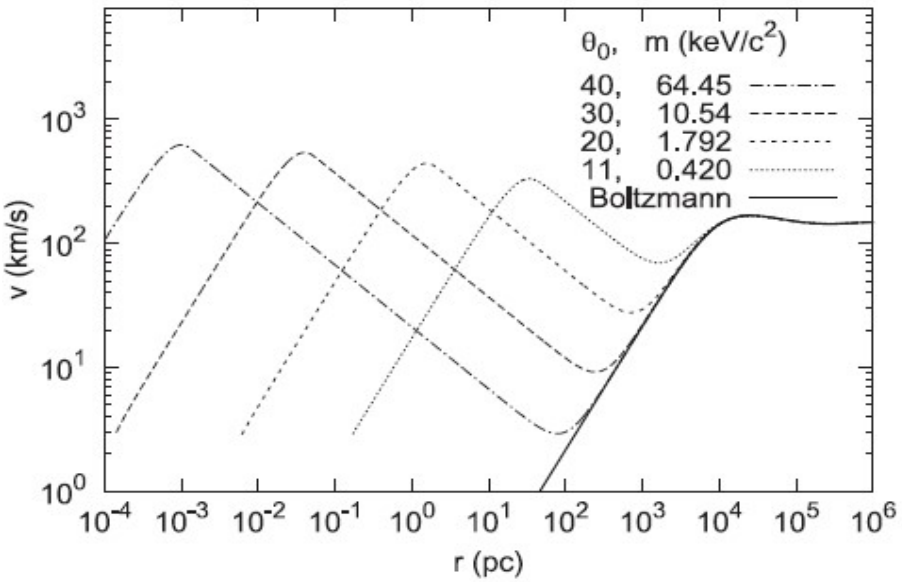

Figure 4.3: Rotation curves for different ino masses m and the model parameters from 10^{-4} pc to 10^6 pc. The rotation curves for the RAR model are compared with the Boltzmannian profile [5].

4.2.3 The Central Core

Observations show that the galaxies have a massive compact object at their centers which is thought to be a black hole. The RAR model predicts that the *central core* could be

compact enough to be a black hole, so for $m \sim 10\ keV/c^2$ a degenerate core with mass $M_c \sim 2.7 \times 10^6\ M_\odot$ is obtained as an alternative to the black hole Sgr A*, but r_c is greater by a factor of about $\sim 10^2$ than the radius obtained with the S2 star, it is the closest observed star to Sgr A*. It can also be seen that the core mass is strongly dependent on the ino mass whereas in the classical region, the Boltzmannian distribution is independent of m.

In spiral galaxies, for $m \sim 10\ keV/c^2$, the *compactness of the quantum core* is $\sim 10^{-6}$, so here Newtonian gravity can be used instead of the general relativistic approach because the solution of equilibrium equations in the former case gives the same results as the latter one. The *critical mass* value for the gravitational collapse is $M_{cr} \sim m_{Planck}^3/m^2$. Core masses of about $\sim 10^9\ M_\odot$ are observed in the active galactic nuclei. This value overcomes the critical mass value for the fermions in keV range and these cores have to be necessarily black holes. Then general relativistic effects are necessary with different boundary conditions as used here.

The central cores predicted in the RAR model are valid if the inter-particle mean distance is less than or equal to the thermal de-Broglie wavelength of the inos, that is $\lambda_B \gtrsim 3l_c$, $\lambda_B = h/\sqrt{2\pi mkT}$, and $l_c \sim n_c^{-1/3}$ where n_c is the core particle density. This shows that the less degenerate quantum cores have larger sizes.

In the model, phase space density is maximum at the center of the core, $Q_{max}^c \sim \rho_0^c m^{-4}\sigma_c^{-3}$ given by the Fermi-Dirac statistics and the maximum phase space density at the center of halo, $Q_{max}^h \sim \rho_0^h m^{-4}\sigma_h^{-3}$, where $\sigma_h = \sqrt{2/5}v_h$ is given by the Maxwellian distribution. Here all the quantum solutions satisfy the condition, $Q_{max}^c > Q_{max}^h$. For less degenerate quantum cores ($\theta_0 \approx 10$), the two limits become comparable

The RAR model, for the first time was able to link the dark central cores with the dark matter halos. For $m = 10\ keV/c^2$, the $M_c - M_h$ *correlation law* is

$$\frac{M_c}{10^6\ M_\odot} = 2.35 \left(\frac{M_h}{10^{11}\ M_\odot}\right)^{0.52}, \tag{4.22}$$

valid for the core masses $\sim [10^4, 10^7]\ M_\odot$ (corresponding to the dark matter halo masses $\sim [10^7, 10^{12}]\ M_\odot$) [5].

4.3 The RAR Model with Energy Cutoff

In the AKRR paper [13], a cutoff is added in the RAR model by introducing an *energy cutoff* parameter in the phase space distribution. This parameter gives a finite galaxy size and more compact solutions which give a core alternative to the central black hole. A *Fermi-Dirac distribution function* including an energy cutoff ϵ_c is considered here which is obtained by considering the effects of violent relaxation and evaporation as a quasi-stationary solution of the generalized Fokker-Planck equation for fermions. The fermionic equations of state are

given as

$$\rho = \frac{2m}{h^3}\int_0^{\epsilon_c} f_c(p)\left[1+\frac{\epsilon(p)}{mc^2}\right]d^3p, \tag{4.23}$$

$$P = \frac{2}{3h^3}\int_0^{\epsilon_c} f_c(p)\left[1+\frac{\epsilon(p)}{mc^2}\right]^{-1}\left[1+\frac{\epsilon(p)}{2mc^2}\right]\epsilon d^3p, \tag{4.24}$$

where $f_c(\epsilon \leq \epsilon_c) = \frac{1-e^{(\epsilon-\epsilon_c)/k_BT}}{e^{(\epsilon-\mu)/k_BT}+1}$ and $f_c(\epsilon > \epsilon_c) = 0$ is the distribution function with $\epsilon \leq \epsilon_c$. Along with the thermodynamic equilibrium conditions of Tolman and Klein we have another condition which is obtained from the energy conservation along a geodesic

$$e^{\nu/2}(\epsilon + mc^2) = constant. \tag{4.25}$$

This gives the *cutoff condition* as

$$(1 + W\beta) = e^{(\nu_b-\nu)/2}, \tag{4.26}$$

where $\nu_b = \nu(r_b)$ is the metric function at the boundary and r_b is the tidal radius. Also $\epsilon_c(r_b) = 0$, so $W(r_b) = 0$. In the classical limit $c \to \infty$, $e^{\nu/2} \approx 1 + \phi/c^2$, then the cutoff condition reduces to the escape velocity condition, where $V = m\phi$ such that $V(r_b) = 0$ and ϕ is the Newtonian gravitational potential. Along with the other equilibrium equations, an equation for the cutoff parameter is introduced with an initial condition $W(0) = W_0$ for core, given by [13]

$$W(r) = W_0 + \theta(r) - \theta_0. \tag{4.27}$$

The same dimensionless quantities are also introduced here as the original RAR model. In this paper a third parameter is introduced that is the *cutoff parameter* given by

$$W = \frac{\epsilon_c}{k_BT}. \tag{4.28}$$

In the limit $W \to \infty$, the system reduces to the original RAR model. The boundary conditions for the halo are

$$M = 2 \times 10^{11}\ M_\odot, \quad r = 40\ kpc, \tag{4.29}$$

$$M = 5 \times 10^{10}\ M_\odot, \quad r = 12\ kpc, \tag{4.30}$$

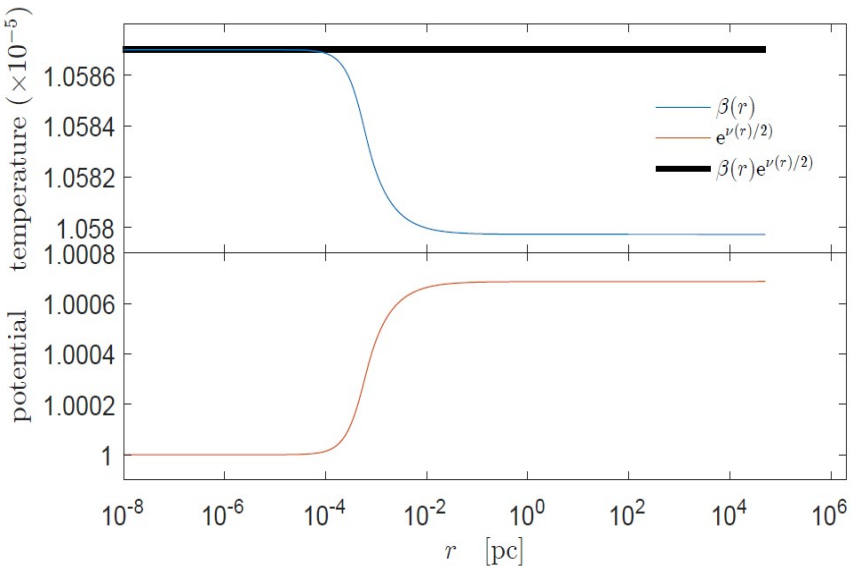

Figure 4.4: The upper graph shows the temperature parameter $\beta(r)$ changing with the radial distance and the lower graph shows the gravitational potential $e^{\nu/2}$. Comparing both the graphs, we see that the temperature is higher where the potential is deeper. Also, the gravitational red-shift temperature is plotted given in the black solid line.

$$M = 4 \times 10^6 \ M_\odot, \quad r = 6 \times 10^{-4} \ pc. \tag{4.31}$$

In this paper, first the three RAR model parameters are plotted as a function of r for $mc^2 = 48 \ keV$ in fig. 4.4 and 4.5, for the three parameters three different regimes are seen.

4.3.1 Density Profiles

The density profiles for the RAR model with the cutoff effects are plotted as a function of radial distance r, for different values of m along with the NFW density profile shown in fig.4.6. Three regimes are obtained: the degenerate quantum core with constant density and for which the degeneracy parameter has positive value, the transition region followed by an extended plateau in which the density decreases sharply and the degeneracy parameter transitions from positive to negative values, and the Boltzmannian regime with $\rho \propto r^{-n}$ where $n > 2$ because of including the energy cutoff. The cutoff conditions are applied to the outer halo by taking boundary radius $r_b = 50 \ kpc$ such that $\rho(r_b) = 10^{-5} \ M_\odot pc^{-3}$, then $W(r_b) \approx 0$. For $r \gtrsim r_b$ the exact condition $W(r) = 0$ is fulfilled giving $\rho(r) = 0$ [13].

Recently in the sixteenth Marcel-Grossmann meeting, it was discussed that the fermions of mass 56 keV, calling them the *darkinos*, give a compact quantum core with mass $\sim 3.6 \times 10^6 \ M_\odot$ giving a good approximation as an alternative to Sgr A* [75].

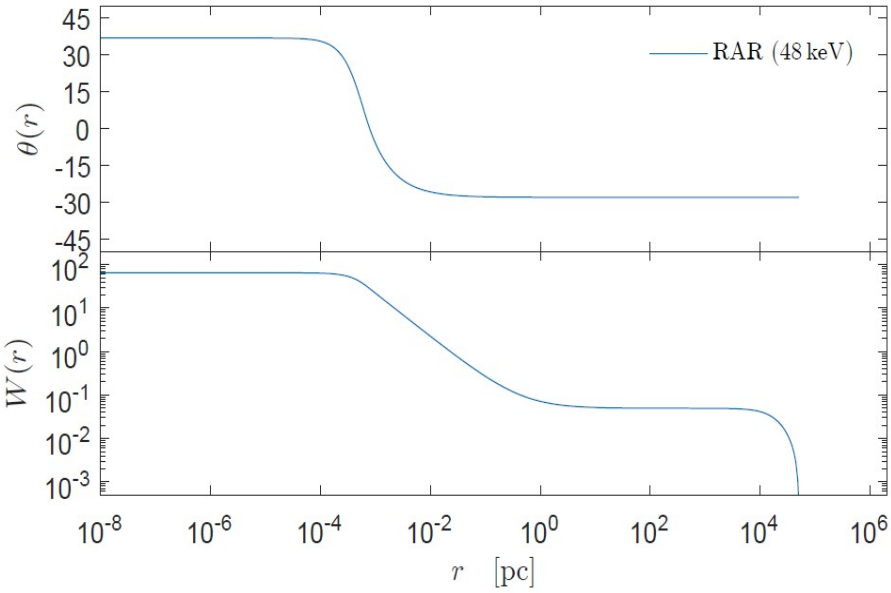

Figure 4.5: The upper graph is for the degeneracy parameter $\theta(r)$ changing with radial distance and the lower graph is for the cutoff parameter $W(r)$ changing with the radial distance.

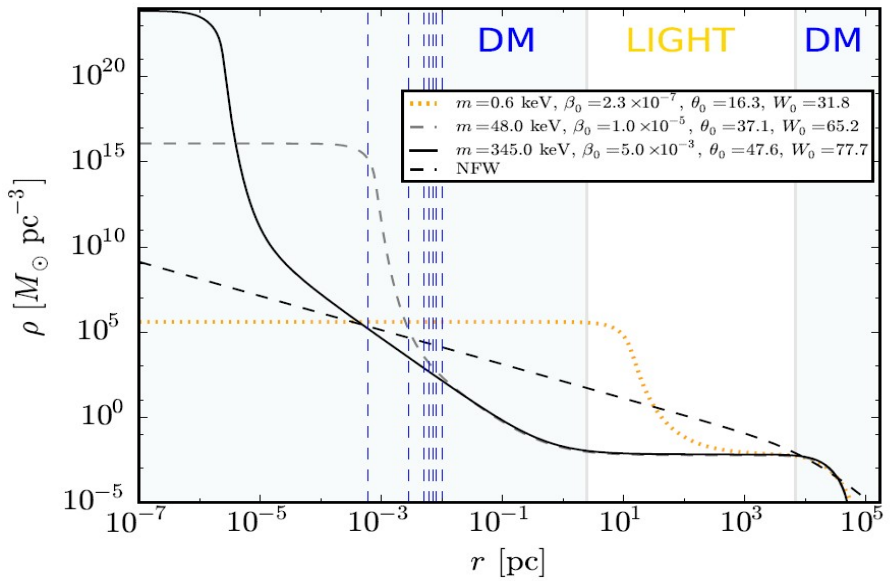

Figure 4.6: Density profiles for ino masses: 0.6 keV, 48 keV, and 345 keV with the corresponding model parameters, along with the NFW density profile in the given range. The dashed blue lines indicate the position of the S-cluster stars. [9]

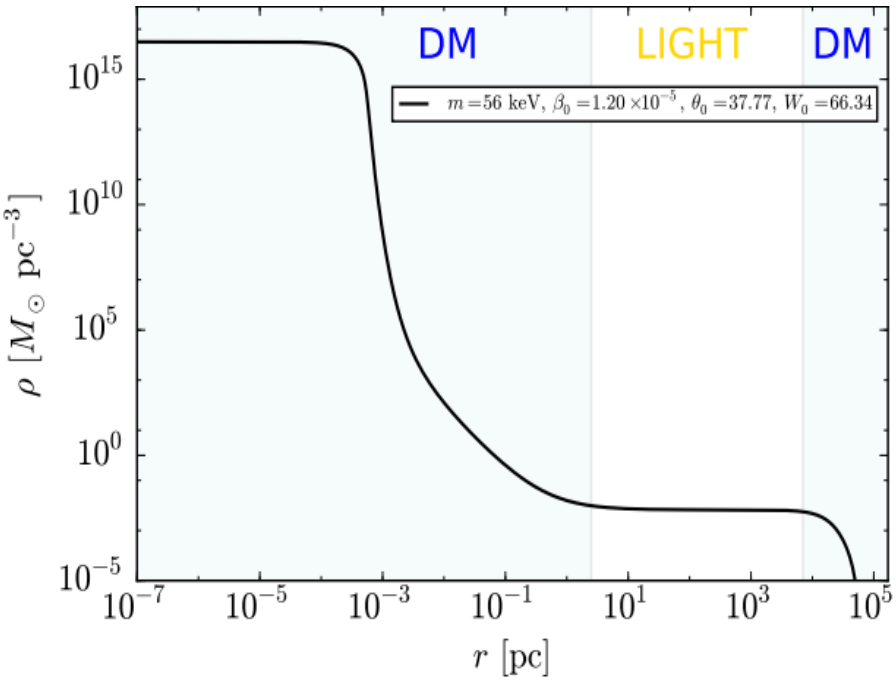

Figure 4.7: Density profile for ino mass 56 keV and the corresponding free model parameters in a given range. [10]

4.3.2 Rotation Curves

The rotation curves for different values of m are given in fig. 4.8. The three rotation curves show the dark matter contribution showing different regimes: the first region shows the velocity increasing linearly with distance as $v \propto r$ till it reaches the first maximum at $r = r_c$ which gives the core size, by further increasing the distance $r > r_c$ is the second region in which the velocity decreases as $v \propto r^{-1/2}$, after a certain distance it again starts linearly increasing as $v \propto r$ reaching the second maximum at $r = r_h$ which gives the halo size, for $r > r_h$ the rotation curve becomes flat. By introducing the cutoff effects it would not continue indefinitely. The curve in red shows both the baryonic and dark matter contributions. This shows that the data of the RAR model is consistent with that of the Milky Way in range $mc^2 = 48\ keV - 345\ keV$. This provides an alternative case for the Sgr A* black hole [13]. The matter components of the Galaxy are divided in four mass distribution laws:

1. From distance ($r \sim 10^{-3} - 2\ pc$) is the central region which has young S-stars and gas. Then the central region is seen to obey Keplerian law $v \propto r^{-1/2}$ under the influence of an object with mass $M_c = 4 \times 10^6\ M_\odot$.

2. Then comes the intermediate region from ($r \sim 3 - 10^3\ pc$) with spheroidal bulge, having the older stars in majority. The exponential spheroid model explains the inner and main components, the density is

$$\rho(r) = \rho_c e^{-r/a_b}, \tag{4.32}$$

where ρ_c is the central density and a_b is the scale length for bulge.

3. The other region from ($r \sim 10^3 - 10^4\ pc$) is a flat disk. Disk is a star forming region with dust and gas, whose surface mass density is described by an exponential law

$$\Sigma(R) = \Sigma_0 e^{-R/a_d}, \quad \Sigma_0 = M_d/(2\pi a_d^2), \tag{4.33}$$

where M_d is the disk mass, Σ_0 is the central density, and a_d is the scale length for disk.

4. From ($r \sim 10^4 - 10^5\ pc$) is the halo region, it has dark matter in abundance. The outer halo shows the density decreasing as r^{-2}. The dark matter circular velocity is given by equation 4.21.

It is assumed in the papers that baryonic and dark matter interact only gravitationally, so the rotation curve is obtained by adding square of circular velocities of nucleus, bulge, disk which is the baryonic part, and of halo which is the dark matter part, given as

$$v_{tot}^2(r) = v_b^2(r) + v_d^2(r) + v_{DM}^2(r). \tag{4.34}$$

From this the *total gravitational potential* can be obtained

$$v_{rot}^2 = r\frac{d\Phi_{tot}}{dr}, \tag{4.35}$$

where $\Phi_{tot} = \Phi_b + \Phi_d + \Phi_{DM}$.

4.3.3 Ino Mass Ranges

The range of ino masses is analyzed as:

1. For $m \lesssim 10\ keV/c^2$, the dark matter rotation curve exceeds from the observed velocity in the region with baryon domination that is the bulge where $r \approx 2 - 100\ pc$, as shown in fig. 4.8 for $m = 0.6\ keV/c^2$. So this limit is discarded as it should hold for accurate inner baryonic models and does not provide an alternative to the black hole scenario in Sgr A*.

2. For $mc^2 = 10\ keV - 48\ keV$, the rotation curve agrees with the observations but it does not explain the alternative to the central black hole case with a less dense core.

3. For $mc^2 = 48\ keV - 345\ keV$, the rotation curve agrees with the observations and explains an alternative to the central black hole scenario with a dense core $4 \times 10^6\ M_\odot$.

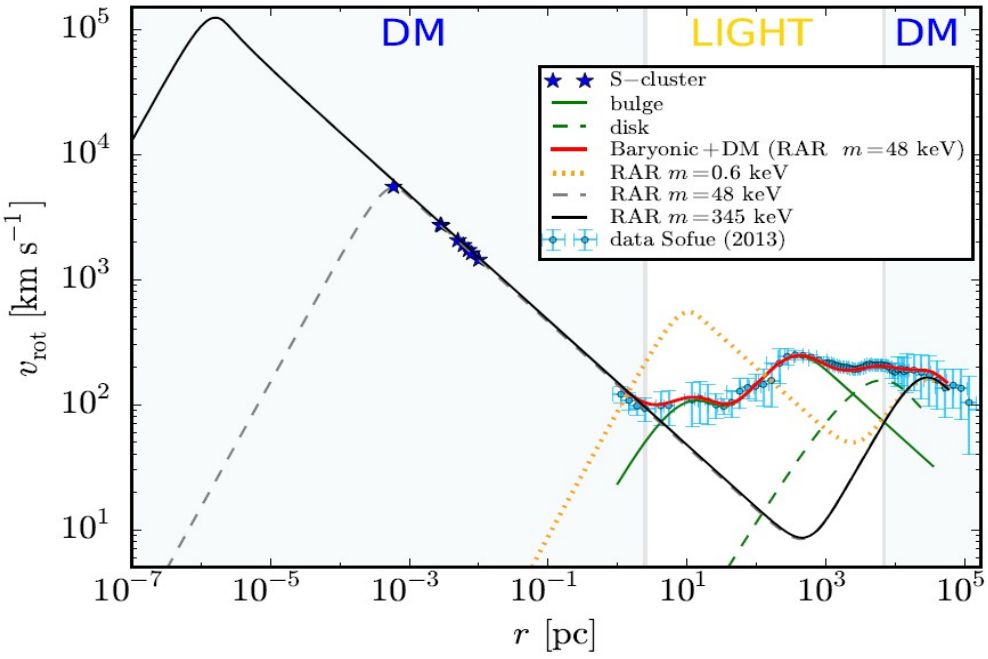

Figure 4.8: Rotation curves for fermion masses: 0.6 keV, 48 keV, and 345 keV with the corresponding model parameters in a given range. These solutions are in agreement with all the Milky Way observables within a certain range from $\backsim 10^{-3}$ pc to $\backsim 10^{5}$ pc. For $mc^2 = 48$ keV, the total rotation curve is included (red thick curve) that includes the total baryonic (bulge + disk) component. The stars show the eight best resolved S-cluster stars. [9]

$mc^2 = 345$ keV is the last stable value beyond which gravitational collapse occurs. The critical core mass formula is given as $M_c^{cr} \propto m_p^3/m^2$ with core radius $r_c \approx 4r_{Sch}$ where r_{Sch} is the Schwarzschild radius of the black hole with mass 4×10^6 $M_\odot$ [13].

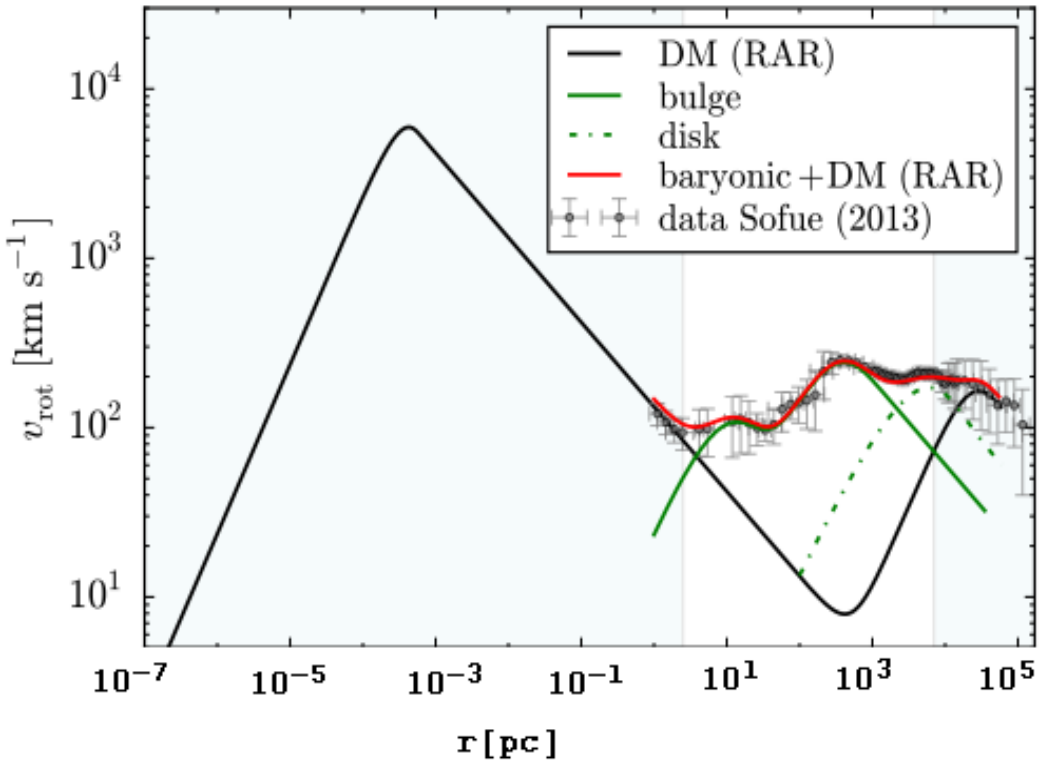

Figure 4.9: Rotation curve for fermion mass 56 keV with the corresponding model parameters within the given range. The total rotation curve (red thick curve) is also included that includes bulge + disk components. [10]

Chapter 5

Massive Sterile Neutrinos for Dark Matter Halos

In this final chapter, I will explain my work on the RAR model with and without including the energy cutoff. The problem I will work on is how dark matter is distributed in a galaxy from core to halo and how the degenerate fermions in keV range fall into the degenerate core and whether it would form a black hole. These fermions are to provide the non-baryonic dark matter. Such fermions lie outside the standard model of Particle Physics and are talked of as sterile neutrinos or neutralinos which are supposedly the heavy versions of neutrinos that are not associated with any generation of quarks and leptons. Other than dark matter, baryonic matter is also present in the core of a galaxy, so I will find out how much baryonic matter falls into the degenerate core so that it would collapse to form a black hole. The RAR model provides a good explanation of the distribution of dark matter in different galaxies than any other model. It explains the matter distribution in each component of a galaxy separately, giving a very good explanation of the dark matter halos, and predicting a compact dense quantum core at the galactic center. We will see a Fermi degenerate core surrounded by a partially degenerate halo.

In the previous chapter, we discussed about the problem of the missing black holes in intermediate mass range and the formation of supermassive black holes soon after the Big Bang. The problem is that normally, we cannot see how we could get black holes such massive. We do not know how were they formed so early when the Universe was still an infant. The only way we know how large black holes can be formed is by coalescence of stellar-mass black holes. But the time was not enough for the stars to collapse into black holes, then collide, and coalesce into supermassive black holes. The first generation of stars, the Population III stars were formed about 200 million years after the Big Bang, then over millions of years they evolved, and eventually in supernovae they became black holes with masses say about 100 $M_\odot$ and the supermassive black holes are thought to have formed about 600 million years after the Big Bang. So how could a black hole with mass from a few million to a few billion solar masses have formed in such short time? For a stellar-mass black hole even 13

billion years are not enough to become supermassive by just accreting the mass. We also know that every galaxy hosts a supermassive black hole at its center, so we consider that to be a dense compact quantum core here, made up of the degenerate fermions. In this way, we can try explaining the formation of the central supermassive black holes. We say that there is a large gravitational potential well, matter is falling into it, and produce central black holes. Other than this, astronomers are looking for the intermediate-mass black holes which are known as the missing links between the stellar-mass black holes and the supermassive black holes.

The RAR model, as discussed in the previous chapter consists of a system of self-gravitating massive fermions in thermodynamic equilibrium and spherical symmetry. To find the matter distribution in galaxies, we will solve the equations of equilibrium for a system of self-gravitating fermions with free parameters of the model that is the temperature parameter and the degeneracy parameter within General Relativity. Firstly, the simplest case of self-gravitating bare massive fermions obeying the *Fermi-Dirac statistics* is considered and neglecting any additional interactions. It proposes the fermion masses to be above keV. We consider the mass range from 4 keV to 345 keV. The particles considered are not weakly interacting, called the inos. Then we consider the RAR model that consists of a system of self-gravitating massive fermions with introducing the energy cutoff effects in the fermionic phase space distribution, in order to be consistent with the observations in Sgr A*. By introducing the cutoff effects we get the finite galaxy size and more compact cores as compared to the RAR model without the cutoff effects. An interesting prediction of this model is a dense quantum core at the center, by adding the cutoff effects we get a solution for the core which is an alternative to the central black hole. The fermionic mass range from 48 keV to 345 keV considered here, below the Fermi temperature, gives the dark matter halo distribution forming a fully degenerate core which agrees with the data obtained from the rotation curves of the Milky Way galaxy.

A system of self-gravitating fermions following the Boltzmann distribution, giving a classical dilute regime overall, if applied to the galaxies, undergoes a core collapse. But a system of self-gravitating collisionless particles with central degeneracy does not give a classical regime and the system is stable because of Pauli's exclusion principle. With the thermodynamical considerations, the effects of violent relaxation which are important for the virialization in galaxies are considered. An extension of this includes the violent relaxation with evaporation.

We are interested in the fermionic dark matter, these fermions lie outside the Standard Model. Particle Physics beyond the standard model suggests sterile neutrino or neutralino which could be the possible candidates for dark matter.

5.1 Central Density and Pressure

We now consider a system of self-gravitating massive fermions and neglect all the interactions other than the gravitational interaction, fulfilling the Fermi-Dirac distribution due to the

collisionless relaxation process, predicting a degenerate core at the center. The fermionic equations of state for phase space density and pressure, without the energy cutoff are given in equations 4.1 and 4.2, respectively. From the first equation, we compute the central density of a galaxy at $r = 0$. Substituting the Fermi-Dirac distribution function in both the equations, we get

$$\rho = \frac{2m}{h^3} \int_0^\infty \left[e^{(\epsilon-\mu)/k_B T} + 1 \right]^{-1} \left[1 + \frac{\epsilon(p)}{mc^2} \right] d^3p. \tag{5.1}$$

Due to the spherical symmetry, $d^3p = 4\pi p^2 dp$. Substituting the value of kinetic energy, the above equation becomes

$$\rho = \frac{8\pi m}{h^3} \int_0^\infty \left[e^{(\sqrt{c^2p^2+m^2c^4}-mc^2-\mu)/k_B T} + 1 \right]^{-1} \left[1 + \frac{\sqrt{c^2p^2+m^2c^4} - mc^2}{mc^2} \right] p^2 dp. \tag{5.2}$$

Using the approximation $p \gg mc$, the kinetic energy reduces to cp which gives the relativistic degenerate cores, and the equation becomes

$$\rho = \frac{8\pi m}{h^3} \int_0^\infty \left[e^{(cp-\mu)/k_B T} + 1 \right]^{-1} \left[1 + \frac{cp}{mc^2} \right] p^2 dp, \tag{5.3}$$

$$\rho = \frac{8\pi m}{h^3} \int_0^\infty \frac{\left[1 + \frac{cp}{mc^2} \right]}{\left[e^{(cp-\mu)/k_B T} + 1 \right]} p^2 dp. \tag{5.4}$$

Further simplifying the above equation, we have

$$\rho = \frac{8\pi}{c^2h^3} \int_0^\infty \frac{(mc^2 + cp)}{e^{(cp-\mu)/k_B T}} p^2 dp, \tag{5.5}$$

$$\rho = \frac{8\pi}{c^2h^3} \int_0^\infty \frac{mc^2}{e^{(cp-\mu)/k_B T}} p^2 dp + \frac{8\pi}{c^2h^3} \int_0^\infty \frac{cp}{e^{(cp-\mu)/k_B T}} p^2 dp, \tag{5.6}$$

$$\rho = \frac{8\pi m}{c^2h^3} \int_0^\infty \frac{c^2p^2}{e^{cp/k_B T} e^{-\mu/k_B T}} dp + \frac{8\pi}{c^4h^3} \int_0^\infty \frac{c^3p^3}{e^{cp/k_B T} e^{-\mu/k_B T}} dp. \tag{5.7}$$

Put $cp = z$, such that $dp = dz/c$, we get

$$\rho = \frac{8\pi m}{c^3h^3} \int_0^\infty \frac{z^2}{e^{z/k_B T} e^{-\mu/k_B T}} dz + \frac{8\pi}{c^5h^3} \int_0^\infty \frac{z^3}{e^{z/k_B T} e^{-\mu/k_B T}} dz. \tag{5.8}$$

Consider the degeneracy and temperature parameters from the equation 4.13 and substitute in the above equation, which gives

$$\rho = \frac{8\pi m}{c^3 h^3} \int_0^\infty \frac{z^2}{e^{z/\beta_0 mc^2} e^{-\theta_0}} dz + \frac{8\pi}{c^5 h^3} \int_0^\infty \frac{z^3}{e^{z/\beta_0 mc^2} e^{-\theta_0}} dz. \tag{5.9}$$

To solve the above equation, we find the values of the two free parameters β_0 and θ_0 for different values of the ino mass m. The central degeneracy parameter θ_0 is obtained by

$$\theta(m) = \theta_0^* + 12.52 \log \left[\frac{m}{10\ keV/c^2} \right], \tag{5.10}$$

where the value of θ_0^* varies for different types of galaxies, we here consider $\theta_0^* \approx 29.6$. If we know the value of the central degeneracy parameter, we can find the value of m.

During the early stages of the Universe, when the fermions had just been produced, the temperature at that stage of the Universe was approximately 100 keV or $\sim 10^9$ K, the fermions decoupled and froze out. Then the Universe cooled as it expanded and reached the *Fermi degeneracy temperature*. At that time, the gas of fermions became a *degenerate Fermi gas* and the degenerate cores collected at the centers of galaxies and grew. The Fermi temperature is given by

$$T_F = \frac{mc^2}{k_B}. \tag{5.11}$$

Substituting the value of mc^2 and k_B, we get the Fermi temperature. We can find the Fermi temperature for any value of the ino mass by equation5.11. The central temperature parameter β_0 is obtained by a trial and error procedure until the values of v_h and M_h are obtained at r_h. We have now the constants, central degeneracy parameter, and central temperature parameter, substitute them in the equation 4.23. Numerically integrate the resulting equation and get the central density for any value of the ino mass.

Similarly, we can work for the central pressure of a galaxy at $r = 0$ using the equation 4.2, substituting the Fermi-Dirac function, we have

$$P = \frac{2}{3h^3} \int_0^\infty \left[e^{(\epsilon-\mu)/k_B T} + 1 \right]^{-1} \left[1 + \frac{\epsilon(p)}{mc^2} \right]^{-1} \left[1 + \frac{\epsilon(p)}{2mc^2} \right] \epsilon d^3 p. \tag{5.12}$$

We simplify the equation for pressure same as we did for the equation of density, this will give the central pressure. In the table 5.1, different values of θ_0, β_0, and central density for different values of m are given. To find different variables we will move on to a set of Einstein equations.

Table 5.1: Core properties including the central degeneracy parameter, temperature parameter, and central density for different ino masses fulfilling the halo boundary conditions given in equation 4.14.

$m(keV/c^2)$	θ_0	β_0	$\rho_c(M_\odot/pc^3)$
4.323	25	3.32×10^{-7}	6.3×10^{8}
10.54	29.8	7.4×10^{-8}	3×10^{10}
48	38.12	5.13×10^{-9}	1.76×10^{13}
64.45	39.72	3.1×10^{-9}	6.25×10^{13}
100	42.1	1.44×10^{-9}	3.92×10^{14}
200	45.88	4.34×10^{-10}	7.53×10^{15}
300	48.1	2.14×10^{-10}	4.2×10^{16}
345	48.85	1.68×10^{-10}	7.61×10^{16}

5.2 Einstein Equations

A finite mass distribution is obtained by solving the Einstein equations for a thermal and semi-degenerate fermionic gas, described by a perfect fluid in the hydrostatic equilibrium. In the previous chapter, Einstein equations 4.4 - 4.8 for a spherically symmetric metric along with the thermodynamic equilibrium conditions were given. Those equations can be solved to find certain parameters varying with distance which give variables like $M(r)$, $\theta(r)$, $\nu(r)$, $\beta(r)$ with initial conditions $M(0) = 0$, $\theta(0) = \theta_0$, $\nu(0) = 0$, $\beta(0) = \beta_0$.

5.3 Core Mass

The equation 4.4 gives the core mass by solving it numerically for a constant value of the central density obtained from the equation 4.23. Place the dimensionless quantities from equation 4.9 in equation 4.4. We plug in the value of central density and solve the equation numerically. At $M(r_c)$, we get M_c that is the core mass and r_c is the core size which will be discussed later. We see that the core mass is strongly dependent on the ino mass. For different values of m, the corresponding core masses are given in the table 5.2. Using the core mass and the core radius we will see in the coming sections, whether it forms a black hole or not.

5.4 Density Profiles

The phase space density distribution shows both, the quantum and classical regimes. Density profiles show density varying with distance at the fixed parameters of the model that is the

Table 5.2: Core masses for different values of ino mass, the corresponding central degeneracy, and temperature parameters.

m(keV/c^2)	$M_c(M_\odot)$
4.323	1.43×10^7
10.54	2.74×10^6
48	1.56×10^5
64.45	9×10^4
100	3.91×10^4
200	1.07×10^4
300	5×10^3
345	3.84×10^3

degeneracy and temperature parameters. Earlier, we obtained the central density ρ_c from the Fermi-Dirac phase space distribution using the fermionic equation of state, now we need the density varying with distance that is $\rho(r)$. We start with the standard fermionic equation of state given by

$$\rho(r) = \frac{2m}{h^3} \int_0^\infty \left[e^{(\epsilon - \mu(r))/k_B T} + 1 \right]^{-1} d^3p. \tag{5.13}$$

For the spherically symmetric solutions, we have

$$\rho(r) = \frac{8\pi m}{h^3} \int_0^\infty \frac{p^2}{e^{\epsilon/k_B T - \theta(r)} + 1} dp, \tag{5.14}$$

where $\theta(r) = \frac{\mu(r)}{k_B T}$ is the degeneracy parameter and $\mu(r)$ is the chemical potential. Using the approximation $p \ll mc$, the kinetic energy reduces to $p^2/2m$, so the equation becomes

$$\rho(r) = \frac{8\pi m}{h^3} \int_0^\infty \frac{p^2}{e^{p^2/2mk_B T - \theta(r)} + 1} dp. \tag{5.15}$$

To find density as a function of distance, we use the following substitution

$$y^2 = \frac{p^2}{2mk_B T}. \tag{5.16}$$

We have

$$\rho = \frac{8\pi m(2mk_BT)^{3/2}}{h^3}\int_0^\infty \frac{y^2}{e^{y^2-\theta(r)}+1}dy, \tag{5.17}$$

$$\rho = \frac{2m(2\pi mk_BT)^{3/2}}{h^3}\frac{4}{\sqrt{\pi}}\int_0^\infty \frac{y^2}{e^{y^2-\theta(r)}+1}dy, \tag{5.18}$$

where $\lambda_B = \frac{h}{\sqrt{2\pi mk_BT}}$ is the thermal de Broglie wavelength of inos, so

$$\rho = \frac{2m}{\lambda_B^3}\frac{4}{\sqrt{\pi}}\int_0^\infty \frac{y^2}{e^{y^2-\theta(r)}+1}dy, \tag{5.19}$$

where $\rho_B = \frac{2m}{\lambda_B^3}$, the equation becomes

$$\frac{\rho(r)}{\rho_B} = \frac{4}{\sqrt{\pi}}\int_0^\infty \frac{y^2}{e^{y^2-\theta(r)}+1}dy. \tag{5.20}$$

Solving the standard fermionic equation of state for pressure using the similar substitutions, the equation of pressure is given by

$$\frac{P(r)}{P_B} = \frac{8}{3\sqrt{\pi}}\int_0^\infty \frac{y^4}{e^{y^2-\theta(r)}+1}dy, \tag{5.21}$$

where $P_B = \rho_B\sigma^2$ and $\sigma^2 = k_BT/2m$ is the velocity dispersion.

Now to solve such Fermi integrals, polylogarithms are used given by

$$\int_0^\infty \frac{y^{2n}}{e^{y^2-\theta(r)}+1}dy = -\frac{(2n)!}{n!4^n}\frac{\sqrt{\pi}}{2}Li_{\frac{1}{2}+n}(-e^{\theta(r)}), \tag{5.22}$$

where $n \in$ N. For density n=1 and for pressure n=2, we have

$$\int_0^\infty \frac{y^2}{e^{y^2-\theta(r)}+1}dy = -\frac{\sqrt{\pi}}{4}Li_{\frac{3}{2}}(-e^{\theta(r)}), \tag{5.23}$$

so the density and pressure will be

$$\frac{\rho(r)}{\rho_B} = -Li_{\frac{3}{2}}(-e^{\theta(r)}), \tag{5.24}$$

$$\frac{P(r)}{P_B} = -Li_{\frac{5}{2}}(-e^{\theta(r)}). \tag{5.25}$$

We need density in terms of ρ_0, so we re-scale the above equation for density. Starting at $r = 0$, equation 5.24 reduces to

$$\frac{\rho_0}{\rho_B} = -Li_{\frac{3}{2}}(-e^{\theta_0}), \tag{5.26}$$

$$\frac{\rho(r)}{\rho_B} = \frac{\rho(r)}{\rho_0}\left[-Li_{\frac{3}{2}}(-e^{\theta_0})\right]. \tag{5.27}$$

From equation 5.24, we have

$$\rho(r) = \rho_0 \frac{-Li_{\frac{3}{2}}(-e^{\theta(r)})}{-Li_{\frac{3}{2}}(-e^{\theta_0})}. \tag{5.28}$$

To solve this equation, the degeneracy parameter $\theta(r)$ is required which will be discussed in detail in the coming sections. So, by using the values of $\theta(r)$ and θ_0, we can find the density variable. Now we can easily find out the values of density at any distance and hence the density profiles for different ino masses with the corresponding central degeneracy and temperature parameters are obtained.

By fixing the fermion mass m, we construct different solutions depending on the degeneracy and temperature parameters at the center. The mass density profiles clearly show in fig. 5.1a and 5.1b different regimes: the first regime is the central degenerate compact core which obeys the quantum statistics, then is the transition region where density is seen sharply decreasing followed by an extended plateau, then is the classical Boltzmann regime representing the halo ending in a power law behavior r^2. The density of such a system at large radii scales as r^2, independent of the values of the central density, providing the flat rotation curve.

For $\theta_0 \ll -1$, the central degeneracy is very low. Now the Fermi-Dirac distribution does not apply, we instead use the Boltzmann approximation (see fig. 5.2), from equation 5.29 which reduces to

$$\frac{\rho(r)}{\rho_B} = \int_0^\infty \frac{y^2}{e^{y^2-\theta(r)}} dy, \tag{5.29}$$

$$\frac{\rho(r)}{\rho_B} = \int_0^\infty y^2 e^{y^2-\theta(r)} dy. \tag{5.30}$$

Integrating the above equation we have

$$\frac{\rho(r)}{\rho_B} = \frac{\sqrt{\pi}}{4} e^{\theta(r)}, \tag{5.31}$$

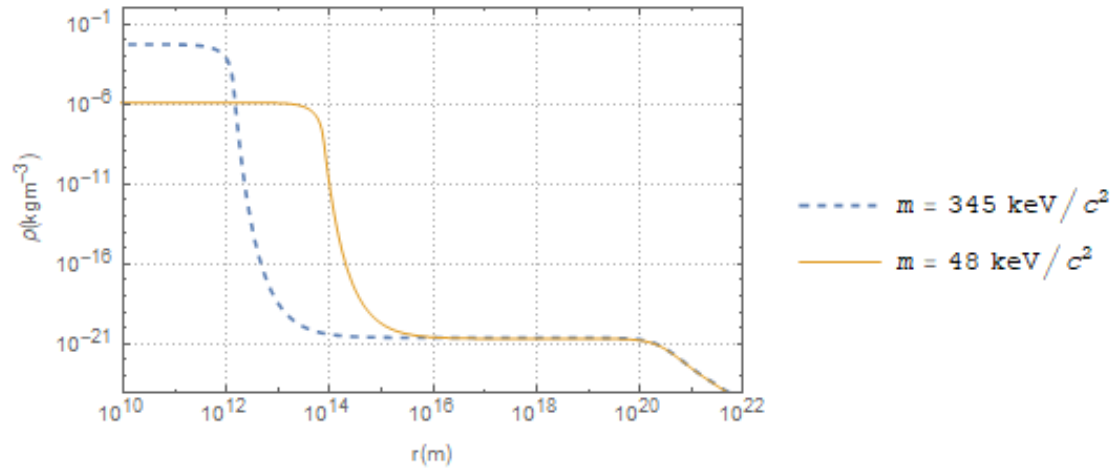

(a)

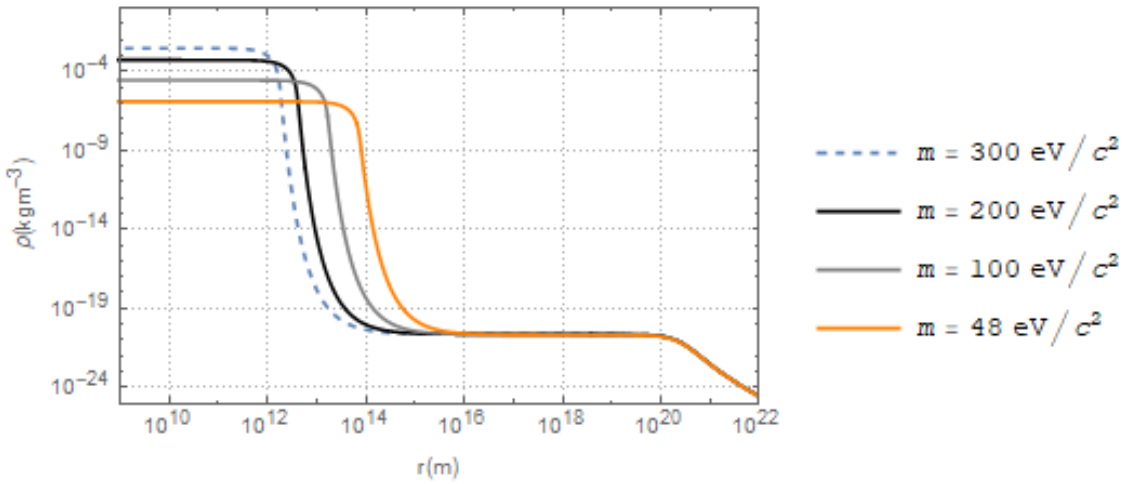

(b)

Figure 5.1: Density profiles for ino masses 345 keV and 48 keV given in fig. 5.1a and 300 keV, 200 keV, 100 keV, and 48 keV given in fig. 5.1b with the corresponding central degeneracy parameters θ_0 and temperature parameters β_0 , showing three different regimes from quantum to classical. The density profiles fulfill the boundary conditions given in equation 4.14.

where $\frac{\rho_0}{\rho_B} = e^{\theta_0}$.

$$\rho(r) = \frac{\sqrt{\pi}}{4}\rho_0 e^{\theta(r)-\theta_0}. \tag{5.32}$$

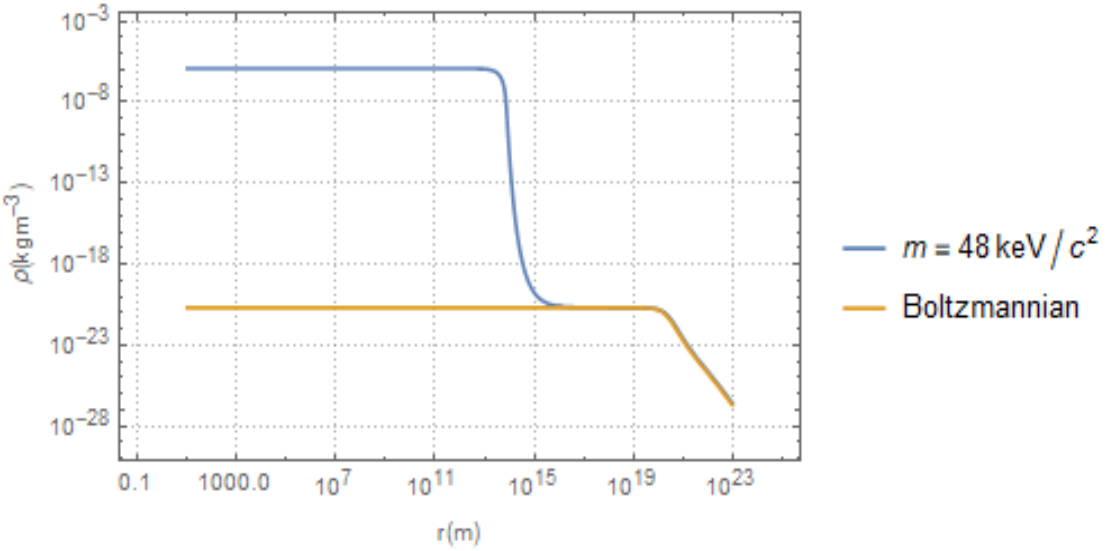

Figure 5.2: The RAR model density profile for $m = 48\ keV/c^2$ is compared with the Boltzmann density profile. The comparison shows that the RAR density profile eventually reduces to the Boltzmann classical regime.

5.5 Mass Profiles

Mass profiles show how the mass in a galaxy is distributed over large distances from the core to halo for different ino masses and the corresponding degeneracy and temperature parameters. The Einstein equation for mass given by equation 4.4 in its dimensionless form is given by

$$\frac{dM(r)}{dr} = 4\pi r^2 \rho(r), \tag{5.33}$$

$$M(r) = \int_0^r 4\pi r^2 \rho(r) dr. \tag{5.34}$$

Substitute the value of $\rho(r)$ from equation 5.28, we have

$$M(r) = \int_0^r 4\pi r^2 \rho_0 \frac{-Li_{\frac{3}{2}}(-e^{\theta(r)})}{-Li_{\frac{3}{2}}(-e^{\theta_0})} dr. \tag{5.35}$$

The mass distribution $M(r)$ is obtained by numerically integrating the above equation with the initial condition $M(0) = 0$. Now we can simply find the value of M at any distance. The plots of mass distribution for different values of ino mass m with the corresponding free parameters of the model are given in fig. 5.3a and 5.3b.

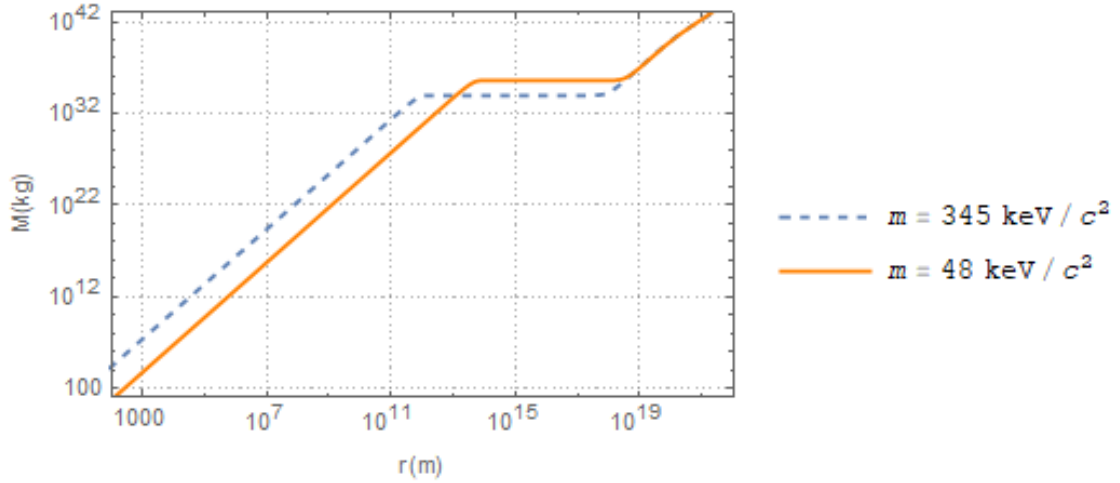

(a)

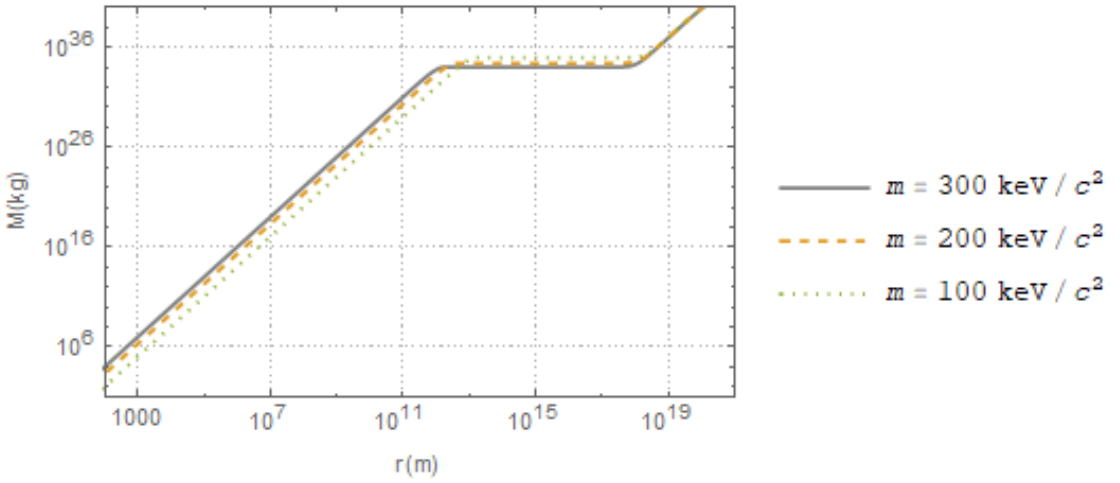

(b)

Figure 5.3: Mass profiles for ino masses 345 keV and 48 keV given in fig. 5.3a and 300 keV, 200 keV, and 100 keV given in fig. 5.3b with the corresponding central degeneracy and temperature parameters.

For a less central degeneracy, mass will reduce to the Boltzmann distribution(see fig. 5.4), we have

$$M(r) = \int_0^r \pi^{3/2} r^2 \rho_0 e^{\theta(r)-\theta_0} dr. \tag{5.36}$$

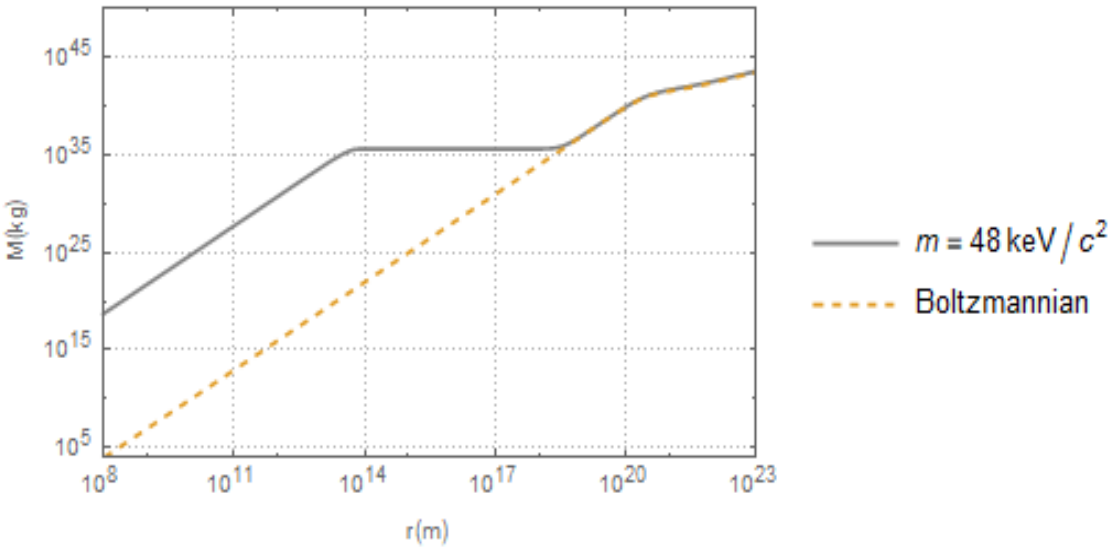

Figure 5.4: The RAR model mass profile for $m = 48\ keV/c^2$ is compared with the Boltzmann mass profile. The comparison shows the RAR mass profile eventually reduces to the Boltzmann classical regime.

5.6 The Degeneracy Parameter

The degeneracy parameter in our model determines the degeneracy of a galaxy from the core to halo, varying with the distance. To find the degeneracy parameter $\theta(r)$, we start with considering Keplerian

$$\frac{d\phi}{dr} = \frac{GM(r)}{r^2}, \tag{5.37}$$

where $\phi(r)$ is the potential. Equations 5.34 and 5.37 give the Poisson equation as

$$\frac{1}{r^2}\frac{d}{dr}\left[r^2\frac{d\phi}{dr}\right] = 4\pi G\rho(r). \tag{5.38}$$

The equilibrium of galaxies is explained by the classical hydrostatic equation given by

$$\frac{d\phi}{dr} = -\frac{1}{\rho(r)}\frac{dP}{dr}. \tag{5.39}$$

Using the following Polylogarithm formula

$$\frac{d}{dx}Li_n(x) = \frac{1}{x}Li_{n-1}(x), \tag{5.40}$$

and then comparing with the equation 5.39, we get a relation between $\phi(r)$ and $\theta(r)$

$$\phi(r) - \phi_0 = -\sigma^2[\theta(r) - \theta_0], \tag{5.41}$$

where

$$\sigma^2 = \phi_R/2, \tag{5.42}$$

and ϕ_R is the scaling factor given by

$$\phi_R = 4\pi G R^2 \rho_0. \tag{5.43}$$

Comparing both the relations we get the scaling radius

$$R^2 = \frac{\sigma^2}{2\pi G\rho_0}. \tag{5.44}$$

From equation 5.41, put $\phi(r) = -\sigma^2\theta(r)$ in the Poisson equation 5.38, we get

$$\frac{-\sigma^2}{r^2}\frac{d}{dr}\left[r^2\frac{d\theta}{dr}\right] = 4\pi G\rho(r). \tag{5.45}$$

Substituting the value of σ^2 from equation 5.44, we have

$$\frac{R^2}{r^2}\frac{d}{dr}\left[r^2\frac{d\theta}{dr}\right] = -2\frac{\rho(r)}{\rho_0}. \tag{5.46}$$

From equation 5.28, we get

$$\frac{R^2}{r^2}\frac{d}{dr}\left[r^2\frac{d\theta}{dr}\right] = -2\frac{-Li_{\frac{3}{2}}(-e^{\theta(r)})}{-Li_{\frac{3}{2}}(-e^{\theta_0})}. \tag{5.47}$$

So the final equation will be of the form

$$R^2\frac{d^2\theta}{dr^2} + \frac{2R^2}{r}\frac{d\theta}{dr} = -2\frac{-Li_{\frac{3}{2}}(-e^{\theta(r)})}{-Li_{\frac{3}{2}}(-e^{\theta_0})}. \tag{5.48}$$

A relation between the intrinsic parameters of the model that is the ino mass m, central degeneracy parameter θ_0, and observables that is σ and ρ_0 is given by

$$m^4 \left[-Li_{\frac{3}{2}}(-e^{\theta_0})\right] = \frac{(2\pi)^{3/2}\hbar^3\rho_0}{2\sigma^3}, \tag{5.49}$$

$$\sigma^2 = \frac{(2\pi)\hbar^2\rho_0^{2/3}}{m^{8/3}\left[-Li_{\frac{3}{2}}(-e^{\theta_0})\right]^{2/3}}. \tag{5.50}$$

Substituting this value in equation 5.44, we get the value for R^2, now we can solve the equation for the degeneracy parameter. We can find the value of degeneracy parameter for any value of r. The plots for the degeneracy parameter for different values of m and the corresponding free parameters of the model are given in the fig. 5.5a and 5.5b. It clearly shows three regimes: the first one where $\theta(r) > 0$ is the degenerate quantum core at $r = r_c$, in the second regime $\theta(r)$ transitions from positive to negative values at $r > r_c$ and in this regime the quantum corrections are still applicable upto the classical regime, the third regime is the classical one described by the Boltzmann statistics where the quantum corrections are no longer applicable and $\theta(r) \ll -1$ at $r \gtrsim r_h$.

For the classical regime, Poissonian becomes

$$\frac{R^2}{r^2}\frac{d}{dr}\left[r^2\frac{d\theta}{dr}\right] = -2e^{\theta(r)-\theta_0}, \tag{5.51}$$

$$R^2\frac{d^2\theta}{dr^2} + \frac{2R^2}{r}\frac{d\theta}{dr} = -2(-e^{\theta(r)-\theta_0}). \tag{5.52}$$

The value of R is given by equation 5.44 and for the value of σ, we use the relation

$$\sigma^2 = \frac{(2\pi)\hbar^2\rho_0^{2/3}}{m^{8/3}(e^{\theta_0})^{2/3}}. \tag{5.53}$$

5.7 Rotation Curves

The circular velocity is given by

$$v_c^2 = r\frac{d\phi}{dr}, \tag{5.54}$$

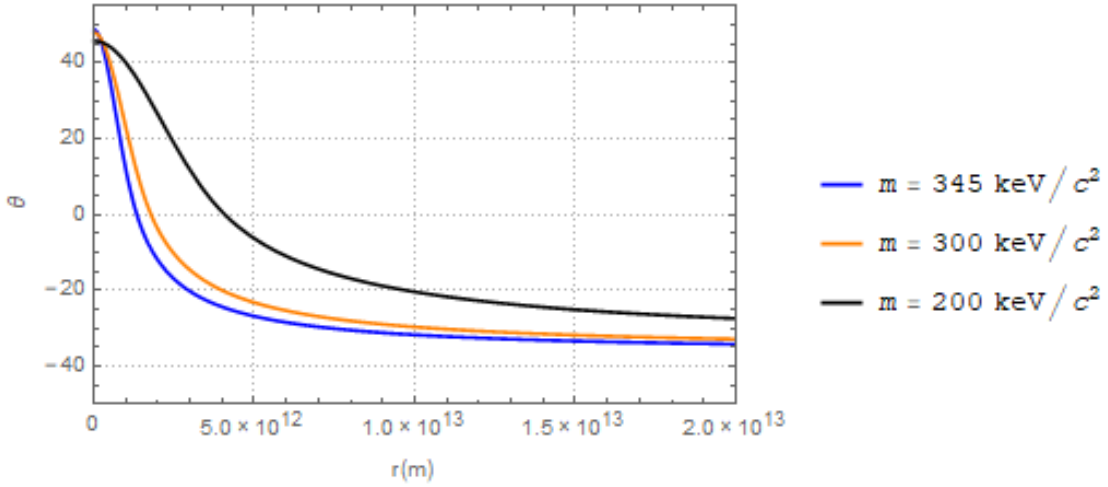

(a)

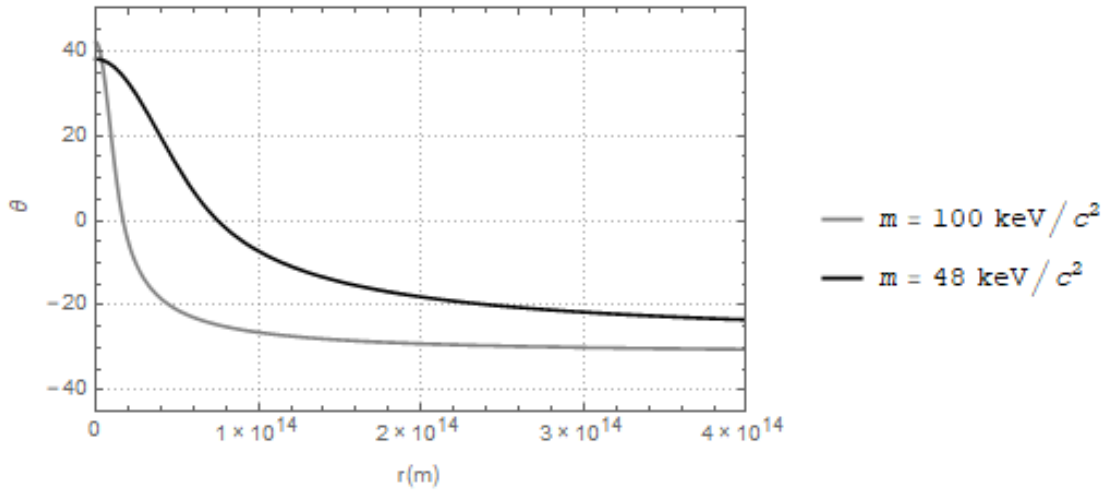

(b)

Figure 5.5: Degeneracy parameters varying with distance for ino masses 345 keV, 300 keV, and 200 keV in fig. 5.5a, and 100 keV and 48 keV given in fig. 5.5b with the corresponding central degeneracy parameters θ_0 and temperature parameters β_0, profiles fulfill the boundary conditions given in equation 4.14.

where ϕ is the potential.

$$v_{DM}(r) = \sqrt{\frac{GM(r)}{r - 2GM(r)/c^2}}. \tag{5.55}$$

We plug in the value of $M(r)$ from equation 5.36. Also $v(r = r_c) = v_c$ and $v(r = r_h) = v_h$. We then plot this velocity as a function of distance which gives the rotation curves for

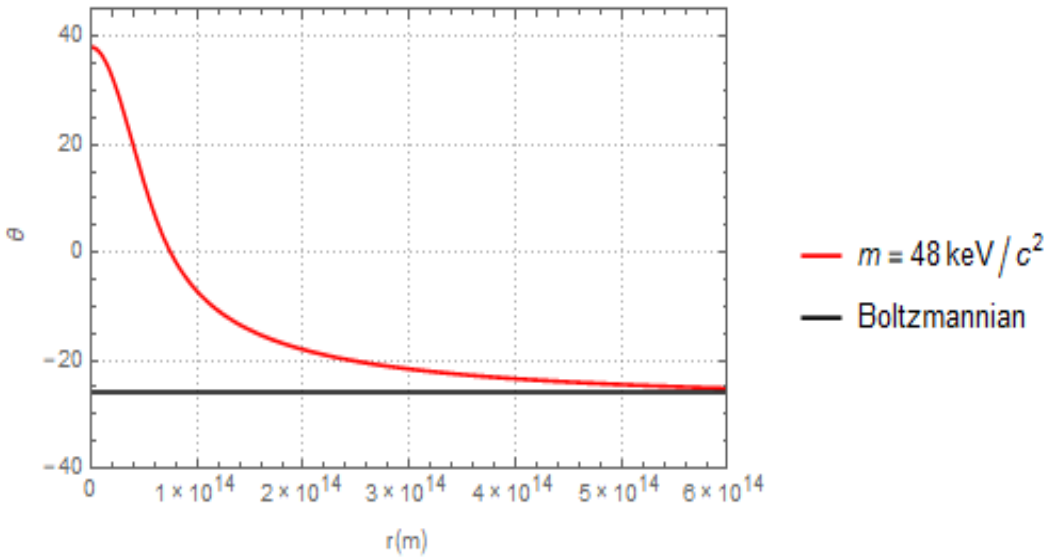

Figure 5.6: The RAR model degeneracy parameter for $m = 48\ keV/c^2$ is compared with the degeneracy parameter for the Boltzmann classical distribution which applies when the central degeneracy is very low, that is $\theta_0 \ll -1$. The comparison shows the RAR degeneracy parameter reduces to the classical regime.

different ino masses and the free parameters of the model. We consider the fixed boundary conditions for the spiral galaxies like our galaxy Milky Way as given in equation 4.14, to obtain the same flat rotation curves for any value of ino mass.

We see four regions in the rotation curves given in fig. 5.7a - 5.7e, each with a characteristic slope. Region I shows a degenerate core in which the velocity goes as $v_c \propto r$, then it reaches its first maximum at $r = r_c$ which gives the core size. Increasing the values of radial coordinate $r > r_c$ is region II, this is the Keplerian region in which the velocity varies as $v_c \propto r^{-1/2}$. Further, increasing the values of radial coordinate we have region III where the velocity again behaves as $v_c \propto r$, it reaches $r = r_h$ which is the second maximum giving the halo size. Finally, reaching region IV when $r > r_h$, after some oscillations the circular velocity tends to a constant value, corresponding to a pure classical Boltzmannian regime. The solution leads to the isothermal sphere with $\rho \propto r^{-2}$ density profile, leading the dark matter halo to a flat rotation curve. A cutoff in the momentum space is introduced so that the flat region of the rotation curves does not seem to continue indefinitely. The flatness of the rotation curves verify the existence of dark matter in galaxies.

As discussed in the previous chapter, the matter components of a galaxy can be divided into three parts: nucleus, baryonic matter, and dark matter. Baryonic matter further includes the matter in bulge and disk. So the total rotation curve can be calculated by equations 4.34 and 4.35. We will here plot the rotation curves for baryonic matter in the bulge and disk using the observational data from the Milky Way galaxy. So the circular velocities for the inner bulge, the main bulge, and the disk parts of the Galaxy are given by

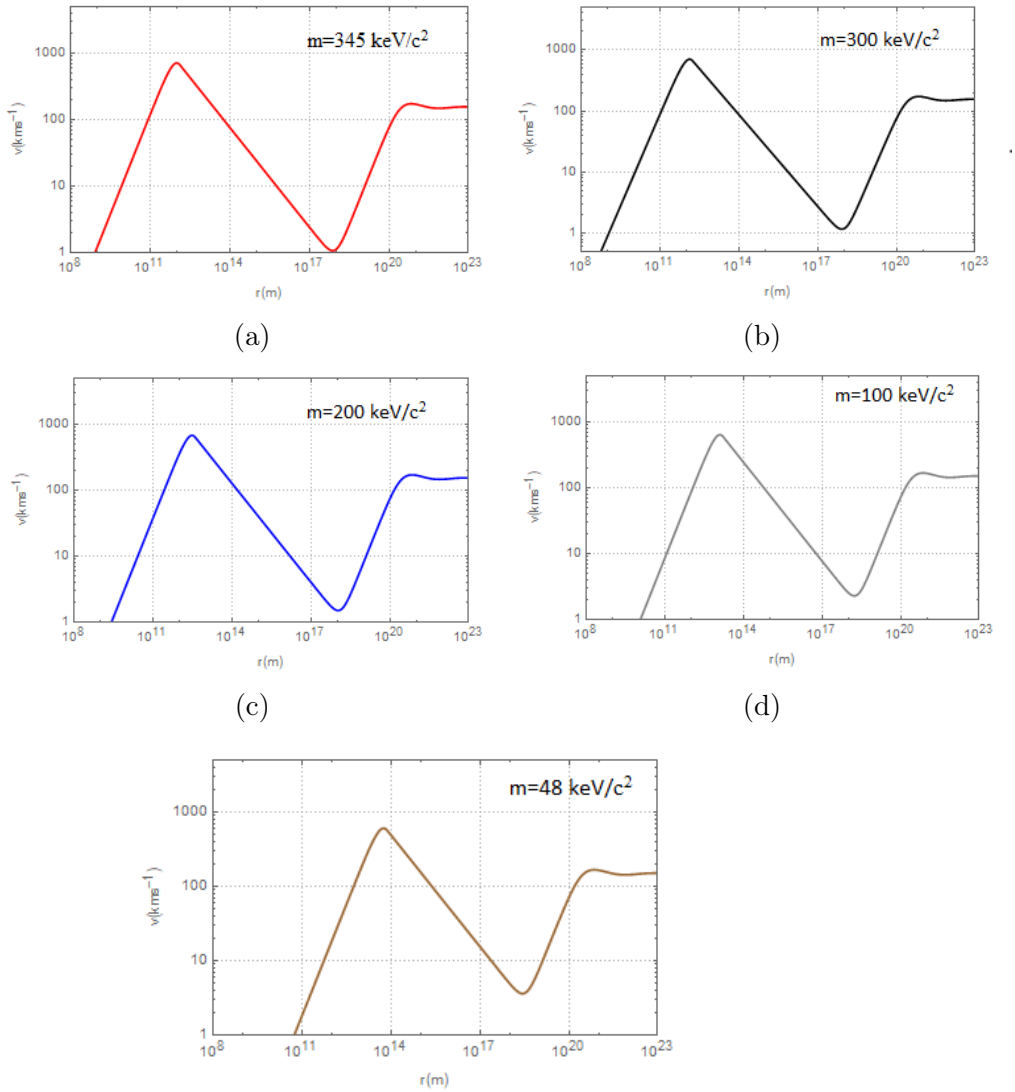

(a) (b) (c) (d) (e)

Figure 5.7: Rotation curves for different ino masses m with the corresponding central degeneracy parameters θ_0 and temperature parameters β_0 are given. The plots show different regions.

$$v_b^2 = \frac{2GM_{ib}}{r} + \frac{2GM_{ob}}{r} + \frac{2GM_d}{r}, \tag{5.56}$$

where M_{ib} and M_{ob} are the masses of the inner bulge and the outer bulge and M_d is the mass of the disk. These masses are obtained by

$$M(r) = M_0(1 - e^{-r/a} - (r/a)e^{-r/a}), \tag{5.57}$$

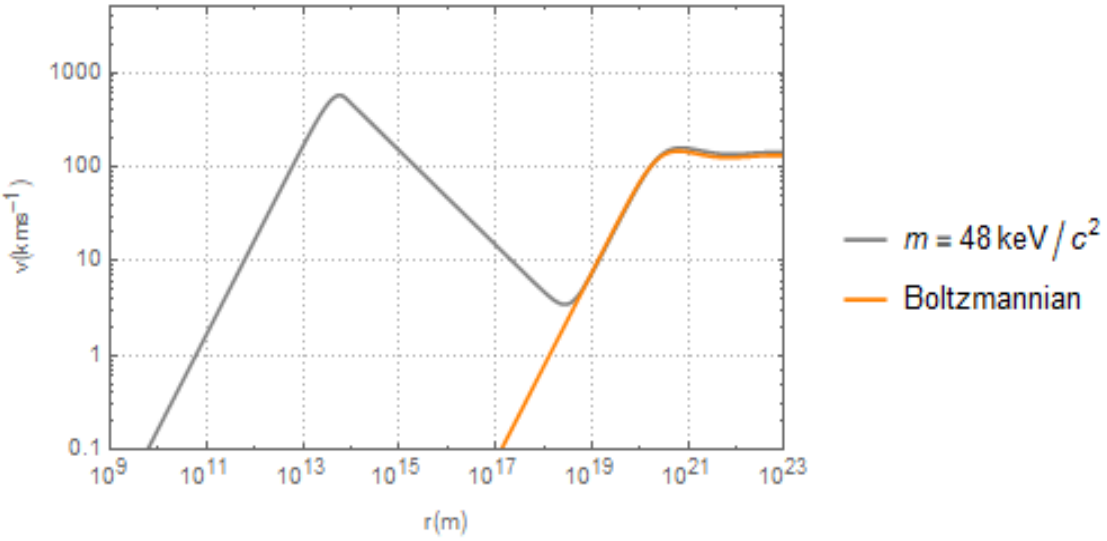

Figure 5.8: The RAR model rotation curve for $m = 48\ keV/c^2$ is compared with the rotation curve for Boltzmannian classical distribution which applies when the central degeneracy is very low that is $\theta_0 \ll -1$. The comparison shows the RAR degeneracy parameter reduces to the Boltzmann classical regime.

Table 5.3: Core properties including the core radius for different ino masses.

m(keV/c^2)	$r_c(pc)$
4.323	2.5×10^{-1}
10.54	4×10^{-2}
48	1.83×10^{-3}
64.45	1×10^{-3}
100	4.1×10^{-4}
200	1×10^{-4}
300	4.35×10^{-5}
345	3.27×10^{-5}

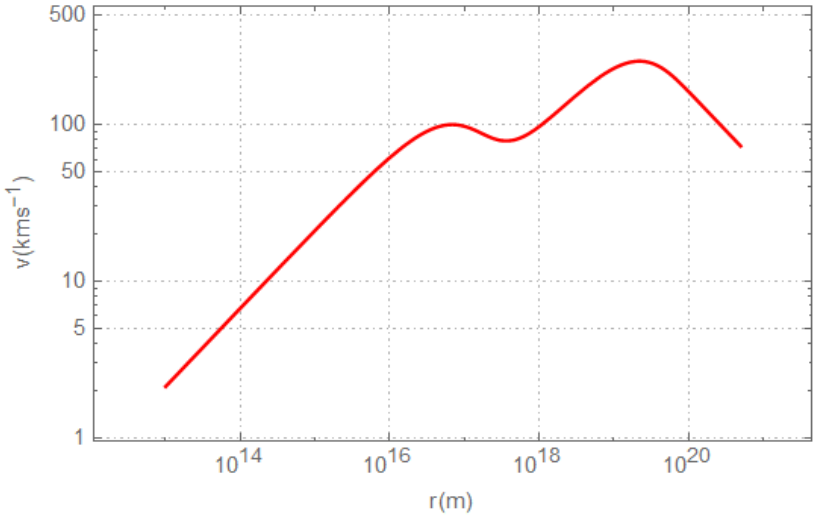

Figure 5.9: The graph shows the velocity varying with distance for the bulge of the Milky Way galaxy which is the baryonic part of a galaxy. The bulge consists of an inner bulge and the outer bulge.

where for the inner bulge $M_0 \approx 4.2 \times 10^6\ M_\odot$ and $r \approx 1.15\ pc$, for the outer bulge $M_0 \approx 1 \times 10^{10}\ M_\odot$ and $r \approx 400\ pc$, and for the disk $M_0 \approx 4.4 \times 10^{10}\ M_\odot$ and $r \approx 3.5\ kpc$.

5.8 Black Hole Formation

Using the values of the core mass and core size we will check whether the core is compact enough to collapse into a black hole or not. The condition is given as

$$\text{If} \quad \frac{2GM_c}{r_c c^2} < 1, \quad \text{The core is not a black hole;} \tag{5.58}$$

$$\text{if} \quad \frac{2GM_c}{r_c c^2} > 1, \quad \text{The core is a black hole.} \tag{5.59}$$

The compactness of cores with the corresponding masses and sizes mentioned in the above tables, is given in the table 5.4.

At $m = 10.54\ keV/c^2$, we get a core mass of $2.7 \times 10^6\ M_\odot$ which is approximately equal to the mass of Sgr A* black hole. Its observed mass is about $4 \times 10^6\ M_\odot$, so the core of the RAR model can be considered as an alternative to the Sgr A* black hole. But the core radius we obtained is about $1.2 \times 10^{12}\ km$ and the one obtained when S2 star (which is the closest star to Sgr A*) came closest to Sgr A* is $1 \times 10^{10}\ km$. We need to introduce the cutoff effects in order to get more compact cores.

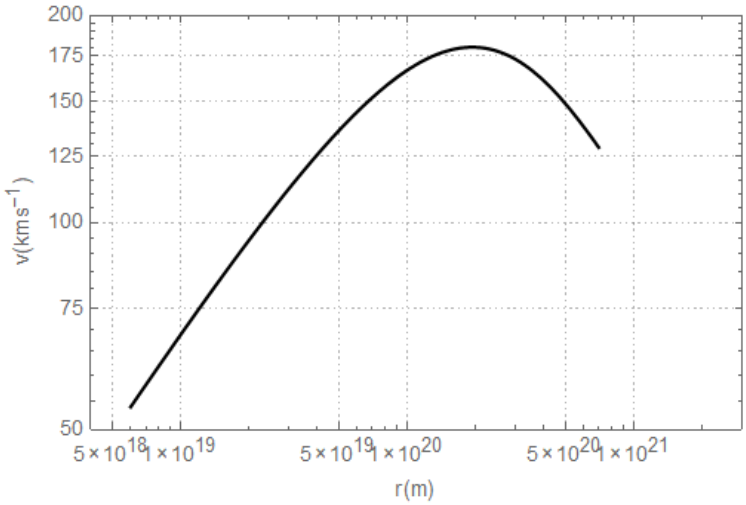

Figure 5.10: The graph shows the velocity varying with distance for the disk of the Milky Way galaxy which is the baryonic part of a galaxy other than the bulge.

Table 5.4: Core compactness values for different core masses and core sizes at different ino masses.

m(keV/c^2)	$2GM_c/r_cc^2$
4.323	5.5×10^{-6}
10.54	6.58×10^{-6}
48	8.2×10^{-6}
64.45	8.64×10^{-6}
100	9.16×10^{-6}
200	1.03×10^{-5}
300	1.1×10^{-5}
345	1.13×10^{-5}

5.9 The RAR Model with Cutoff Effects

We now discuss the RAR model by including the energy cutoff in the fermion phase space distribution. This gives the finite size of galaxies and the profiles will not go on indefinitely. Also, we get more compact cores than the cores obtained from the RAR model without the cutoff effects. In the ino mass range $48 - 345\ keV$, it gives a new solution with a compact quantum core as an alternative to the central black hole scenario for Sgr A*.

5.9.1 Central Density and Pressure

The fermionic equations of state for the phase space density and pressure with an energy cutoff are given in the previous chapter in equations 4.23 and 4.24. The limits now go from 0 to ϵ_c instead of infinity, that is the upper limit is at $\epsilon \leq \epsilon_c$, and the phase space distribution function is also different from the standard Fermi-Dirac distribution function given by $f_c(\epsilon \leq \epsilon_c) = \frac{1-e^{(\epsilon-\epsilon_c)/k_BT}}{e^{(\epsilon-\mu)/k_BT}+1}$ and $f_c(\epsilon > \epsilon_c) = 0$. Particles with energy $\epsilon > \epsilon_c$ are too fast and considered as lost, this is what causes a cutoff in the phase space distribution. We solve these equations to obtain central density and pressure at $r = 0$ in the same way as we did previously without the cutoff. So the equation for density after substituting the distribution function becomes

$$\rho = \frac{2m}{h^3}\int_0^{\epsilon_c}\left[\frac{1-e^{(\epsilon-\epsilon_c)/k_BT}}{e^{(\epsilon-\mu)/k_BT}+1}\right]\left[1+\frac{\epsilon(p)}{mc^2}\right]d^3p. \tag{5.60}$$

Also, we consider the system to be spherically symmetric

$$\rho = \frac{8\pi m}{h^3}\int_0^{\epsilon_c}\left[\frac{1-e^{(\epsilon-\epsilon_c)/k_BT}}{e^{(\epsilon-\mu)/k_BT}+1}\right]\left[1+\frac{\epsilon(p)}{mc^2}\right]p^2dp. \tag{5.61}$$

Using the same approximation $p \gg mc$, reduces the kinetic energy to cp and substituting this value in the above equation, we have

$$\rho = \frac{8\pi}{h^3c^2}\int_0^{\epsilon_c}\left[\frac{1-e^{(cp-\epsilon_c)/k_BT}}{e^{(cp-\mu)/k_BT}+1}\right](mc^2+cp)p^2dp. \tag{5.62}$$

Further simplifying the equation, we get

$$\begin{aligned}\rho &= \frac{8\pi m}{h^3c^2}\int_0^{\epsilon_c}\frac{c^2p^2}{e^{(cp-\mu)/k_BT}}dp + \frac{8\pi}{h^3c^4}\int_0^{\epsilon_c}\frac{c^3p^3}{e^{(cp-\mu)/k_BT}}dp \\ &- \frac{8\pi m}{h^3c^2}\int_0^{\epsilon_c}\frac{c^2p^2}{e^{\epsilon_c/k_BT}e^{-\mu/k_BT}}dp - \frac{8\pi}{h^3c^4}\int_0^{\epsilon_c}\frac{c^3p^3}{e^{\epsilon_c/k_BT}e^{-\mu/k_BT}}dp.\end{aligned} \tag{5.63}$$

To account for the value of energy cutoff ϵ_c, we introduce a cutoff parameter W as given in equation 4.28 other than the previously introduced temperature and degeneracy parameters from equation 4.13. Also, using the same substitutions for cp as we did for computing the density and pressure without cutoff, so

$$\begin{aligned}\rho &= \frac{8\pi m}{h^3c^3}\int_0^{\epsilon_c}\frac{z^2}{e^{z/\beta mc^2}e^{-\theta}}dz + \frac{8\pi}{h^3c^5}\int_0^{\epsilon_c}\frac{z^3}{e^{z/\beta mc^2}e^{-\theta}}dz \\ &- \frac{8\pi m}{h^3c^3}\int_0^{\epsilon_c}\frac{z^2}{e^{W}e^{-\theta}}dz - \frac{8\pi}{h^3c^5}\int_0^{\epsilon_c}\frac{z^3}{e^{W}e^{-\theta}}dz.\end{aligned} \tag{5.64}$$

To solve this equation, we find the values of the model parameters β_0, θ_0, and W_0 for different values of m. The central degeneracy parameter is obtained by equation 5.10 with $\theta_0^* \approx 28.684$. The central temperature parameter is obtained by the eigen value problem until we get the fixed halo observables of the model for spiral galaxies in our case.

First making the core mass dimensionless by using the values from equation 4.9 and then solving it for β_0. Using all the above discussed constants, we can now numerically integrate the resulting equation and get the central density for any value of the ino mass. The central cutoff parameter W_0 is obtained by

$$W_0 = (1+\alpha)\theta_0, \tag{5.65}$$

where $\alpha \approx 0.7564$ for spiral galaxies, $\alpha \approx 0.6324$ for dwarf galaxies, and $\alpha \approx 0.951$ for elliptical galaxies. Similarly, we can work for the central pressure of a galaxy at $r = 0$ with cutoff, using the equation 4.24, substituting the Fermi-Dirac function, we have

$$P = \frac{2}{3h^3}\int_0^{\epsilon_c}\frac{1-e^{(\epsilon-\epsilon_c)/k_BT}}{e^{(\epsilon-\mu)/k_BT}+1}\left[1+\frac{\epsilon(p)}{mc^2}\right]^{-1}\left[1+\frac{\epsilon(p)}{2mc^2}\right]\epsilon d^3p. \tag{5.66}$$

The equation for pressure is simplified the same way as the equation for density, this will give the central pressure. In the following table different values for the central degeneracy parameter, central temperature parameter, and central density for different values of the ino mass are given. To find different variables we will move on to a set of Einstein equations.

Table 5.5: Core properties including the central degeneracy parameter, temperature parameter, cutoff parameter, and central density for different ino masses fulfilling the halo boundary conditions given in equation 4.14.

m(keV/c^2)	θ_0	β_0	W_0	$\rho_c^c(M_\odot/pc^3)$
48	36.93	1×10^{-5}	65	9.7×10^{15}
54	37.57	1.13×10^{-5}	66	2.95×10^{16}
56	37.76	1.21×10^{-5}	66.32	4.12×10^{16}
58	37.96	1.3×10^{-5}	66.7	5.8×10^{16}
100	40.92	1.8×10^{-5}	71.8	9.88×10^{18}
200	44.69	2×10^{-4}	73	6.86×10^{21}
250	45.9	2.2×10^{-3}	75.1	5.6×10^{22}
300	46.89	3.7×10^{-3}	76.5	3.13×10^{23}
320	47.24	4.3×10^{-3}	77.1	5.76×10^{23}
340	47.57	4.7×10^{-3}	77.6	1.02×10^{24}
345	47.65	5×10^{-3}	77.7	1.17×10^{24}

5.9.2 Core Mass

The Einstein equations in the RAR model are given in equations 4.4 4.8. In order to account for the cutoff in momentum space, an additional equation is included given by

$$W(\hat{r}) = W_0 + \theta(\hat{r}) - \theta_0. \tag{5.67}$$

The equations can be solved to find the parameters varying with distance like $M(r)$, $\theta(r)$, $\nu(r)$, $\beta(r)$ with initial conditions $M(0) = 0$, $\theta(0) = \theta_0$, $\nu(0) = 0$, $\beta(0) = \beta_0$, $W(0) = W_0$. We solve these equations after making them dimensionless by using the dimensionless quantities from equation 4.9. The first equation gives the core mass by solving it numerically with a constant central density, obtained from the equation 5.64, we have

$$\frac{dM}{dr} = 4\pi r^2 \rho_c^c, \tag{5.68}$$

where ρ_c^c is the central density obtained from the fermionic equations of state with energy cutoff. We plug in the value of central density and solve it numerically. At $M(r_c^c)$, we get M_c^c that is the core mass and r_c^c is the core size which will be discussed later. For different values of m, the corresponding core masses are given in the following table.

Table 5.6: Core masses for different ino masses and the corresponding central degeneracy and temperature parameters.

m(keV/c^2)	$M_c^c(M_\odot)$
48	3.18×10^6
54	3.46×10^6
56	3.54×10^6
58	3.65×10^6
100	5.4×10^6
200	8.86×10^6
250	1.04×10^7
300	1.18×10^7
320	1.24×10^7
340	1.29×10^7
345	1.31×10^7

5.9.3 Density Profiles and Rotation Curves

The phase space density distribution as we have previously seen, shows a quantum regime which transitions into a classical one. Now we will see the density profiles for different ino masses with the effects of cutoff. The density is studied varying with the distance at certain fixed parameters that is the central degeneracy parameter, temperature parameter, and cutoff parameter. The central density ρ_c^c was calculated from the Fermi-Dirac phase space distribution using the fermionic equation of state with energy cutoff, now we need the density varying with distance that is $\rho(r)$. We start with the standard fermionic equation of state with the distribution function including the cutoff given by

$$\rho(r) = \frac{2m}{h^3} \int_0^{\epsilon_c} \left[\frac{1 - e^{(\epsilon - \epsilon_c(r))/k_B T}}{e^{(\epsilon - \mu(r))/k_B T} + 1} \right] d^3p. \tag{5.69}$$

For the spherically symmetric solutions, we have

$$\rho(r) = \frac{8\pi m}{h^3} \int_0^{\epsilon_c} \left[\frac{1 - e^{(\epsilon/k_B T - \epsilon_c/k_B T)}}{e^{(\epsilon/k_B T - \theta(r))} + 1} \right] p^2 dp, \tag{5.70}$$

where $\theta(r) = \mu(r)/k_B T$ is the degeneracy parameter and $\mu(r)$ is the chemical potential, $W(r) = \epsilon_c(r)/k_B T$ is the cutoff parameter, and ϵ_c is the energy cutoff. The distribution function is considered as the fermionic King model. To account for different regimes, we use the approximation $p \ll mc$, the kinetic energy reduces to $p^2/2m$, so the equation becomes

$$\rho(r) = \frac{8\pi m(2mk_BT)}{h^3}\int_0^{\epsilon_c}\left[\frac{1-e^{(p^2/2mk_BT-\epsilon_c/k_BT)}}{e^{(p^2/2mk_BT-\mu/k_BT)}+1}\right]\frac{p^2}{2mk_BT}dp. \tag{5.71}$$

To find density as a function of distance, we use the following substitution

$$y^2 = \frac{p^2}{2mk_BT}. \tag{5.72}$$

The equation becomes

$$\rho(r) = \frac{2m(2\pi mk_BT)^{3/2}}{h^3}\frac{4}{\sqrt{\pi}}\int_0^{\epsilon_c}\left[\frac{1-e^{(y^2-W(r))}}{e^{(y^2-\theta(r))}+1}\right]y^2dy, \tag{5.73}$$

$$\rho(r) = \frac{2m}{\lambda_B^3}\frac{4}{\sqrt{\pi}}\int_0^{\epsilon_c}\left[\frac{1-e^{(y^2-W(r))}}{e^{(y^2-\theta(r))}+1}\right]y^2dy, \tag{5.74}$$

where $\lambda_B = \frac{h}{\sqrt{2\pi mk_BT}}$ is the thermal de Broglie wavelength of inos. In the limit $W_0 \longrightarrow \infty$, we get the Fermi-Dirac distribution without cutoff. This gives the density profiles as we obtained earlier with a compact quantum core of constant density, a transition region with a sharp decrease in density, and a classical halo after the sharp decrease, for high mass particles it obeys a power law $\rho \propto r^{-n}$ where n>2. We saw earlier that for low mass particles, it obeys a power law $\rho \propto r^{-2}$ which is an isothermal sphere. The halo is now not continuing indefinitely, it is finite with a cutoff at certain value. Using the density given above we can get finite mass profiles given by the equation

$$M(r) = 4\pi r^2\frac{2m}{\lambda_B^3}\frac{4}{\sqrt{\pi}}\int_0^{\epsilon_c}\left[\frac{1-e^{(y^2-W(r))}}{e^{(y^2-\theta(r))}+1}\right]y^2dy. \tag{5.75}$$

Using the above mass we get the rotation curves by the circular velocity formula given in equation 5.55. The curves show a similar increasing behavior at the beginning, $v \propto r$, reaching the core radius r_c at the first maximum, core sizes for different ino masses are given in the table 5.7, then a Keplerian decrease $v \propto r^{-1/2}$ to a minimum showing a transition from the quantum to dilute regime and again increasing to a second maximum that gives the halo radius r_h. But this time the flat rotation curve going infinite is finite due to the cutoff effects.

Table 5.7: Core properties including the core radii for different ino masses.

m(keV/c^2)	$r_c^c(pc)$
48	6.4×10^{-4}
54	4.56×10^{-4}
56	4.1×10^{-4}
58	3.7×10^{-4}
100	7.65×10^{-5}
200	1.02×10^{-5}
250	5.33×10^{-6}
300	3.14×10^{-6}
320	2.6×10^{-6}
340	2.18×10^{-6}
345	2.07×10^{-6}

5.10 Black Hole Formation

The values of core mass and core size obtained by the RAR model with cutoff can be used to check whether the core is compact enough to collapse into a black hole or not, as we did earlier in the RAR model without cutoff. The conditions are given as

$$\text{If} \quad \frac{2GM_c}{r_c c^2} < 1, \quad \text{The core is not a black hole;} \tag{5.76}$$

$$\text{if} \quad \frac{2GM_c}{r_c c^2} > 1, \quad \text{The core is a black hole.} \tag{5.77}$$

The values of the core compactness with the corresponding masses and sizes mentioned in the above tables are given in the table 5.8.

At $mc^2 = 56\ keV$, we get a core mass $3.6 \times 10^6\ M_\odot$ which is approximately equal to the mass of Sgr A* black hole. Its observed mass is about $4 \times 10^6\ M_\odot$, so the core of the RAR model can be considered as an alternative to Sgr A* black hole, with the core radius about $4.1 \times 10^{-4}\ pc$ which is almost equal to the one obtained when S2 star came closest to Sgr A*.

5.11 Baryonic Matter in Galaxies

Along with the dark matter, baryonic matter is also present in the galaxies. The dark matter cores for different ino masses in the given range do not form black holes. We consider the

Table 5.8: Core compactness values for different core masses and core sizes at different ino masses.

m(keV/c^2)	$2GM_c^c/r_c^c c^2$
48	4.77×10^{-4}
54	7.3×10^{-4}
56	8.3×10^{-4}
58	9.48×10^{-4}
100	6.78×10^{-3}
200	8.34×10^{-2}
250	1.87×10^{-1}
300	3.61×10^{-1}
320	4.58×10^{-1}
340	5.68×10^{-1}
345	6.08×10^{-1}

core to be a gravitational potential well, so as yet there is no matter that has fallen in. There are the partially degenerate fermions outside the core, so for it to collapse into a black hole, it must have baryonic matter falling in. Some of the baryonic matter in the core of a galaxy will tend to fall into the degenerate core and may form black hole inside. But they all come from a time after nucleosynthesis, so the number of baryons that must fall in may provide a sharper constraint on the fermion masses. So with expecting the fermions, what will be the amount of mass of baryons that must come in to make it into a black hole?

We already worked out the dark matter core masses for different ino masses, so now we can find out the critical masses for cores for different ino masses by using following equation

$$M_c^{cr} = \frac{3\sqrt{\pi}}{16}\frac{m_p^3}{m^2}\left(1 + \frac{2\pi^2}{\theta_0^2}\right)^{3/2}, \tag{5.78}$$

where m is the ino mass, m_p is the Planck mass, and θ_0 is the central degeneracy parameter. So, the values for critical core mass for different ino masses is given in table 5.10. For high central degeneracy, $\theta_0 \gg 2\sqrt{\pi}$, so the critical core mass becomes independent of θ_0 and it becomes proportional to m_p^3/m^2.

We have the values for the dark matter core mass and the values for the critical core mass, we will add a certain amount of baryonic matter in the dark matter cores such that the cores reach the critical mass and collapse into black holes.

Table 5.9: Critical Core masses for different values of the ino mass and the central degeneracy parameter.

$m(keV/c^2)$	$M_c^{cr}(M\odot)$
10.54	5.053×10^9
48	2.409×10^8
64.45	1.332×10^8
100	5.528×10^7
200	1.378×10^7
300	6.116×10^6
345	4.623×10^6

Table 5.10: Baryonic matter masses for different values of the ino mass and the central degeneracy parameter.

$m(keV/c^2)$	$M_b(M\odot)$
10.54	5.05×10^9
48	2.407×10^8
64.45	1.331×10^8
100	5.524×10^7
200	1.377×10^7
300	6.111×10^6
345	4.62×10^6

5.12 Conclusion

One of the aims of modern Astrophysics now is to know the nature of dark matter after various pieces of evidence on its existence. It is assumed that the particle composing it, would be beyond the Standard Model of Particle Physics. Basically, we assumed that the supermassive object at the center of a galaxy is made up of the degenerate fermions, the halo is made up of the same fermions but non-degenerate, and that the same fermions are responsible for the dark matter at the center and in the halo. In the Milky Way galaxy, a continuous distribution of dark matter was observed.

We considered the RAR model in the framework of General Relativity which includes a spherically symmetric self-gravitating system of massive fermions with masses in the range $10 - 345\ keV$ and $48 - 345\ keV$. Also, the system has certain free parameters like the degeneracy parameter θ_0, the temperature parameter β_0, and the cutoff parameter W_0. We found the core masses using the fermionic equations of state with and without the cutoff effects. Then for the thermal and semi-degenerate fermion gas, considering a perfect fluid in the hydrostatic equilibrium, we found the mass distributions both infinite and finite, using Einstein's equation. Firstly, we considered the Fermi-Dirac phase space distribution and the fermions obeying the quantum statistics with no additional interactions. This gave us the density profiles for different fermion masses at fixed dark matter halo constraints for spiral galaxies. The density profiles showed different regimes: the degenerate quantum core, a transition region from quantum to classical, and the classical Boltzmann regime. We also considered the Boltzmann distribution, compared it with different RAR profiles, and we concluded that the different profiles eventually reach the classical regime in halo region. The rotation curves were then obtained giving different regions: first an increasing behavior was seen till it reached the first maximum which gave the core size, after this the curve deceased and then increased to a second maximum which was the halo size. We saw a flat rotation curve in the outer regions due to the constant circular velocities at the halo scales, this indicated the presence of dark matter. So, the flat rotation curves are the classical pieces of evidence of dark matter.

We first used the model and proceeded with the calculations without the cutoff effects, which resulted in not so compact cores. At about $10\ keV$ fermionic mass, the core mass was $\sim 3 \times 10^6\ M_\odot$ and the core size of the order $\sim 10^{-2}\ pc$ which is greater of the order 10^2 from the size of the core observed due to S2 star.

We then considered the fermionic dark matter RAR model with cutoff effects in the phase space distribution. This gave a degenerate quantum core and a diluted halo with cutoff effects, providing with sufficient compactness of the quantum core. It can now be considered as an alternative to the central black hole scenario. We observed that at fermion mass $56\ keV$, the core mass is $\sim 3.6 \times 10^6\ M_\odot$ with the core size $\sim 4.1 \times 10^{-4}\ pc$. The calculations in this thesis were performed on spiral galaxies, we can also use the constraints for dwarf spheroidal galaxies or the elliptical galaxies to extend this work.

The model predicts a particle as a possible candidate for dark matter. The density profiles

and the rotation curves show the distribution of matter from the degenerate compact cores to the dark matter halos. Flat rotation curves are seen at large distances which indicate the presence of dark matter. The model gives a degenerate fermionic compact core which provides an alternatives to the central black hole scenario. It is a consistent proposal for the explanation of the problem of the formation of supermassive black holes shortly after the Big Bang and the missing intermediate-mass black holes. Other than the dark matter, baryonic matter is also present in the cores of galaxies, it will tend to fall into the degenerate cores and may even form black holes inside. We have the dark matter core masses and the critical core masses for different ino masses, so we worked out the respective baryonic matter masses by adding them into the dark matter cores and get the cores to collapse. We also saw the distribution of baryonic matter in the bulge and disk parts of the Milky Way galaxy.

What the RAR model gives is an explanation but we need evidence for such fermions, the model needs to be tested. This would be done by considering the effect of such structures as they form on the cosmic microwave background as an imprint of the formation of the cores. We should trace back early times, when the cosmic microwave background was coming out, then these fermions should leave an imprint on the cosmic microwave background. Due to the formation process there will be the inhomogeneities, then we should be able to make a prediction of what to see. We can then compare the spectrum of cosmic microwave background with the actual spectrum with the prediction. Then we shall be able to see the degenerate fermion core. Then we say how do they form into one central core? So in the start these fermions will be presumably uniformly distributed, there will be fluctuations, and they will collapse. They will collapse in various spaces. Over time, these collapsed things will go on coalescing more and more. It forms degeneratly not at one place but at one momentum, they can be on different places and correlated. Finally, the gravitational force will pull it all together and there will be a central black hole. How do these form can make a difference to what could be predicted. This is left as an open problem for the present.

Bibliography

[1] V. Sahni and A. Starobinsky, "The Case for a Positive Cosmological λ-Term," *International Journal of Modern Physics D*, vol. **9**, pp. 373–443, (2000).

[2] J. A. Peacock, *Cosmological Physics*. Cambridge University Press, (1999).

[3] V. C. Rubin and W. K. Ford Jr, "Rotation of the Andromeda Nebula from a Spectroscopic Survey of Emission Regions," *The Astrophysical Journal*, vol. **159**, (1970).

[4] Y. Heymann, "Dark Matter, the Correction to Newton's Law in a Disk," *Progress in Physics*, vol. **12**, pp. 347–352, (2016).

[5] R. Ruffini, C. R. Argüelles, and J. A. Rueda, "On the Core-Halo Distribution of Dark Matter in Galaxies," *Monthly Notices of the Royal Astronomical Society*, vol. **451**, pp. 622–628, (2015).

[6] J. F. Navarro, C. S. Frenk, and S. D. White, "A Universal Density Profile from Hierarchical Clustering," *The Astrophysical Journal*, vol. **490**, (1997).

[7] J. Einasto, "On the Construction of a Composite Model for the Galaxy and on the Determination of the System of Galactic Parameters," *Trudy Astrofizicheskogo Instituta Alma-Ata*, vol. **5**, pp. 87–100, (1965).

[8] J. Einasto and U. Haud, "Galactic Models with Massive Corona. I-Method. II-Galaxy," *Astronomy and Astrophysics*, vol. **223**, pp. 89–106, (1989).

[9] S. Gillessen, F. Eisenhauer, T. Fritz, H. Bartko, K. Dodds-Eden, O. Pfuhl, T. Ott, and R. Genzel, "The Orbit of the Star S2 Around Sgr A* from Very Large Telescope and Keck Data," *The Astrophysical Journal Letters*, vol. **707**, (2009).

[10] E. Becerra-Vergara, C. Argüelles, A. Krut, J. Rueda, and R. Ruffini, "Geodesic Motion of S2 and G2 as a Test of the Fermionic Dark Matter Nature of our Galactic Core," *Astronomy & Astrophysics*, vol. **641**, (2020).

[11] J. Gao, M. Merafina, and R. Ruffini, "The Semidegenerate Configurations of a Selfgravitating System of Fermions," *Astronomy and Astrophysics*, vol. **235**, pp. 1–7, (1990).

[12] M. Baldeschi, G. Gelmini, and R. Ruffini, "On Massive Fermions and Bosons in Galactic Halos," *Physics Letters B*, vol. **122**, pp. 221–224, (1983).

[13] C. R. Argüelles, A. Krut, J. Rueda, and R. Ruffini, "Novel Constraints on Fermionic Dark Matter from Galactic Observables I: The Milky Way," *Physics of the Dark Universe*, vol. **21**, pp. 82–89, (2018).

[14] G. Ingrosso, M. Merafina, R. Ruffini, and F. Strafella, "System of Self-Gravitating Semidegenerate Fermions with a Cutoff of Energy and Angular Momentum in their Distribution Function," *Astronomy and Astrophysics*, vol. **258**, pp. 223–233, (1992).

[15] N. Bilic, F. Munyaneza, G. B. Tupper, and R. D. Viollier, "The Dynamics of Stars Near Sgr A* and Dark Matter at the Center and in the Halo of the Galaxy," *Progress in Particle and Nuclear Physics*, vol. **48**, pp. 291–300, (2002).

[16] A. Qadir, *An Introduction to the Special Theory.* World Scientific, (1989).

[17] A. Qadir, *Einstein's General Theory of Relativity.* Cambridge University Press, (2020).

[18] R. M. Wald, *General Relativity.* The University of Chicago Press, (2010).

[19] O. Hans C, *Gravitation and Spacetime.* Cambridge University Press, (2013).

[20] M. S. Swanson, *Classical Field Theory and the Stress-Energy Tensor.* Morgan and Claypool, (2015).

[21] A. Eckart, *The Black Hole at the Center of the Milky Way.* Imperial College Press, (2005).

[22] V. P. Frolov and I. D. Novikov, *Black Hole Physics Basic Concepts and New Developments.* Springer, (1998).

[23] B. Ryden, *Introduction to Cosmology.* Cambridge University Press, (2016).

[24] C. W. Misner, K. Thorne, and J. Wheeler, *Gravitation.* W. H. Freeman", (1973).

[25] H. Kumar Mohajan, "Development of Einstein's Static Cosmological Model of the Universe," *Journal of Scientific Achievements*, vol. **2**, pp. 18–29, (2017).

[26] C. O'Raifeartaigh, M. O'Keeffe, W. Nahm, and S. Mitton, "Einstein's 1917 Static Model of the Universe: A Centennial Review," *The European Physical Journal H*, vol. **42**, pp. 431–474, (2017).

[27] M. Li, X.-D. Li, S. Wang, and Y. Wang, "Dark Energy," *Commun. Theor. Phys.*, vol. **56**, pp. 525–604, (2011).

[28] M. Li, X.-D. Li, S. Wang, and Y. Wang, "Dark Energy," *The Universe*, vol. **1**, pp. 24–45, (2013).

[29] A. Faessler, R. Hodak, S. Kovalenko, and F. Simkovic, "Search for the Cosmic Neutrino Background," in *Journal of Physics: Conference Series*, vol. **580**, IOP Publishing, (2015).

[30] D. Griffiths, *Introduction to Elementary Particles*. (2008).

[31] A. V. Patwardhan, G. M. Fuller, C. T. Kishimoto, and A. Kusenko, "Diluted Equilibrium Sterile Neutrino Dark Matter," *Physical Review D*, vol. **92**, (2015).

[32] J. Conrad, C. Ignarra, G. Karagiorgi, M. Shaevitz, and J. Spitz, "Sterile Neutrino Fits to Short-Baseline Neutrino Oscillation Measurements," *Advances in High Energy Physics*, vol. **2013**, (2013).

[33] A. Boyarsky, M. Drewes, T. Lasserre, S. Mertens, and O. Ruchayskiy, "Sterile Neutrino Dark Matter," *Progress in Particle and Nuclear Physics*, vol. **104**, pp. 1–45, (2019).

[34] C. d. S. Pires, "A Cosmologically Viable eV Sterile Neutrino Model," *Physics Letters B*, vol. **800**, (2020).

[35] D. V. Naumov, "The Sterile Neutrino: A Short Introduction," *EPJ Web Conf.*, vol. **207**, (2019).

[36] H. De Vega, P. Salucci, and N. Sanchez, "Observational Rotation Curves and Density Profiles Versus the Thomas-Fermi Galaxy Structure Theory," *Monthly Notices of the Royal Astronomical Society*, vol. **442**, pp. 2717–2727, (2014).

[37] N. A. Bahcall, "Dark Matter Universe," *Proceedings of the National Academy of Sciences*, vol. **112**, pp. 12243–12245, (2015).

[38] K. Garrett and G. Duda, "Dark Matter: A Primer," *Advances in Astronomy*, vol. **2011**, (2011).

[39] A. Boyarsky, O. Ruchayskiy, D. Iakubovskyi, A. V. Maccio, and D. Malyshev, "New Evidence for Dark Matter," *arXiv preprint arXiv:0911.1774*, (2009).

[40] H. De Vega and N. Sanchez, "The Dark Matter Distribution Function and Halo Thermalization from the Eddington Equation in Galaxies," *International Journal of Modern Physics A*, vol. **31**, (2016).

[41] J. R. Primack, "Dark Matter and Structure Formation," in *Midrasha Mathematicae in Jerusalem: Winter School in Dynamical Systems*, (1997).

[42] E. Morgante, *Aspects of WIMP Dark Matter Searches at Colliders and Other Probes*. PhD thesis, (2016).

[43] J. R. Primack and M. A. Gross, "Hot Dark Matter in Cosmology," in *Current Aspects of Neutrino Physics*, pp. 287–308, Springer, 2001.

[44] L. Hui, J. P. Ostriker, S. Tremaine, and E. Witten, "Ultralight Scalars as Cosmological Dark Matter," *Physical Review D*, vol. **95**, (2017).

[45] S. Raha, S. Banerjee, A. Bhattacharyya, S. K. Ghosh, E.-M. Ilgenfritz, B. Sinha, E. Takasugi, and H. Toki, "Strangeness, Cosmological Cold Dark Matter and Dark Energy," *Journal of Physics G: Nuclear and Particle Physics*, vol. **31**, (2005).

[46] S. Colombi, S. Dodelson, and L. M. Widrow, "Large Scale Structure Tests of Warm Dark Matter," *Astrophys. J.*, vol. **458**, (1996).

[47] S. Hannestad and R. J. Scherrer, "Selfinteracting Warm Dark Matter," *Phys. Rev. D*, vol. **62**, (2000).

[48] W. Arnett, "Degenerate Matter," in *Summer School of Theoretical Physics*.

[49] E. Riazuddin and A. Qadir, "Physics and Contemporary Needs 5: Proceedings/[5th International Summer College on Physics and Contemporary Needs], Nathiagali, June 16-July 4, 1980,"

[50] L. Susskind and J. Lindesay, *An Introduction to Black Holes, Information and the String Theory Revolution: The Holographic Universe*. World Scientific, (2005).

[51] D. Nardo, *Black Holes*. Lucent Books, (2004).

[52] V. Frolov and I. Novikov, *Black Hole Physics: Basic Concepts and New Developments*, vol. **96**. Springer Science & Business Media, (2012).

[53] H. C. Ohanian and R. Ruffini, *Gravitation and Spacetime*. Cambridge University Press, (2013).

[54] M. P. Hobson, G. P. Efstathiou, and A. N. Lasenby, *General Relativity: An Introduction for Physicists*. Cambridge University Press, (2006).

[55] S. Chandrasekhar and S. Chandrasekhar, *An Introduction to the Study of Stellar Structure*, vol. **2**. Courier Corporation, (1957).

[56] T. Nakajima, "Future Studies of Brown Dwarfs from Space," *Advances in Space Research*, vol. **25**, pp. 2225–2232, (2000).

[57] T. Nakajima, B. Oppenheimer, S. Kulkarni, D. Golimowski, K. Matthews, and S. Durrance, "Discovery of a Cool Brown Dwarf," *Nature*, vol. **378**, pp. 463–465, (1995).

[58] F. C. Adams, G. Laughlin, and G. J. Graves, "Red Dwarfs and the End of the Main Sequence," in *Revista Mexicana de Astronomia y Astrofisica Conference Series*, vol. **22**, pp. 46–49, (2004).

[59] A. Chiavassa, E. Pasquato, A. Jorissen, S. Sacuto, C. Babusiaux, B. Freytag, H. G. Ludwig, P. Cruzalèbes, Y. Rabbia, A. Spang, *et al.*, "Photocentric Variability of Red Supergiant Stars and Consequences on Gaia Measurements," in *SF2A-2010: Proceedings of the Annual Meeting of the French Society of Astronomy and Astrophysics*, (2010).

[60] A. Lobel, "Two Decades of Hypergiant Research," *arXiv preprint astro-ph/0108358*, (2001).

[61] M. Bessell, "The Formation and Evolution of White Dwarfs," in *Proceedings of the Astronomical Society of Australia*, vol. **3**, pp. 220–224, (1978).

[62] J. Provencal, "The Importance of White Dwarf Stars as Tests of Stellar Physics and Galactic Evolution,"

[63] H. Shipman, "White Dwarf Evolution: A Review," in *12th European Workshop on White Dwarfs*, vol. **226**, (2001).

[64] A. Y. Potekhin, "The Physics of Neutron Stars," *Physics-Uspekhi*, vol. **53**, (2010).

[65] J. M. Lattimer and M. Prakash, "The Physics of Neutron Stars," *Science*, vol. **304**, pp. 536–542, (2004).

[66] J. M. Lattimer, "Neutron Star Physics and EoS," in *EPJ Web of Conferences*, vol. **109**, EDP Sciences, (2016).

[67] A. J. Burgasser, J. Bloom, K. Cruz, M. Cushing, S. Leggett, K. Lodders, A. Mainzer, M. Marley, S. Metchev, S. Mohanty, *et al.*, "Toward the End of Stars: Discovering the Galaxy's Coldest Brown Dwarfs," *arXiv preprint arXiv:0902.2604*, (2009).

[68] J. Binney and S. Tremaine, *Galactic Dynamics*. Princeton University Press, (2011).

[69] C. J. Conselice, "The Fundamental Properties of Galaxies and a New Galaxy Classification System," *Monthly Notices of the Royal Astronomical Society*, vol. **373**, pp. 1389–1408, (2006).

[70] D. Lynden-Bell, "Statistical Mechanics of Violent Relaxation in Stellar Systems," *Monthly Notices of the Royal Astronomical Society*, vol. **136**, (1967).

[71] R. W. Michie, "On the Distribution of High Energy Stars in Spherical Stellar Systems," *Monthly Notices of the Royal Astronomical Society*, vol. **125**, pp. 127–139, (1962).

[72] I. R. King, "The Structure of Star Clusters. IV. Photoelectric Surface Photometry in Nine Globular Clusters," *The Astronomical Journal*, vol. **71**, (1966).

[73] R. C. Tolman, "On the Weight of Heat and Thermal Equilibrium in General Relativity," *Physical Review*, vol. **35**, (1930).

[74] O. Klein, "On the Thermodynamical Equilibrium of Fluids in Gravitational Fields," *Reviews of Modern Physics*, vol. **21**, (1949).

[75] E. Becerra-Vergara, C. Argüelles, A. Krut, J. Rueda, and R. Ruffini, "Hinting a Dark Matter Nature of Sgr A* via the S-Stars," *Monthly Notices of the Royal Astronomical Society: Letters*, vol. **505**, pp. L64–L68, (2021).